

**UCLA**

**UCLA Electronic Theses and Dissertations**

**Title**

Dissecting the Regulatory Strategies of NFkappaB RelA Target Genes in the Inflammatory Response

**Permalink**

<https://escholarship.org/uc/item/2bw1217w>

**Author**

Ngo, Kim Anh

**Publication Date**

2019

**Supplemental Material**

<https://escholarship.org/uc/item/2bw1217w#supplemental>

Peer reviewed|Thesis/dissertation

UNIVERSITY OF CALIFORNIA

Los Angeles

Dissecting the Regulatory Strategies of NFkappaB RelA Target Genes  
in the Inflammatory Response

A dissertation submitted in partial satisfaction of the  
requirements for the degree Doctor of Philosophy  
in Microbiology, Immunology, and Molecular Genetics

by

Kim Anh Ngo

2019

© Copyright by

Kim Anh Ngo

2019

## ABSTRACT OF THE DISSERTATION

### Dissecting the Regulatory Strategies of NF $\kappa$ B RelA Target Genes in the Inflammatory Response

by

Kim Anh Ngo

Doctor of Philosophy in Microbiology, Immunology, and Molecular Genetics

University of California, Los Angeles, 2019

Professor Alexander Hoffmann, Chair

The NF $\kappa$ B family member RelA is a ubiquitously expressed potent transcriptional activator that is induced by exposure to pathogens and inflammatory cytokines to activate the expression of a large number of inflammatory and immune-response genes. Its nuclear activity is induced from a latent cytoplasmic pool by stimulus-responsive degradation of I $\kappa$ B proteins, and the complex signaling mechanisms that regulate its activity are well understood. Less well characterized are the mechanisms that allow nuclear NF $\kappa$ B RelA activity to select its target genes and produce gene-specific expression. While many genes have been identified to be potentially NF $\kappa$ B regulated, there is no database that lists the NF $\kappa$ B target genes in a particular physiological condition, defined cell types and stimulus.



Chapter 1 presents a general overview of IKK-I $\kappa$ B-NF $\kappa$ B signaling system. Chapter 2 reports the primary study in this dissertation in which includes approaches such as biochemistry, molecular biology, mouse genetics, Next-Generation Sequencing, and mathematical modeling to dissect the regulatory strategies of NF $\kappa$ B RelA endogenous target genes in the inflammatory response. Chapter 3 summarizes our findings and provide a future direction to this study.

In Chapter 2, to dissect gene-specific regulatory strategies resulting from NF $\kappa$ B activation in response to inflammation, we stringently defined a list of direct RelA target genes by integrating physical/DNA binding (ChIP-seq) and functional/transcriptional data (RNA-seq) datasets. We then dissected each gene's regulatory strategy by testing RelA variants in a novel primary-cell genetic complementation assay. All endogenous target genes required that RelA makes DNA-base-specific contacts, and none could be activated by the DNA binding domain alone. However, endogenous target genes differed widely in how they employ the two transactivation domains (TAD). Through model-aided analysis of the dynamic timecourse data we reveal gene-specific synergy and redundancy of TA1 and TA2. Given that post-translational modifications control TA1 activity and affinity for coactivators determines TA2 activity, the differential TA logics suggests context-dependent vs. context-independent control of endogenous RelA-target genes. While some inflammatory initiators appear to require co-stimulatory TA1 activation, inflammatory resolvers are a part of the NF $\kappa$ B RelA core response where TA2 activity mediates activation even when TA1 is inactive.

The dissertation of Kim Anh Ngo is approved.

Arnold J. Berk

Lili Yang

Siavash K. Kurdistani

Alexander Hoffmann, Committee Chair

University of California, Los Angeles

2019

## DEDICATION

I dedicate this work to my family, especially my parents for giving me life. To my mom Hoa Ho, and to my siblings Caroline Ngo, Tri Ngo, Hoang Minh Ngo, and Le Ngo for their constant support and encouragement.

To my principal investigator and advisor, Professor Alexander Hoffmann at UCLA. His passion and enthusiasm for doing science have inspired me and are the reasons why I went to graduate school.

## TABLE OF CONTENTS

ABSTRACT OF THE DISSERTATION	ii
COMMITTEE PAGE	iv
DEDICATION	v
TABLE OF CONTENTS	vi
LIST OF FIGURES	viii
LIST OF SUPPLEMENTARY TABLES	x
ACKNOWLEDGEMENTS	xi
VITA	xv
PUBLICATIONS	xvi
CHAPTER 1: General Introduction	1
NF $\kappa$ B, I $\kappa$ B, and IKK PROTEIN FAMILIES	2
NF $\kappa$ B SIGNALING SYSTEM	9
DNA RECOGNITION BY NF $\kappa$ B DIMERS	14
NF $\kappa$ B TRANSACTIVATION	16
FOCUS OF STUDY	17
REFERENCES	20
CHAPTER 2: Dissecting the Regulatory Strategies of NF $\kappa$ B RelA Target Genes in the Inflammatory Response	29
ABSTRACT	30

INTRODUCTION	31
RESULTS	35
Stringent identification of TNF-responsive NF $\kappa$ B RelA target genes	35
An experimental system to dissect regulatory strategies of NF $\kappa$ B RelA target genes	40
All TNF-induced NF $\kappa$ B target genes require that RelA makes base-specific contacts within the $\kappa$ B element	48
All TNF-induced NF $\kappa$ B target genes are regulated by two C-terminal TA domains	55
A model-aided analysis reveals gene-specific logic gates formed by RelA TA1 and TA2	61
A knock-in mouse reveals that regulatory strategies of RelA target genes are generally conserved in different cell types but are often stimulus-specific	66
MATERIALS AND METHODS	78
ACKNOWLEDGEMENTS	88
REFERENCES	90
CHAPTER 3: Conclusions and Future Directions	95
REFERENCES	103

## LIST OF FIGURES

### CHAPTER 1: General Introduction

Figure 1.1 NFκB protein family	4
Figure 1.2 IκB and IKK protein families	8
Figure 1.3 Two NFκB signaling pathways	12
Figure 1.4 Cross-talk in NFκB pathways	13
Figure 1.5 RelA modular domain structures	19

### CHAPTER 2: Dissecting the regulatory strategies of NFκB RelA target genes in the inflammatory response

Figure 2.1 Identifying NFκB RelA target genes in the TNF response of murine embryonic fibroblasts	38
Figure 2.2 p53 deficiency does not affect TNF-induced gene expression	41
Figure 2.3 A RelA genetic complementation system for studying the control of endogenous NFκB RelA target genes	44
Figure 2.4 Retroviral transduction of RelA in <i>p53<sup>+</sup>crel<sup>-</sup>rela<sup>-</sup></i> MEF provide a suitable complementation system for studying NFκB RelA target genes	46
Figure 2.5 High affinity binding by RelA is required for the TNF-induced expression of all NFκB target genes	50
Figure 2.6 High affinity DNA binding by RelA is required for all TNF-induction of NFκB target genes	52
Figure 2.7 The RelA C-terminal portion is required for TNF induction of all NFκB target genes	57

Figure 2.8 RelA transactivation domains TA1 and TA2 both contribute to the TNF response of NF- $\kappa$ B target genes	59
Figure 2.9 A math model-aided analysis reveals gene-specific requirements for TA1 and TA2	64
Figure 2.10 Generation of a RelA Transactivation Domain mutant knock-in mouse strain	67
Figure 2.11 A knock-in mouse reveals that the dual TAD-requirement pertains to other cell-types and stimuli	68
Figure 2.12 Lack of RelA-TAD-dependence in the transcriptional response of MEFs to TNF or LPS is not due to cRel compensation	72

### CHAPTER 3: Conclusions and Future Directions

Figure 3.1 The RelA TA2 domain functions primarily via intrinsic affinity for CBP/p300	100
--	-----

## LIST OF SUPPLEMENTARY TABLES

*The following items are available as external Excel files.*

Supplementary Table 2.1 List of RelA binding locations and TNF-induced gene expression for 104 NF $\kappa$ B target genes

Supplementary Table 2.2: Gene names and relative expression data plotted in Figure 2.11B for the 37 TNF-responsive genes in wild-type and RelA<sup>TATA</sup> MEFs and BMDMs

Supplementary Table 2.3: Gene names and relative expression data plotted in Figure 2.11B for the 481 LPS-responsive genes in wild-type and RelA<sup>TATA</sup> MEFs and BMDMs

Supplementary Table 2.4: Gene names and percentage of expression data plotted in Figure 2.11C for 37 TNF-responsive genes in RelA<sup>TATA</sup> MEFs and BMDMs

Supplementary Table 2.5: Gene names and percentage of expression data plotted in Figure 2.11C for 481 LPS-responsive genes in RelA<sup>TATA</sup> MEFs and BMDMs

Supplementary Table 2.6: Gene names and relative expression data plotted in Figure 2.11E for the 146 TNF and LPS-responsive genes in wild-type and RelA<sup>TATA</sup> MEFs

Supplementary Table 2.7: Gene names and relative expression data plotted in Figure 2.11E for the 185 TNF and LPS-responsive genes in wild-type and RelA<sup>TATA</sup> BMDMs

Supplementary Table 2.8: Gene names and percentage of expression data plotted in Figure 2.11F for 146 TNF and LPS-responsive genes in RelA<sup>TATA</sup> and *crel*<sup>-/-</sup>RelA<sup>TATA</sup> MEFs

Supplementary Table 2.9: Gene names and percentage of expression data plotted in Figure 2.11F for 185 TNF and LPS-responsive genes in RelA<sup>TATA</sup> BMDMs

Supplementary Table 2.10: Gene names and relative expression data plotted in Figure 2.12A for the 146 TNF and LPS-responsive genes in *crel*<sup>-/-</sup> and *crel*<sup>-/-</sup>RelA<sup>TATA</sup> MEFs



## ACKNOWLEDGEMENTS

Accomplishing this dissertation and enjoying doing scientific research would not have been possible without the contribution and help from many people. I would first like to thank my principal investigator and advisor, Professor Alexander Hoffmann, for his enthusiasm, mentorship, and support throughout these 8 years of graduate study. His great success has had a profound impact on my scientific career. When I started my scientific research career as a soon-to-be college graduate, Alex's enthusiasm and passion for science inspired me to pursue a career in research. Alex has provided an excellent lab environment and resources for all lab members. He has taught me how to think more objectively and write more critically. I really appreciate Alex for his constant encouragement and for giving me the opportunity to mentor undergraduate students and lab assistants. I am very grateful to have had the pleasure of working in his lab in various roles: starting out as an undergraduate volunteer, then becoming a lab assistant and manager for 3 years, and coming back as a graduate student. Thank you for everything.

Special thanks to Professor Gourisankar Ghosh, who is a wonderful scientist and mentor, as a neighboring principal investigator at UCSD. He has so much enthusiasm for science and was a kind, helpful, and encouraging collaborator. His lab members kindly provided help and guidance before and during my first 3 years of graduate study. Jessica Ho and Vivien Ya-Fan Wang were helpful in giving technical advice as well as general advice about graduate school. Dr. Smarajit Polley and Dr. Yidan Li are wonderful friends and were very helpful in providing technical and scientific advice. I am grateful to have worked next to Professor Gourisankar Ghosh's lab.

I want to sincerely thank the other members of my doctoral committee, Professor Arnold J. Berk, Professor Lili Yang, and Professor Siavash K. Kurdistani, for their insightful advices on my project and their expert input on genome-wide sequencing data analysis. Additionally, I want to acknowledge and thank the UCLA Warsaw Fellowship and National Institute of Health (NIH) grants GM117134 and AI12784 for funding support of this dissertation work.

I would especially like to thank all the former and current lab mates in the Signaling Systems Laboratory with whom I've crossed paths, for making this lab a fun place to work. I have so many great memories with this group and have enjoyed being a part of it. Thank you to Dr. Soumen Basak, for teaching me biochemical techniques and how to make effective presentations even before my graduate study. As a key senior lab mate, he shared his extensive knowledge of NF $\kappa$ B signaling, his experience in doing scientific research, and many scientific ideas. Dr. Masataka Asigiri, a visiting scholar from Japan, whom is a knowledgeable immunologist had provided me with so much help in our scientific discussions. Jonathan Almaden, also known as my "big brother" in lab, for supporting and guiding me in my project and life as a graduate student. Eason (Yu-Sheng) Lin, for being in the same program year as me and for allowing me to vent on stressful days. Dr. Jesse Vargas for helpful guidance and feedback on my research proposals. Dr. Roberto Spreafico, for being another wonderful "big brother" in lab. He is a phenomenal scientist, immunologist, and bioinformatician and has taught me how to analyze sequencing data in the R program and how to use UNIX-based terminal commands. A big thank-you to Marie Grossett, Dr. Simon Mitchell, Dr. Marie Metzigg, Dr. Catera Wilder, Dr. Stefanie Luecke, Diane Lefaudeux, Dr. Yi Liu, Emily Chen, and Brian Kim for their friendship, encouragement, and my outlet for frustration. I especially want to thank my

two undergraduate assistants for their help with sequencing analysis, Kensei Kishimoto and Aditya Pimplaskar. They also contributed to the work in Chapter 2 of this dissertation. Diane Lefaudeux, Katherine Sheu, Ning Wang, and Adewunmi Adelaja for technical help in R programming. I also want to thank everyone for their great feedback during sub-group and lab meetings.

I want to thank my friends from neighboring labs on the third floor of Natural science building (NSB) at UCSD from Professor Patricia Jennings' and Professor Partho Ghosh's labs for making the third floor of NSB fun and interactive. DJ Burban, Kendra Hailey, and Kaitlin Fisher from the Jennings lab for their friendship, support, and desserts. Brent Hamaoka from the Partho lab for his technical advice in protein chemistry and for being a great beach volleyball coach.

My utmost gratitude to my family, relatives, and friends for their endless support and understanding. My mom and siblings, for always being supportive and encouraging me to push forward to completion. My dad Thong Viet Ngo and grandpa Morris Wilson who are no longer here but who always believed that I have the talents to succeed. A special thanks to my second family at Tinh Xa Ngoc Dang Buddhist Temple in San Diego, for their support and care. My wonderful friends since grade school, college, and graduate school, for all their unwavering support and friendship. My best friends, Amy Hoang and Loan Tran, for always being great friends and listeners when I need to vent on stressful days.

This dissertation would not have been possible without the people who have contributed directly to the work presented in Chapter 2. Dr. Roberto Spreafico and Dr. Frank (Zhang) Cheng processed sequencing data and helped with some downstream analysis. Jeremy Davis-Turak

helped with the control gene expression analysis comparing WT and p53<sup>-/-</sup> mouse fibroblast cells. Kensei Kishimoto and Aditya Pimplaskar helped with downstream ChIP- and RNA-sequencing analyses and contributed to sequencing results shown in Chapter 2. Emily Chen helped with generating RNA libraries for chromatin-associated RNA-seq experiment; Ning Wang helped with HOMER motif enrichment analysis; Dr. Simon Mitchell and Amy Tam contributed to the mathematical modeling results shown in Chapter 2. Dr. Yi Liu helped with BMDM isolation. Eason Lin helped with documenting the knock-in mutant mice phenotypes. Lastly, Diane Lefaudeux for her teaching and providing her amazing technical advice in R programming.

## VITA

### Education

- 2008 Bachelor of Science, University of California, San Diego
- 2013 Master of Science, University of California, San Diego

### Academic Research Experience

- 2007-2008 Undergraduate Assistant, Signaling Systems Lab, UCSD
- 2008-2010 Lab Assistant III and Manager, Signaling Systems Lab, UCSD
- 2011-2019 Graduate Research, Signaling Systems Lab, UCLA and UCSD

### Industrial Research Experience

- 2010-2011 Research Associate Scientist, Atrium Staffing

### Awards and Fellowships

- 2015 Sidney Rittenberg Award, UCLA, Department of MIMG
- 2017-2018 Warsaw Fellowship, UCLA, Department of MIMG

## PUBLICATIONS

**Ngo KA**, Kishimoto K, Davis-Turak J, Pimplaskar A, Cheng Z, Spreafico R, Chen EYH, Tam A, Mitchell S, Hoffmann A. (2019). Dissecting the Regulatory Strategies of NFkappaB RelA Target Genes in the Inflammatory Response Reveals Differential Logics of Two Transactivation Domains. *Submitted*.

Fortmann KT, Lewis RD, **Ngo KA**, Fagerlund R, Hoffmann A. (2015). A Regulated, Ubiquitin-Independent Degron in I $\kappa$ B $\alpha$ . *J. Mol. Biol.* 427, 2748-2756.

Tsui R, Kearns JD, Lynch C, Vu D, **Ngo KA**, Basak S, Ghosh G, Hoffmann A. (2015). I $\kappa$ B $\beta$  enhances the generation of the low-affinity NF $\kappa$ B/RelA homodimer. *Nat. Commun.* 6: 7068.

Almaden JV, Tsui R, Liu YC, Birnbaum H, Shokhirev MN, **Ngo KA**, Davis-Turak JC, Otero D, Basak S, Rickert RC, Hoffmann A. (2014). A pathway switch directs BAFF signaling to distinct NF $\kappa$ B transcription factors in maturing and proliferating B cells. *Cell Rep.* 9: 2098-2111.

# **CHAPTER 1:**

## **General Introduction**

## **NFκB, IκB, and IKK PROTEIN FAMILIES**






Nuclear Factor kappaB (NFκB) was first discovered as a DNA-binding complex in activated B-cells (Sen and Baltimore, 1986). It was then characterized as a ubiquitously expressed potent transcriptional activator that is activated by a wide range of intracellular and extracellular signals, such as inflammatory cytokines, bacterial pathogens, viruses, environmental stress, genotoxic stress, and developmental inter-cellular signals, to induce the expression of many genes (Baeuerle and Henkel, 1994; Hoffmann et al., 2006; Liu et al., 2017; Stanic et al., 2004; Zhang et al., 2017). NFκB is widely recognized as a master regulator of inflammatory response, but at the same time it is a major transcription factor for both innate and adaptive immune system that controls the transcription of genes involved in many cellular processes such as inflammation, cell survival, cell proliferation, cell differentiation, viral response, and apoptosis. In addition, NFκB signaling is activated by two distinct pathways known as canonical (“classical”) and non-canonical (“alternative”) pathways, which are important for inflammatory gene expression and genes involved in developmental processes, respectively. Improper regulation of NFκB activity has been linked to inflammatory and autoimmune diseases, such as rheumatoid arthritis and Crohn’s disease, septic shock, non-Hodgkin B cell lymphoma, viral infection, and cancer (Hoesel and Schmid, 2013; Liu and Malik, 2006; Monaco and Paleolog, 2004; Nakshatri et al., 1997; Tak and Firestein, 2001; Xia et al., 2014). NFκB transcriptional activity can have important physiological functions and however, pathophysiological functions if not appropriately controlled. Because of its important role in health and disease, NFκB signaling has been a potential therapeutic target in the prevention and


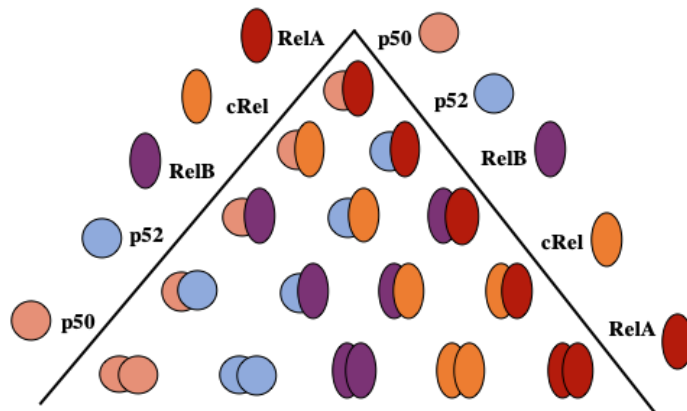


treatment of cancer and human diseases (Greten and Karin, 2004; Gupta et al., 2010; Luo et al., 2005; Monaco and Paleolog, 2004; Roman-Blas and Jimenez, 2006; Sarkar and Li, 2008).

The NF $\kappa$ B family of transcription factors consists of 5 proteins: RelA (also called p65), RelB, cRel, p50, and p52 encoded by RELA, RELB, REL, NFKB1, and NFKB2 genes, respectively. These proteins all share an N-terminal Rel homology region (RHR) that is 300 amino acids long and has three functions: sequence-specific DNA binding, dimerization and inhibitory protein binding (Figure 1.1) (Ghosh et al., 2012, 1998; Siebenlist et al., 1994). These five NF $\kappa$ B subunits can form 15 possible combinations of NF $\kappa$ B dimers through homo- and hetero-dimerization. Following the RHR is a nuclear localization sequence (NLS), and a C-terminal transcription activation domain (TAD) that is unique to RelA, RelB, and cRel proteins. p50 and p52 result from precursor proteins: p105 (NFKB1) and p100 (NFKB2), respectively, through post-translational cleavage of a C-terminal region containing ankyrin repeat domains (ARDs) (Baeuerle and Henkel, 1994; Fan and Maniatis, 1991). Hence, p50 and p52 can act as transcriptional activators when forming heterodimers with Rel-containing members with a C-terminal TAD. On the other hand, p50 and p52 homodimers function as transcriptional repressors due to the lack of TAD (Cramer et al., 1997; Ghosh et al., 1995; Müller et al., 1995). Of all the NF $\kappa$ B dimers, RelA:p50 heterodimer is predominant, and was the first NF $\kappa$ B dimer to be described (Kopp and Ghosh, 1995; Verma et al., 1995). Further, RelA/p65 is ubiquitously expressed and was characterized to contain two transactivation sub-domains that are within its C-terminal TAD; however, cRel-containing dimers are found to be more highly expressed in mature lymphoid cells (Boffa et al., 2003; Köntgen et al., 1995; Tumang et al., 1998).

**A**

Gene	Polypeptide	Length
<i>rela</i>	RelA 	551
<i>crel</i>	cRel 	619
<i>relb</i>	RelB 	557
<i>nfkb1</i>	p50 	433
<i>nfkb2</i>	p52 	447


**B**

**Figure 1.1 NFκB protein family.** (A) Members of NFκB family. Left column: gene symbol, middle column: protein name, right column: the number of amino acids in the human protein. RHR, Rel homology region; TAD, transactivation domain. (B) Five NFκB subunits can form 15 possible different combinations of NFκB dimers through homo- and hetero-dimerization. Adapted from Hoffmann and Baltimore, 2006; O’Dea and Hoffmann, 2009.

Inhibitors of  $\kappa$ B (I $\kappa$ B) are a family of inhibitory proteins that regulate NF $\kappa$ B activity by sequestering NF $\kappa$ B dimers in the cytoplasm of resting cells and releasing them upon signaling input. I $\kappa$ B blocks the nuclear localization of NF $\kappa$ B dimers by blocking their nuclear localization signal (NLS), and regulates DNA-binding of NF $\kappa$ B dimers through the formation of stable I $\kappa$ B:NF $\kappa$ B complexes that inhibit NF $\kappa$ B binding to NF $\kappa$ B-binding sites, called  $\kappa$ B DNA (Baeuerle and Baltimore, 1988; Huxford et al., 1998; Jacobs and Harrison, 1998; Kearns et al., 2006; Nolan et al., 1991; Thanos and Maniatis, 1995; Truhlar et al., 2006; Zabel and Baeuerle, 1990). The I $\kappa$ B family consists of I $\kappa$ B $\alpha$ , I $\kappa$ B $\beta$ , I $\kappa$ B $\epsilon$ , I $\kappa$ B $\delta$ , I $\kappa$ B $\gamma$ , I $\kappa$ B $\xi$ , and Bcl3 that are encoded by NFKBIA, NFKBIB, NFKBIE, NFKB2, NFKB1, NFKBIZ, and BCL3, respectively (Figure 1.2A). Of note, NFKB2 and NFKB1 also encode for NF $\kappa$ B proteins, p52 and p50, respectively. However, the C-terminal containing ARDs in their precursor proteins, p100 and p105, respectively, make them as I $\kappa$ B-like proteins. Hence, p100 and p105 homodimers, I $\kappa$ B $\delta$  and I $\kappa$ B $\gamma$ , respectively, can bind to NF $\kappa$ B dimers and inhibit their translocation into the nucleus. The C-terminal region of I $\kappa$ B proteins contain ARDs, which is the hallmark of the I $\kappa$ B proteins. The ARDs of I $\kappa$ Bs associate with the RHR of NF $\kappa$ B dimers to form the I $\kappa$ B:NF $\kappa$ B complex (Huxford et al., 1998; Jacobs and Harrison, 1998; Malek et al., 2003). I $\kappa$ B proteins also have other functional domains, such as the signal response domain (SRD) in the N-terminus or C-terminus. I $\kappa$ B $\alpha$  and I $\kappa$ B $\beta$  additionally contain an acidic carboxy-terminal region that is rich in the amino acids proline (P), glutamic acid (E), serine (S), and threonine (T), known as the PEST-like region, in which is required for inhibiting NF $\kappa$ B binding to DNA (Ernst et al., 1995). However, I $\kappa$ B $\beta$  has an additional essential and positive function, which is to stabilize the low




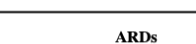



affinity RelA:RelA homodimer. Also, it may be considered a bona fide chaperone for the RelA:RelA homodimer formation (Tsui et al., 2015). Furthermore, classical I $\kappa$ Bs (I $\kappa$ B $\alpha$ , I $\kappa$ B $\beta$ , I $\kappa$ B $\epsilon$ ) and I $\kappa$ B $\delta$ , and I $\kappa$ B $\gamma$  are primarily found in the cytoplasm, which inhibit nuclear NF $\kappa$ B activity by masking their nuclear localization signals (NLS) and by interfering with the capacity of NF $\kappa$ B to bind to DNA (Baeuerle and Baltimore, 1988; Huxford et al., 1998; Jacobs and Harrison, 1998; Nolan et al., 1991; Zabel and Baeuerle, 1990). Importantly, these I $\kappa$ B promoter regions contain NF $\kappa$ B binding sites that positively regulate the expression of the I $\kappa$ Bs; hence, I $\kappa$ Bs are target genes of NF $\kappa$ B and their expression is important for the negative feedback control of NF $\kappa$ B activity (Hoffmann et al., 2002, 2006). The atypical I $\kappa$ B-like proteins (Bcl3, and I $\kappa$ B $\xi$ ) are found primarily in the nucleus where they are strongly induced after NF $\kappa$ B activation and modulate NF $\kappa$ B activity both positively and negatively depending on the target genes (Muta, 2006; Muta et al., 2003; Trinh et al., 2008; Zhang et al., 1994).

An essential component in the activation of NF $\kappa$ B signaling pathway is the I $\kappa$ B kinase (IKK) complex that is the gatekeeper for NF $\kappa$ B activation because IKK protein complex mediates the signaling-dependent degradation of I $\kappa$ B proteins in which frees NF $\kappa$ B to translocate into the nucleus and activate gene transcription (Israel, 2010; Rushe et al., 2008; Yamaoka et al., 1998; DiDonato et al., 1997; Mercurio et al., 1997; Zandi et al., 1997; Malinin et al., 1997). Structural studies have provided protein structural information on the IKK complexes which were shown to form a multimeric complex with NF $\kappa$ B and I $\kappa$ B. In the canonical or “classical” NF $\kappa$ B pathway, IKK complex contains two kinase subunits, IKK $\alpha$  (or IKK1) and IKK $\beta$  (or IKK2), and a non-catalytic subunit, NF $\kappa$ B essential modulator (NEMO or IKK $\gamma$ ). IKK $\alpha$  and


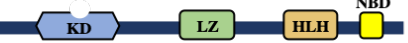


IKK $\beta$  are structurally similar in that both proteins contain an amino-terminal kinase domain and two protein-protein interaction motifs in their carboxyl terminus, called the leucine zipper (LZ) and helix-loop-helix domain (HLH) (Figure 1.2B). Another important domain within C-terminal portion of IKK $\alpha$  and IKK $\beta$  proteins is a NEMO binding domain (NBD) that allows the IKK complex formation. NEMO protein does not harbor any kinase domain or enzymatic activity, but instead it acts as an adapter protein. NEMO contains two coiled-coil domains (CC1/2), a leucine zipper domain, and a zinc finger domain. The N-terminal CC1 region of NEMO interacts with the IKK C-terminal kinase tails and the CC2-LZ domains mediate oligomerization and polyubiquitin binding, key features that govern NEMO function (Grubisha et al., 2010). NEMO is essential for the activation of the IKK complex in the canonical NF $\kappa$ B signaling pathway. Deficiency in these IKK proteins have been shown to cause developmental defects in neurulation and liver degeneration in mice (Li et al., 2000; Rudolph et al., 2000). When activated, IKK $\alpha$  and IKK $\beta$  directly phosphorylate I $\kappa$ Bs at their signal response domain (SRD), triggering ubiquitination and rapid degradation of the inhibitors by the 26S proteasome. This process releases the NF $\kappa$ B dimer, which then stably translocates to the nucleus and activates expression of many genes. On the other hand, NF $\kappa$ B-inducing kinase (NIK) is required for the activation of the “alternative” or non-canonical NF $\kappa$ B pathway where NIK has been shown to only phosphorylate IKK $\alpha$ , and not IKK $\beta$  *in vitro* (Ling et al., 1998; Malinin et al., 1997; Régnier et al., 1997; Xiao et al., 2001). Of note, MAP3K14 is the gene encoding NIK because it was first identified as a mitogen-activated protein (MAP) kinase kinase kinase (MAP3K) related kinase due to its homology with other MAP3Ks in its enzymatic domain (Malinin et al., 1997). In response to a developmental stimulus, activated NIK phosphorylates and activates IKK $\alpha$  through

its C-terminal kinase domain. Also, a unique molecular component of NIK is in its carboxyl region called the TRAF2-binding domain (TBD), in which it allows its association to the TRAF2 adaptor protein for its stabilization in NF $\kappa$ B activation (Song et al., 1997).

**A**

Gene	Polypeptide	Length
<i>nfkbia</i>	I $\kappa$ B $\alpha$ 	317
<i>nfkbib</i>	I $\kappa$ B $\beta$ 	356
<i>nfkbie</i>	I $\kappa$ B $\epsilon$ 	361
<i>nfkbl</i>	I $\kappa$ B $\gamma$ p105 	539
<i>nfkbl2</i>	I $\kappa$ B $\delta$ p100 	484
<i>nfkblz</i>	I $\kappa$ B $\zeta$ 	718
<i>bcl3</i>	Bcl3 	454

**B**

Gene	Polypeptide	Length
<i>ikbka</i>	IKK $\alpha$ 	745
<i>ikbbb</i>	IKK $\beta$ 	756
<i>ikbkg</i>	NEMO (IKK $\gamma$ ) 	419
<i>map3k14</i>	NIK 	947

**Figure 1.2 I $\kappa$ B and IKK protein families.** Members of the (A) I $\kappa$ B and (B) IKK families. Left column: gene symbol, middle column: protein name, right column: number of amino acids in each human protein. RHR, Rel homology region; SRD, signal response domain; ARDs, ankyrin repeat domains; DD, death domain; PEST, proline, glutamic acid, serine, and threonine rich-like region; KD, kinase domain; LZ, leucine zipper domain; HLH, helix-loop-helix domain; CC1/2, coiled-coil domains; Z; zinc finger domain; NBD, NEMO-binding domain; BR, basic region; PRR, proline rich region; TBD: TRAF binding domain. These schematics are adapted from Hayden and Ghosh, 2008; Malinin et al., 1997; O’Dea and Hoffmann, 2009; Régnier et al., 1997; Thu and Richmond, 2010.

## NFκB SIGNALING SYSTEM

NFκB dimers can be activated through two different pathways referred to as the canonical and non-canonical NFκB signaling pathways (Hayden and Ghosh, 2008; O’Dea and Hoffmann, 2009; Pomerantz and Baltimore, 2002). These pathways differ in respect of inducers, activating kinases, and specific IκB and NFκB molecules involved (Figure 1.3). Genes activated by the canonical pathway are activated rapidly and are generally involved in inflammation, whereas the genes induced by the non-canonical pathway are generally important for developmental programs (Pomerantz and Baltimore, 2002; Sun, 2011).

### *The canonical NFκB pathway*

Activation of the canonical or “classical” NFκB signaling pathway is triggered by a variety of inflammatory and pathogen-derived signals, and through receptors like members of the TNF receptor (TNFR) super-family, Toll-like receptors (TLRs), Interleukin receptors, antigen of B and T cells. Signaling through these results in the innate immune and inflammatory response (Figure 1.3A). The downstream signaling complex that is activated is a trimeric IKK complex of the catalytic subunits IKKα, IKKβ, and the regulatory subunit NEMO. Although NFκB activation is regulated/prevented by the three prototypical inhibitors, IκBα, IκBβ, and IκBε (Baeuerle, 1998; Huxford et al., 1998; Jacobs and Harrison, 1998; Kearns et al., 2006; Malek et al., 2003); IκBα is the key regulator of the dynamics of NFκB activity in the canonical pathway because deficiency in IκBα in mice was shown to exhibit neonatal lethality due to elevated NFκB activity (Beg et al., 1995). The primary NFκB dimers that are activated are RelA and cRel-containing homo- and hetero-dimers. In response to a stimulus, IκBs are phosphorylated by

the NEMO/IKK complex, particularly by IKK $\alpha$  and IKK $\beta$ , leading to subsequent ubiquitination and proteasomal degradation (Ghosh et al., 1998). I $\kappa$ B degradation frees NF $\kappa$ B to translocate to the nucleus and bind DNA which then activates transcription of numerous of target genes. While the activation of the canonical NF $\kappa$ B pathway is essential for eliciting the inflammatory response, prolonged NF $\kappa$ B activity is detrimental, for example, causing chronic inflammation (Tak and Firestein, 2001). Hence, a second important molecular event in the canonical NF $\kappa$ B signaling is the inducible synthesis and activation of the I $\kappa$ Bs which results in a post-induction repression of the NF $\kappa$ B response, referred to as the negative feedback control of NF $\kappa$ B activity (Hoffmann et al., 2002).

#### *The non-canonical NF $\kappa$ B pathway*

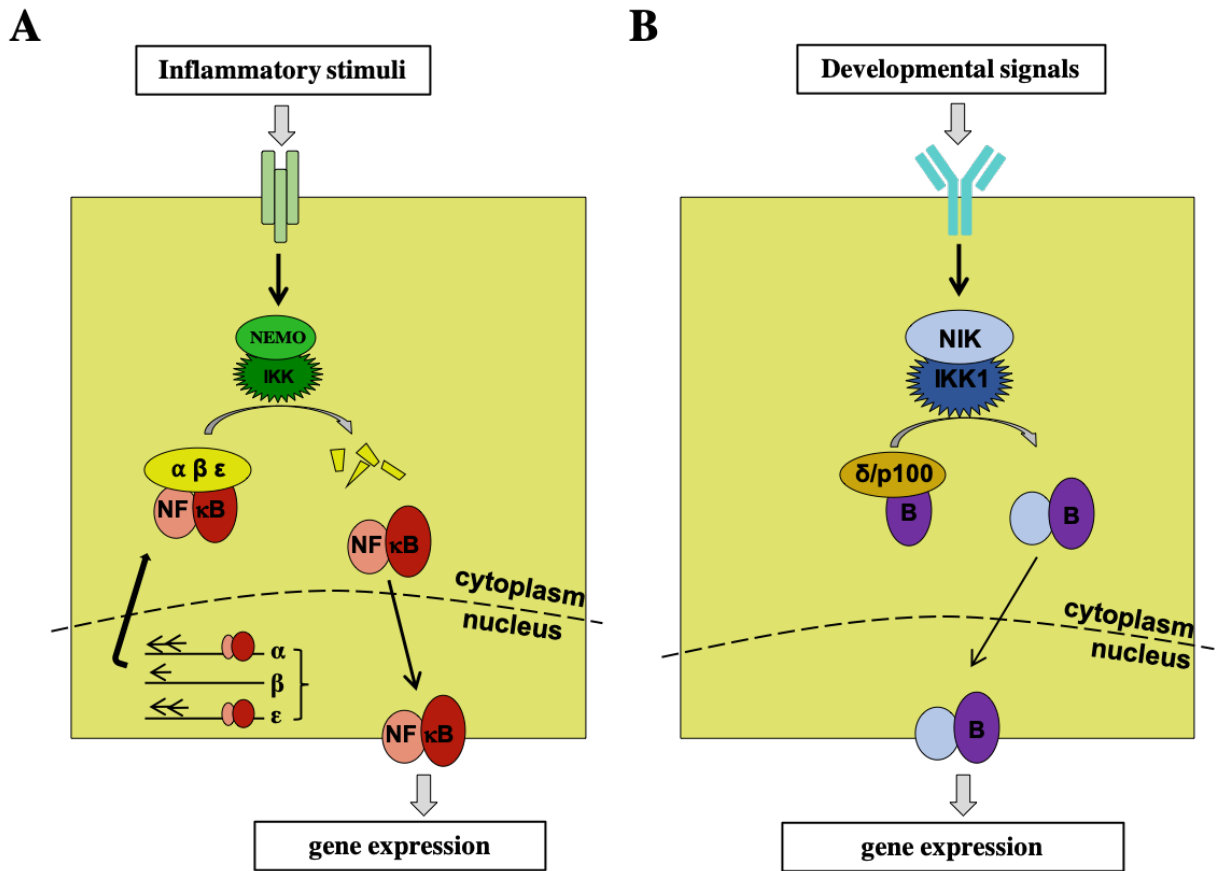
In contrast to the canonical NF $\kappa$ B signaling pathway, activation of the non-canonical or “alternative” NF $\kappa$ B signaling pathway occurs in response to developmental processes that are induced through Lymphotoxin  $\beta$  receptor (LT $\beta$ R), RANK, BAFFR, CD40, and CD27 signaling (Sun, 2011); (Figure 1.3B). Mice deficient in molecular components of the non-canonical NF $\kappa$ B signaling pathway - RELB<sup>-/-</sup>, NF $\kappa$ B2<sup>-/-</sup>, NIK<sup>-/-</sup> - showed defective LT $\beta$ R-induced NF $\kappa$ B transcriptional activity, abnormalities in lymphoid tissue development and antibody responses, and defective Peyer’s Patch tissue development (Weih and Caamaño, 2003; Yilmaz, 2003; Yin et al., 2001). The activation mechanism does not occur through NEMO activity but requires the activity of NF $\kappa$ B-inducing kinase (NIK). Activation of NF $\kappa$ B via the non-canonical pathway involves NIK- and IKK $\alpha$ -dependent phosphorylation of p100 associated with RelB. This induces



the proteolytic processing of p100 to generate the NFκB family member p52 (Coope et al., 2002; Senftleben et al., 2001; Xiao et al., 2001). This then allows the formation of the p52: RelB heterodimer (Sun, 2011), which activates gene expression. Activated non-canonical NFκB signaling results in more sustained signaling where the kinetics involve a slow build-up and long-lasting activity, as opposed to the more transient canonical NFκB signaling pathway.

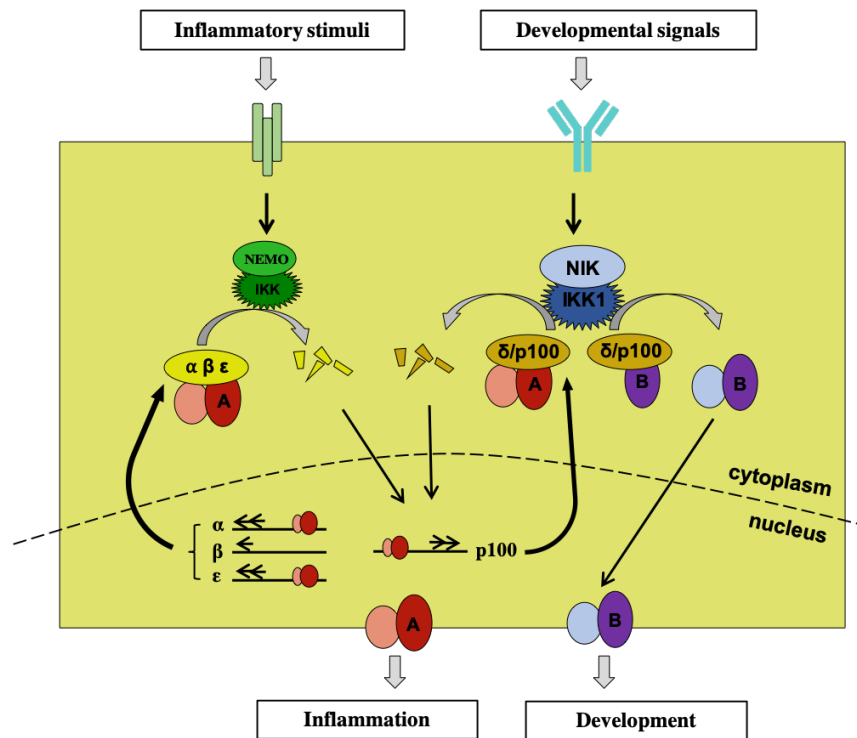
#### *Crosstalk between canonical and non-canonical pathways*

Because activation of the canonical pathway is generally associated with inflammation while activation of non-canonical pathway is mostly associated with developmental signals, these pathways are presumed to transduce signals independently and elicit distinct physiological functions. However, NFκB RelA:p50 dimers can be activated in response to both inflammatory and developmental stimuli via crosstalk signaling between NFκB signaling pathways (Basak and Hoffmann, 2008; Basak et al., 2007; Shih et al., 2011, 2012). This allows the diverse biological functions of NFκB to be adapted to the cell type and context (Figure 1.4). An example of the cross-talk signaling between canonical and non-canonical NFκB signaling pathways is LTβR signaling, in which it is critical for lymphoid organogenesis. LTβR signaling was shown to regulate primary lymphoid development and maturation (B and T lymphocytes), secondary lymphoid development (spleen, lymph nodes, and Peyer's patch), and their microenvironment for antigen recognition (Fütterer et al., 1998; Rennert et al., 1998; Weih and Caamaño, 2003). However, LTβR signaling is not sufficient for lymphoid architecture, but TNFR signaling is also required as inhibition of TNFR signaling during LTβR signaling resulted in a lack of lymph node formation (Rennert et al., 1998).



**Figure 1.3 Two NFκB signaling pathways.** (A) Canonical or “classical” NFκB signaling pathway. Canonical NFκB signaling involves NEMO-dependent IKK complex, prototypical IκBs (IκBα, IκBβ, and IκBε), and NFκB RelA and cRel-containing homo- and heterodimers that are activated in response to inflammatory cytokines and pathogens. (B) Non-canonical or “alternative” NFκB signaling pathway. Non-canonical NFκB signaling is induced in response to developmental stimuli and involves the activation of NIK/IKKα complex and p100 proteasomal processing to p52, resulting in NFκB p52:RelB dimers.

Furthermore, Basak *et al.* reported that activation of LT $\beta$ R signaling in murine embryonic fibroblast (MEF) cells resulted in NF $\kappa$ B DNA binding activity by both pre-existing RelA:p50 and RelB:p50 dimers and a late-induced RelB:p52 dimer. Surprisingly, RelA:p50 was not associated with classical NF $\kappa$ B-I $\kappa$ B complex, but bound to the p100 homodimer/I $\kappa$ B $\delta$ . LT $\beta$ R signaling induces I $\kappa$ B $\delta$  degradation through the non-canonical signaling via NIK and IKK $\alpha$  (Basak *et al.*, 2007). In TNF-primed MEF cells, Basak *et al.* found elevated I $\kappa$ B $\delta$ -NF $\kappa$ B complexes, suggesting a cross-talk mechanism that controls canonical and non-canonical I $\kappa$ B proteins and NF $\kappa$ B signaling.



**Figure 1.4 Cross-talk in NF $\kappa$ B pathways.** Cross-talk mechanism between canonical and non-canonical NF $\kappa$ B signaling pathways for NF $\kappa$ B activation. Adapted from Basak and Hoffmann, 2008; Basak *et al.*, 2007; Shih *et al.*, 2011.

### *Regulation of NFκB activity for immune homeostasis*

Tight regulation of NFκB activity is important for immune homeostasis due to the broad range of genes that NFκB can activate. Dysregulation or misregulation of NFκB transcriptional activity has been implicated in many human malignancies and cancers (Baldwin, 2001). Use of genetic knockouts in NFκB:IκB:IKK signaling components have shown the importance of the NFκB signaling pathways in regulating many biological functions, such as inflammatory responses, lymphoid organogenesis, B-cell survival and maturation, dendritic cell activation, and bone metabolism (Baeuerle, 1998; Xiao et al., 2001). However, aberrant NFκB activity is a hallmark feature of several inflammatory diseases, such as arthritis, Crohn's disease, and atherosclerosis (Bourcier et al., 1997; Brand et al., 1997; Tak and Firestein, 2001) which makes it a therapeutic target for treatments of inflammation. Hence, in healthy condition, NFκB activity is usually transient to mediate a cellular response and is then inactivated by newly synthesized IκB proteins that bind to NFκB dimers and export them back out to the cytoplasm. This negative feedback control of NFκB is important to ensure that NFκB signaling is turned on only when necessary for biological functions and is then properly regulated for immune homeostasis.

### **DNA RECOGNITION BY NFκB DIMERS**

Upon translocation into the nucleus, the NFκB complex binds to sequence-specific DNA known as the “κB sites” on target genes. The contact of both NFκB subunits with the DNA is required for DNA binding and transcriptional activation (Chen et al., 1998b; Kunsch et al., 1992). Structural and functional studies of NFκB-DNA complexes have demonstrated that

NFκB dimers bind to a variety of κB sites where NFκB recognizes 9 to 11 base pairs κB DNA elements of the sequence: 5'-GGGRNNNNYCC-3', where R = A or G; N = any nucleotide (A, C, G, or T); Y = C or T (Chen and Ghosh, 1999; Chen et al., 1998b, 2000; Fujita et al., 1992; Ghosh et al., 1995; Kunsch et al., 1992; Müller et al., 1995; Udalova et al., 2000; Zabel et al., 1991). Additionally, crystal structures of NFκB dimers in active DNA-bound state have revealed how each subunit of NFκB contacts each half-site of the full κB DNA sequence (Chen et al., 1998a, 2000; Huxford et al., 1998; Jacobs and Harrison, 1998). These studies highlight the plasticity of NFκB dimers in recognizing κB site sequences with a single half-site in κB DNA sequences. Each NFκB dimer has distinct binding specificities to κB site sequences that influence the selective regulation of NFκB target genes (Siggers et al., 2012). Siggers et al. have performed a comprehensive unbiased characterization of DNA binding by eight different NFκB dimers using protein-binding microarrays (PBMs)-determined z scores. Their work further separates NFκB dimers into three distinct DNA-binding classes: p50 and p52 homodimer preferentially bind to 11 or 12 bp sites; NFκB heterodimers preferentially bind to 10 bp sites; and cRel or RelA homodimers preferentially bind to 9 bp sites.

Structural studies of NFκB have shown that native NFκB from nuclear extracts occurs in a protein complex of more than 200 kDa, significantly higher than the total combined mass of the reconstituted purified p50 and RelA proteins (115 kDa) (Urban et al., 1991). This suggests that gene regulation by NFκB is more complex as it may act together with a variety of other chromatin-associated factors (Kim et al., 2012; Mukherjee et al., 2013; Ohmori and Hamilton, 1993; Wan and Lenardo, 2009; Zhong et al., 1998). A prominent study indicated the potential for

the DNA-binding domain (DBD) within the N-terminal RHR of NFκB RelA to recruit either histone deacetylase 1 (HDAC1) or histone acetyl transferase CBP/p300 co-activator depending on the phosphorylation status of S276 in RelA (Zhong et al., 2002). Further, recent studies indicated that recruitment to endogenous NFκB targets may be mediated by CBP interacting with the NFκB RelA C-terminal TAD (Lecoq et al., 2017; Mukherjee et al., 2013), suggesting the involvement of cofactors in NFκB-dependent transcription of target genes. Other NFκB cofactors that have been reported to interact with NFκB dimers at gene regulatory regions to mediate gene expression are E2F1 (Lim et al., 2007), FOXM1 (Zhao et al., 2014), and RPS3 (Mulero et al., 2018; Wan et al., 2007).

## **NFκB TRANSACTIVATION**

Transcriptional activation by NFκB occurs in the C-terminal TAD found in NFκB Rel-containing subunits: RelA, RelB, and cRel (Figure 1.1A). As mentioned above, NFκB p50 and p52 members can only act as transcriptional activators when forming heterodimers with Rel-containing members due to their lack in C-terminal TAD. NFκB transactivation can influence the chromatin state through recruitment of chromatin modifying co-activators and repressors (i.e CBP/p300 and HDAC1, respectively). One of the mechanisms that could regulate this selective interaction with NFκB co-factors is the specific post-translational modification (PTM), such as phosphorylation, of NFκB proteins (Zhong et al., 2002). A substantial literature has addressed the identification and potential role of post-translational modifications of NFκB subunits, reviewed in Huang et al., 2010; Perkins, 2006. A prominent study demonstrated the importance

of RelA S276 phosphorylation in mediating CBP/p300 co-activator for NFκB-dependent transcriptional activity as introduction of S276A or S276E mutations showed complex mouse phenotypes and transcriptional defects (Dong et al., 2008). Further, S276 phosphorylation of RelA can regulate RelA acetylation that involves CBP/p300. Phosphorylation of RelA at S276 was shown to promote its acetylation at K310 which enhances transcriptional activity (Chen et al., 2005). Further, acetylation of RelA at K314 was reported to be important for late NFκB-dependent gene expression (Rothgiesser et al., 2010). Such post-translational modifications of NFκB RelA were reported to alter interactions with transcriptional cofactors and regulate NFκB transcriptional activity either by enhancing or repressing NFκB activity, some examples in the regulation of NFκB activity.

## **FOCUS OF STUDY**

Whereas many studies of inflammatory signaling have led to a good understanding of how nuclear NFκB activity is regulated, many questions about how nuclear NFκB selects its target genes and produces gene-specific expression remain to be investigated. Prior structure-function studies of the NFκB RelA subunit identified the domain structure and key amino acid residues in biochemical and transient transfection assays (Figure 1.5). However, numerous reports show that in the native chromatin context gene regulation by NFκB is more complex, as it may collaborate with a variety of other chromatin-associated factors.

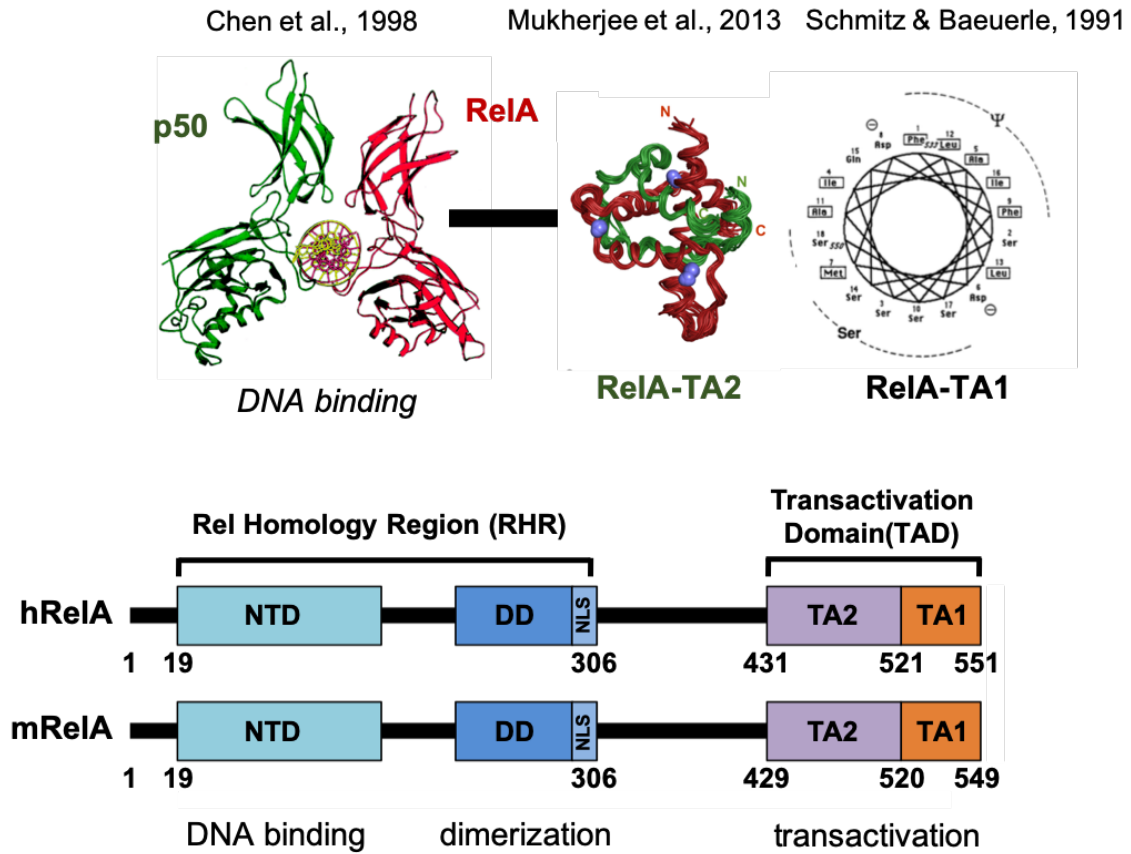
The NFκB RelA (or p65) subunit has been extensively studied because it is known for the strong transcription activating potential of NFκB (Schmitz and Baeuerle, 1991). Indeed,

NFκB RelA is considered the central regulator of inflammation, capable of fast, protein-synthesis-independent activation of gene expression within minutes (Hayden and Ghosh, 2008). The signaling mechanisms involved in regulation of NFκB RelA activity have been elucidated in detail, allowing for the remarkably precise recapitulation of experimental data with mathematical models of the network (Mitchell et al., 2016; Basak et al., 2012). As such, we have focused on RelA to dissect the regulatory strategies of inflammatory response genes that are targets of NFκB RelA.

Aside from containing a conserved amino-terminal RHR, previous reports have identified RelA to have at least two TADs (Moore et al., 1993; Schmitz and Baeuerle, 1991). Transactivation sub-domain 1 (TA1) consist of the most C-terminal 30 amino acids, while Transactivation sub-domain 2 (TA2) is directly adjacent to TA1. It was initially thought that TA1 is the principal transactivation domain for RelA transcriptional activity because structural features of the TA1 domain are highly conserved across species, and because TA1 was shown to be sufficient for inducing transcriptional activity (Schmitz and Baeuerle, 1991). However, when deleting TA1, Schmitz and Baeuerle showed that the unique C-terminal third of RelA contained at least one other distinct activation domain that is directly adjacent to TA1 (Schmitz and Baeuerle, 1991).

In Chapter 2 of this dissertation, I addressed the questions of how NFκB selects target gene binding and by which mechanisms it activates transcription of endogenous target genes. I have established a genetic complementation system for RelA variants to probe their regulatory strategies in the inflammatory response. In this model system, I examined the NFκB transcriptional response to an inflammatory stimulus called tumor necrosis factor (TNF).





**Figure 1.5 RelA modular domain structures.** NF $\kappa$ B RelA functional domain structures were identified from biochemical and exogenous reporter gene assays. RelA N-terminus was identified to contain a DNA-binding domain that binds directly to target gene DNA at  $\kappa$ B sites. RelA C-terminal region was identified to possess transactivation function from its two transactivation sub-domains, TA2 and TA1. The structural domain features were identified through *in vitro* and transient gene reporter studies (Chen et al., 1998; Mukherjee et al., 2013; Schmitz and Baeuerle, 1991) that led to the identification of RelA protein functional domains shown in the schematics for human (hRelA) and mouse (mRelA) RelA protein in amino acid sequences.

## REFERENCES

- Baeuerle, P.A. (1998). I $\kappa$ B–NF- $\kappa$ B Structures: At the Interface of Inflammation Control. *Cell* 95, 729–731.
- Baeuerle, P.A., and Baltimore, D. (1988). I kappa B: a specific inhibitor of the NF-kappa B transcription factor. *Science* 242, 540–546.
- Baeuerle, P.A., and Henkel, T. (1994). Function and Activation of NF-kappaB in the Immune System. *Annu. Rev. Immunol.* 12, 141–179.
- Baldwin, A.S. (2001). Series Introduction: The transcription factor NF- $\kappa$ B and human disease. *J. Clin. Invest.* 107, 3–6.
- Basak, S., and Hoffmann, A. (2008). Crosstalk via the NF-kappaB signaling system. *Cytokine Growth Factor Rev.* 19, 187–197.
- Basak, S., Kim, H., Kearns, J.D., Tergaonkar, V., O’Dea, E., Werner, S.L., Benedict, C.A., Ware, C.F., Ghosh, G., Verma, I.M., et al. (2007). A Fourth I $\kappa$ B Protein within the NF- $\kappa$ B Signaling Module. *Cell* 128, 369–381.
- Basak, S., Behar, M., and Hoffmann, A. (2012). Lessons from mathematically modeling the NF- $\kappa$ B pathway: Mathematical modeling the NF- $\kappa$ B pathway. *Immunol. Rev.* 246, 221–238.
- Beg, A.A., Sha, W.C., Bronson, R.T., and Baltimore, D. (1995). Constitutive NF-kappa B activation, enhanced granulopoiesis, and neonatal lethality in I kappa B alpha-deficient mice. *Genes Dev.* 9, 2736–2746.
- Boffa, D.J., Feng, B., Sharma, V., Dematteo, R., Miller, G., Suthanthiran, M., Nunez, R., and Liou, H.-C. (2003). Selective loss of c-Rel compromises dendritic cell activation of T lymphocytes. *Cell. Immunol.* 222, 105–115.
- Bourcier, T., Sukhova, G., and Libby, P. (1997). The nuclear factor kappa-B signaling pathway participates in dysregulation of vascular smooth muscle cells in vitro and in human atherosclerosis. *J. Biol. Chem.* 272, 15817–15824.
- Brand, K., Page, S., Walli, A.K., Neumeier, D., and Baeuerle, P.A. (1997). Role of nuclear factor-kappa B in atherogenesis. *Exp. Physiol.* 82, 297–304.
- Chen, F.E., and Ghosh, G. (1999). Regulation of DNA binding by Rel/NF-kappaB transcription factors: structural views. *Oncogene* 18, 6845–6852.
- Chen, F.E., Huang, D.-B., Chen, Y.-Q., and Ghosh, G. (1998a). Crystal structure of p50/p65 heterodimer of transcription factor NF- $\kappa$ B bound to DNA. *Nature* 391, 410–413.

- Chen, L.-F., Williams, S.A., Mu, Y., Nakano, H., Duerr, J.M., Buckbinder, L., and Greene, W.C. (2005). NF- $\kappa$ B RelA Phosphorylation Regulates RelA Acetylation. *Mol. Cell. Biol.* 25, 7966–7975.
- Chen, Y.-Q., Ghosh, S., and Ghosh, G. (1998b). A novel DNA recognition mode by the NF- $\kappa$ B p65 homodimer. *Nat. Struct. Mol. Biol.* 5, 67–73.
- Chen, Y.-Q., Sengchanthalangsy, L.L., Hackett, A., and Ghosh, G. (2000). NF- $\kappa$ B p65 (RelA) homodimer uses distinct mechanisms to recognize DNA targets. *Structure* 8, 419–428.
- Coope, H. j., Atkinson, P. g. p., Huhse, B., Belich, M., Janzen, J., Holman, M. j., Klaus, G. g. b., Johnston, L. h., and Ley, S. c. (2002). CD40 regulates the processing of NF- $\kappa$ B2 p100 to p52. *EMBO J.* 21, 5375–5385.
- Cramer, P., Larson, C.J., Verdine, G.L., and Müller, C.W. (1997). Structure of the human NF-kappaB p52 homodimer-DNA complex at 2.1 Å resolution. *EMBO J.* 16, 7078–7090.
- DiDonato, J.A., Hayakawa, M., Rothwarf, D.M., Zandi, E., and Karin, M. (1997). A cytokine-responsive I $\kappa$ B kinase that activates the transcription factor NF- $\kappa$ B. 388, 7.
- Dong, J., Jimi, E., Zhong, H., Hayden, M.S., and Ghosh, S. (2008). Repression of gene expression by unphosphorylated NF- $\kappa$ B p65 through epigenetic mechanisms. *Genes Dev.* 22, 1159–1173.
- Ernst, M.K., Dunn, L.L., and Rice, N.R. (1995). The PEST-like sequence of I kappa B alpha is responsible for inhibition of DNA binding but not for cytoplasmic retention of c-Rel or RelA homodimers. *Mol. Cell. Biol.* 15, 872–882.
- Fan, C.-M., and Maniatis, T. (1991). Generation of p50 subunit of NF- $\kappa$ B by processing of p105 through an ATP-dependent pathway. *Nature* 354, 395.
- Fujita, T., Nolan, G.P., Ghosh, S., and Baltimore, D. (1992). Independent modes of transcriptional activation by the p50 and p65 subunits of NF-kappa B. *Genes Dev.* 6, 775–787.
- Fütterer, A., Mink, K., Luz, A., Kosco-Vilbois, M.H., and Pfeffer, K. (1998). The lymphotoxin beta receptor controls organogenesis and affinity maturation in peripheral lymphoid tissues. *Immunity* 9, 59–70.
- Ghosh, G., Duyne, G.V., Ghosh, S., and Sigler, P.B. (1995). Structure of NF- $\kappa$ B p50 homodimer bound to a  $\kappa$ B site. *Nature* 373, 303–310.
- Ghosh, G., Ya-Fan Wang, V., Huang, D.-B., and Fusco, A. (2012). NF- $\kappa$ B Regulation: Lessons from Structures. *Immunol. Rev.* 246, 36–58.
- Ghosh, S., May, M.J., and Kopp, E.B. (1998). NF- $\kappa$ B AND REL PROTEINS: Evolutionarily Conserved Mediators of Immune Responses. *Annu. Rev. Immunol.* 16, 225–260.

- Greten, F.R., and Karin, M. (2004). The IKK/NF- $\kappa$ B activation pathway—a target for prevention and treatment of cancer. *Cancer Lett.* 206, 193–199.
- Grubisha, O., Kaminska, M., Duquerroy, S., Fontan, E., Cordier, F., Haouz, A., Raynal, B., Chiaravalli, J., Delepierre, M., Israël, A., et al. (2010). DARPIn-assisted crystallography of the CC2-LZ domain of NEMO reveals a coupling between dimerization and ubiquitin binding. *J. Mol. Biol.* 395, 89–104.
- Gupta, S.C., Sundaram, C., Reuter, S., and Aggarwal, B.B. (2010). Inhibiting NF- $\kappa$ B Activation by Small Molecules As a Therapeutic Strategy. *Biochim. Biophys. Acta* 1799, 775–787.
- Hayden, M.S., and Ghosh, S. (2008). Shared Principles in NF- $\kappa$ B Signaling. *Cell* 132, 344–362.
- Hoesel, B., and Schmid, J.A. (2013). The complexity of NF- $\kappa$ B signaling in inflammation and cancer. *Mol. Cancer* 12, 86.
- Hoffmann, A., and Baltimore, D. (2006). Circuitry of nuclear factor  $\kappa$ B signaling. *Immunol. Rev.* 210, 171–186.
- Hoffmann, A., Levchenko, A., Scott, M.L., and Baltimore, D. (2002). The I $\kappa$ B-NF- $\kappa$ B Signaling Module: Temporal Control and Selective Gene Activation. *Science* 298, 1241–1245.
- Hoffmann, A., Natoli, G., and Ghosh, G. (2006). Transcriptional regulation via the NF-kappaB signaling module. *Oncogene* 25, 6706–6716.
- Huang, B., Yang, X.-D., Lamb, A., and Chen, L.-F. (2010). Posttranslational modifications of NF- $\kappa$ B: Another layer of regulation for NF- $\kappa$ B signaling pathway. *Cell. Signal.* 22, 1282–1290.
- Huxford, T., Huang, D.-B., Malek, S., and Ghosh, G. (1998). The Crystal Structure of the I $\kappa$ B $\alpha$ /NF- $\kappa$ B Complex Reveals Mechanisms of NF- $\kappa$ B Inactivation. *Cell* 95, 759–770.
- Israël, A. (2010). The IKK Complex, a Central Regulator of NF- $\kappa$ B Activation. *Cold Spring Harb. Perspect. Biol.* 2.
- Jacobs, M.D., and Harrison, S.C. (1998). Structure of an I $\kappa$ B $\alpha$ /NF- $\kappa$ B Complex. *Cell* 95, 749–758.
- Kearns, J.D., Basak, S., Werner, S.L., Huang, C.S., and Hoffmann, A. (2006). I $\kappa$ B $\epsilon$  provides negative feedback to control NF- $\kappa$ B oscillations, signaling dynamics, and inflammatory gene expression. *J. Cell Biol.* 173, 659–664.
- Kim, J.-W., Jang, S.-M., Kim, C.-H., An, J.-H., Kang, E.-J., and Choi, K.-H. (2012). New Molecular Bridge between RelA/p65 and NF- $\kappa$ B Target Genes via Histone Acetyltransferase TIP60 Cofactor. *J. Biol. Chem.* 287, 7780–7791.

Köntgen, F., Grumont, R.J., Strasser, A., Metcalf, D., Li, R., Tarlinton, D., and Gerondakis, S. (1995). Mice lacking the c-rel proto-oncogene exhibit defects in lymphocyte proliferation, humoral immunity, and interleukin-2 expression. *Genes Dev.* 9, 1965–1977.

Kopp, E.B., and Ghosh, S. (1995). NF-kappa B and rel proteins in innate immunity. *Adv. Immunol.* 58, 1–27.

Kunsch, C., Ruben, S., and Rosen, C. (1992). Selection of optimal kappa B/Rel DNA-binding motifs: interaction of both subunits of NF-kappa B with DNA is required for transcriptional activation. *Mol Cell Bio* 12, 4412–4421.

Lecoq, L., Raiola, L., Chabot, P.R., Cyr, N., Arseneault, G., Legault, P., and Omichinski, J.G. (2017). Structural characterization of interactions between transactivation domain 1 of the p65 subunit of NF- $\kappa$ B and transcription regulatory factors. *Nucleic Acids Res.* 45, 5564–5576.

Li, Q., Estepa, G., Memet, S., Israel, A., and Verma, I.M. (2000). Complete lack of NF- $\kappa$ B activity in IKK1 and IKK2 double-deficient mice: additional defect in neurulation. *Genes Dev.* 14, 1729–1733.

Lim, C.-A., Yao, F., Wong, J.J.-Y., George, J., Xu, H., Chiu, K.P., Sung, W.-K., Lipovich, L., Vega, V.B., Chen, J., et al. (2007). Genome-wide mapping of RELA(p65) binding identifies E2F1 as a transcriptional activator recruited by NF-kappaB upon TLR4 activation. *Mol. Cell* 27, 622–635.

Ling, L., Cao, Z., and Goeddel, D.V. (1998). NF-kappaB-inducing kinase activates IKK-alpha by phosphorylation of Ser-176. *Proc. Natl. Acad. Sci. U. S. A.* 95, 3792–3797.

Liu, S.F., and Malik, A.B. (2006). NF- $\kappa$ B activation as a pathological mechanism of septic shock and inflammation. *Am. J. Physiol.-Lung Cell. Mol. Physiol.* 290, L622–L645.

Liu, T., Zhang, L., Joo, D., and Sun, S.-C. (2017). NF- $\kappa$ B signaling in inflammation. *Signal Transduct. Target. Ther.* 2, 17023.

Luo, J.-L., Kamata, H., and Karin, M. (2005). IKK/NF- $\kappa$ B signaling: balancing life and death – a new approach to cancer therapy. *J. Clin. Invest.* 115, 2625–2632.

Malek, S., Huang, D.-B., Huxford, T., Ghosh, S., and Ghosh, G. (2003). X-ray Crystal Structure of an I $\kappa$ B $\beta$ -NF- $\kappa$ B p65 Homodimer Complex. *J. Biol. Chem.* 278, 23094–23100.

Malinin, N.L., Boldin, M.P., Kovalenko, A.V., and Wallach, D. (1997). MAP3K-related kinase involved in NF- $\kappa$ B induction by TNF, CD95 and IL-1. *Nature* 385, 540.

Mercurio, F., Zhu, H., Murray, B.W., Shevchenko, A., Bennett, B.L., Li, J. wu, Young, D.B., Barbosa, M., Mann, M., Manning, A., et al. (1997). IKK-1 and IKK-2: Cytokine-Activated I $\kappa$ B Kinases Essential for NF- $\kappa$ B Activation. *Science* 278, 860–866.

- Mitchell, S., Vargas, J., and Hoffmann, A. (2016). Signaling via the NF $\kappa$ B system. *Wiley Interdiscip. Rev. Syst. Biol. Med.* 8, 227–241.
- Monaco, C., and Paleolog, E. (2004). Nuclear factor kappaB: a potential therapeutic target in atherosclerosis and thrombosis. *Cardiovasc. Res.* 61, 671–682.
- Moore, P.A., Ruben, S.M., and Rosen, C.A. (1993). Conservation of transcriptional activation functions of the NF-kappa B p50 and p65 subunits in mammalian cells and *Saccharomyces cerevisiae*. *Mol. Cell. Biol.* 13, 1666–1674.
- Mukherjee, S.P., Behar, M., Birnbaum, H.A., Hoffmann, A., Wright, P.E., and Ghosh, G. (2013). Analysis of the RelA:CBP/p300 Interaction Reveals Its Involvement in NF- $\kappa$ B-Driven Transcription. *PLOS Biol.* 11, e1001647.
- Mulero, M.C., Shahabi, S., Ko, M.S., Schiffer, J.M., Huang, D.-B., Wang, V.Y.-F., Amaro, R.E., Huxford, T., and Ghosh, G. (2018). Protein Cofactors Are Essential for High-Affinity DNA Binding by the Nuclear Factor  $\kappa$ B RelA Subunit. *Biochemistry* 57, 2943–2957.
- Müller, C.W., Rey, F.A., Sodeoka, M., Verdine, G.L., and Harrison, S.C. (1995). Structure of the NF- $\kappa$ B p50 homodimer bound to DNA. *Nature* 373, 311–317.
- Muta, T. (2006). I $\kappa$ B- $\zeta$ : An Inducible Regulator of Nuclear Factor- $\kappa$ B. In *Vitamins & Hormones*, (Academic Press), pp. 301–316.
- Muta, T., Yamazaki, S., Eto, A., Motoyama, M., and Takeshige, K. (2003). IkappaB-zeta, a new anti-inflammatory nuclear protein induced by lipopolysaccharide, is a negative regulator for nuclear factor-kappaB. *J. Endotoxin Res.* 9, 187–191.
- Nakshatri, H., Bhat-Nakshatri, P., Martin, D.A., Goulet, R.J., and Sledge, G.W. (1997). Constitutive activation of NF-kappaB during progression of breast cancer to hormone-independent growth. *Mol. Cell. Biol.* 17, 3629–3639.
- Nolan, G.P., Ghosh, S., Liou, H.-C., Tempst, P., and Baltimore, D. (1991). DNA binding and I $\kappa$ B inhibition of the cloned p65 subunit of NF- $\kappa$ B, a rel-related polypeptide. *Cell* 64, 961–969.
- O’Dea, E., and Hoffmann, A. (2009). NF- $\kappa$ B signaling. *Wiley Interdiscip. Rev. Syst. Biol. Med.* 1, 107–115.
- Ohmori, Y., and Hamilton, T. (1993). Cooperative interaction between interferon (IFN) stimulus response element and kappa B sequence motifs controls IFN gamma- and lipopolysaccharide-stimulated transcription from the murine IP-10 promoter. *J. Biol. Chem.* 268, 6677–6688.
- Perkins, N.D. (2006). Post-translational modifications regulating the activity and function of the nuclear factor kappa B pathway. *Oncogene* 25, 6717–6730.
- Pomerantz, J.L., and Baltimore, D. (2002). Two Pathways to NF- $\kappa$ B. *Mol. Cell* 10, 693–695.

- Régnier, C.H., Song, H.Y., Gao, X., Goeddel, D.V., Cao, Z., and Rothe, M. (1997). Identification and characterization of an IkappaB kinase. *Cell* *90*, 373–383.
- Rennert, P.D., James, D., Mackay, F., Browning, J.L., and Hochman, P.S. (1998). Lymph node genesis is induced by signaling through the lymphotoxin beta receptor. *Immunity* *9*, 71–79.
- Roman-Blas, J.A., and Jimenez, S.A. (2006). NF- $\kappa$ B as a potential therapeutic target in osteoarthritis and rheumatoid arthritis. *Osteoarthritis Cartilage* *14*, 839–848.
- Rothgiesser, K.M., Fey, M., and Hottiger, M.O. (2010). Acetylation of p65 at lysine 314 is important for late NF- $\kappa$ B-dependent gene expression. *BMC Genomics* *11*, 22.
- Rudolph, D., Yeh, W.C., Wakeham, A., Rudolph, B., Nallainathan, D., Potter, J., Elia, A.J., and Mak, T.W. (2000). Severe liver degeneration and lack of NF-kappaB activation in NEMO/IKKgamma-deficient mice. *Genes Dev.* *14*, 854–862.
- Rushe, M., Silvan, L., Bixler, S., Chen, L.L., Cheung, A., Bowes, S., Cuervo, H., Berkowitz, S., Zheng, T., Guckian, K., et al. (2008). Structure of a NEMO/IKK-Associating Domain Reveals Architecture of the Interaction Site. *Structure* *16*, 798–808.
- Sarkar, F.H., and Li, Y. (2008). NF-kappaB: a potential target for cancer chemoprevention and therapy. *Front. Biosci. J. Virtual Libr.* *13*, 2950–2959.
- Schmitz, M.L., and Baeuerle, P.A. (1991). The p65 subunit is responsible for the strong transcription activating potential of NF-kappa B. *EMBO J.* *10*, 3805–3817.
- Sen, R., and Baltimore, D. (1986). Inducibility of  $\kappa$  immunoglobulin enhancer-binding protein NF- $\kappa$ B by a posttranslational mechanism. *Cell* *47*, 921–928.
- Senftleben, U., Cao, Y., Xiao, G., Greten, F.R., Krähn, G., Bonizzi, G., Chen, Y., Hu, Y., Fong, A., Sun, S.C., et al. (2001). Activation by IKKalpha of a second, evolutionary conserved, NF-kappa B signaling pathway. *Science* *293*, 1495–1499.
- Shih, V.F.-S., Tsui, R., Caldwell, A., and Hoffmann, A. (2011). A single NF $\kappa$ B system for both canonical and non-canonical signaling. *Cell Res.* *21*, 86–102.
- Shih, V.F.-S., Davis-Turak, J., Macal, M., Huang, J.Q., Ponomarenko, J., Kearns, J.D., Yu, T., Fagerlund, R., Asagiri, M., Zuniga, E.I., et al. (2012). Control of RelB during dendritic cell activation integrates canonical and noncanonical NF- $\kappa$ B pathways. *Nat. Immunol.* *13*, 1162–1170.
- Siebenlist, U., Franzoso, G., and Brown, K. (1994). Structure, Regulation and Function of NF-kappaB. *Annu. Rev. Cell Biol.* *10*, 405–455.
- Siggers, T., Chang, A.B., Teixeira, A., Wong, D., Williams, K.J., Ahmed, B., Ragoussis, J., Udalova, I.A., Smale, S.T., and Bulyk, M.L. (2011). Principles of dimer-specific gene regulation

revealed by a comprehensive characterization of NF- $\kappa$ B family DNA binding. *Nat. Immunol.* *13*, 95.

Song, H.Y., Régnier, C.H., Kirschning, C.J., Goeddel, D.V., and Rothe, M. (1997). Tumor necrosis factor (TNF)-mediated kinase cascades: Bifurcation of Nuclear Factor- $\kappa$ B and c-jun N-terminal kinase (JNK/SAPK) pathways at TNF receptor-associated factor 2. *Proc. Natl. Acad. Sci.* *94*, 9792–9796.

Stanic, A.K., Bezbradica, J.S., Park, J.-J., Matsuki, N., Mora, A.L., Kaer, L.V., Boothby, M.R., and Joyce, S. (2004). NF- $\kappa$ B Controls Cell Fate Specification, Survival, and Molecular Differentiation of Immunoregulatory Natural T Lymphocytes. *J. Immunol.* *172*, 2265–2273.

Sun, S.-C. (2011). Non-canonical NF- $\kappa$ B signaling pathway. *Cell Res.* *21*, 71–85.

Tak, P.P., and Firestein, G.S. (2001). NF- $\kappa$ B: a key role in inflammatory diseases. *J. Clin. Invest.* *107*, 7–11.

Thanos, D., and Maniatis, T. (1995). NF-kappa B: a lesson in family values. *Cell* *80*, 529–532.

Thu, Y.M., and Richmond, A. (2010). NF- $\kappa$ B inducing kinase: a key regulator in the immune system and in cancer. *Cytokine Growth Factor Rev.* *21*, 213–226.

Trinh, D.V., Zhu, N., Farhang, G., Kim, B.J., and Huxford, T. (2008). The nuclear I kappaB protein I kappaB zeta specifically binds NF-kappaB p50 homodimers and forms a ternary complex on kappaB DNA. *J. Mol. Biol.* *379*, 122–135.

Truhlar, S.M.E., Torpey, J.W., and Komives, E.A. (2006). Regions of IkappaBalpha that are critical for its inhibition of NF-kappaB.DNA interaction fold upon binding to NF-kappaB. *Proc. Natl. Acad. Sci. U. S. A.* *103*, 18951–18956.

Tsui, R., Kearns, J.D., Lynch, C., Vu, D., Ngo, K.A., Basak, S., Ghosh, G., and Hoffmann, A. (2015). I $\kappa$ B $\beta$  enhances the generation of the low-affinity NF $\kappa$ B/RelA homodimer. *Nat. Commun.* *6*, 7068.

Tumang, J.R., Owyang, A., Andjelic, S., Jin, Z., Hardy, R.R., Liou, M.L., and Liou, H.C. (1998). c-Rel is essential for B lymphocyte survival and cell cycle progression. *Eur. J. Immunol.* *28*, 4299–4312.

Udalova, I.A., Richardson, A., Denys, A., Smith, C., Ackerman, H., Foxwell, B., and Kwiatkowski, D. (2000). Functional Consequences of a Polymorphism Affecting NF- $\kappa$ B p50-p50 Binding to the TNF Promoter Region. *Mol. Cell. Biol.* *20*, 9113–9119.

Urban, M.B., Schreck, R., and Baeuerle, P.A. (1991). NF-kappa B contacts DNA by a heterodimer of the p50 and p65 subunit. *EMBO J.* *10*, 1817–1825.



- Verma, I.M., Stevenson, J.K., Schwarz, E.M., Antwerp, D.V., and Miyamoto, S. (1995). Rel/NF-kappa B/I kappa B family: intimate tales of association and dissociation. *Genes Dev.* 9, 2723–2735.
- Wan, F., and Lenardo, M.J. (2009). Specification of DNA Binding Activity of NF- $\kappa$ B Proteins. *Cold Spring Harb. Perspect. Biol.* 1, a000067.
- Wan, F., Anderson, D.E., Barnitz, R.A., Snow, A., Bidere, N., Zheng, L., Hegde, V., Lam, L.T., Staudt, L.M., Levens, D., et al. (2007). Ribosomal protein S3: a KH domain subunit in NF-kappaB complexes that mediates selective gene regulation. *Cell* 131, 927–939.
- Weih, F., and Caamaño, J. (2003). Regulation of secondary lymphoid organ development by the nuclear factor- $\kappa$ B signal transduction pathway. *Immunol. Rev.* 195, 91–105.
- Xia, Y., Shen, S., and Verma, I.M. (2014). NF- $\kappa$ B, an Active Player in Human Cancers. *Cancer Immunol. Res.* 2, 823–830.
- Xiao, G., Harhaj, E.W., and Sun, S.C. (2001). NF-kappaB-inducing kinase regulates the processing of NF-kappaB2 p100. *Mol. Cell* 7, 401–409.
- Yamaoka, S., Courtois, G., Bessia, C., Whiteside, S.T., Weil, R., Agou, F., Kirk, H.E., Kay, R.J., and Israël, A. (1998). Complementation Cloning of NEMO, a Component of the I $\kappa$ B Kinase Complex Essential for NF- $\kappa$ B Activation. *Cell* 93, 1231–1240.
- Yilmaz, Z.B. (2003). RelB is required for Peyer's patch development: differential regulation of p52-RelB by lymphotoxin and TNF. *EMBO J.* 22, 121–130.
- Yin, L., Wu, L., Wesche, H., Arthur, C.D., White, J.M., Goeddel, D.V., and Schreiber, R.D. (2001). Defective lymphotoxin-beta receptor-induced NF-kappaB transcriptional activity in NIK-deficient mice. *Science* 291, 2162–2165.
- Zabel, U., and Baeuerle, P.A. (1990). Purified human I kappa B can rapidly dissociate the complex of the NF-kappa B transcription factor with its cognate DNA. *Cell* 61, 255–265.
- Zabel, U., Schreck, R., and Baeuerle, P.A. (1991). DNA binding of purified transcription factor NF-kappa B. Affinity, specificity, Zn<sup>2+</sup> dependence, and differential half-site recognition. *J. Biol. Chem.* 266, 252–260.
- Zandi, E., Rothwarf, D.M., Delhase, M., Hayakawa, M., and Karin, M. (1997). The I $\kappa$ B Kinase Complex (IKK) Contains Two Kinase Subunits, IKK $\alpha$  and IKK $\beta$ , Necessary for I $\kappa$ B Phosphorylation and NF- $\kappa$ B Activation. *Cell* 91, 243–252.
- Zhang, Q., Didonato, J.A., Karin, M., and McKeithan, T.W. (1994). BCL3 encodes a nuclear protein which can alter the subcellular location of NF-kappa B proteins. *Mol. Cell. Biol.* 14, 3915–3926.

Zhang, Q., Lenardo, M.J., and Baltimore, D. (2017). 30 Years of NF- $\kappa$ B: A Blossoming of Relevance to Human Pathobiology. *Cell* 168, 37–57.

Zhao, B., Barrera, L.A., Ersing, I., Willox, B., Schmidt, S.C.S., Greenfeld, H., Zhou, H., Mollo, S.B., Shi, T.T., Takasaki, K., et al. (2014). The NF- $\kappa$ B Genomic Landscape in Lymphoblastoid B-cells. *Cell Rep.* 8, 1595–1606.

Zhong, H., Voll, R.E., and Ghosh, S. (1998). Phosphorylation of NF- $\kappa$ B p65 by PKA Stimulates Transcriptional Activity by Promoting a Novel Bivalent Interaction with the Coactivator CBP/p300. *Mol. Cell* 1, 661–671.

Zhong, H., May, M.J., Jimi, E., and Ghosh, S. (2002). The Phosphorylation Status of Nuclear NF- $\kappa$ B Determines Its Association with CBP/p300 or HDAC-1. *Mol. Cell* 9, 625–636.

## **CHAPTER 2:**

**Dissecting the Regulatory Strategies of NF $\kappa$ B RelA**

**Target Genes in the Inflammatory Response**

## **ABSTRACT**

NFκB RelA is the potent transcriptional activator of inflammatory response genes. We stringently defined a list of direct RelA target genes by integrating physical (ChIPseq) and functional (RNAseq in knockouts) datasets. We then dissected each gene's regulatory strategy by testing RelA variants in a novel primary-cell genetic complementation assay. All endogenous target genes required that RelA makes DNA-base-specific contacts, and none could be activated by the DNA binding domain alone. However, endogenous target genes differed widely in how they employ the two transactivation domains. Through model-aided analysis of the dynamic timecourse data we reveal gene-specific synergy and redundancy of TA1 and TA2. Given that post-translational modifications control TA1 activity and intrinsic affinity for coactivators determines TA2 activity, the differential TA logics suggests context-dependent vs. context-independent control of endogenous RelA-target genes. While some inflammatory initiators appear to require co-stimulatory TA1 activation, inflammatory resolvers a part of the NFκB RelA core response where TA2 activity mediates activation even when TA1 is inactive.

## INTRODUCTION

An impactful concept of molecular biology is the modular domain organization of transcription factors (Keegan et al., 1986), typically distinguishing between a DNA-binding domain (DBD) and a separable transcriptional activation domain (TAD) that could be fused to a heterologous DBD. Prominent mammalian TFs, including NF $\kappa$ B RelA (Schmitz and Baeuerle, 1991; Schmitz et al., 1994), conform to the modular domain model. Such studies utilized exogenous reporter genes that provided a convenient assay for TF activity. However, they lacked the physiological context of endogenous regulatory regions, which may involve complex protein-protein interactions, and are often considerable distances from the transcription start site. Indeed, subsequent studies provided numerous examples where the functional distinction between DNA binding and transcriptional activation did not neatly segregate into distinct structural domains, with the DBD providing transcriptional activity (Corton et al., 1998) or, conversely, not being required for TF recruitment to the target gene (Kovesdi et al., 1986).

Given that the regulatory context of endogenous target genes determines a TF's mode of function, next generation TF structure-function studies may be considered probes of the regulatory diversity of its endogenous target genes. However, only with the advent of quantitative transcriptomic and epigenomic measurement capabilities enabled by Next Generation Sequencing has it become feasible to undertake such studies. The present study is leveraging such technological development to dissect the regulatory strategies of inflammatory response genes that are regulatory targets of NF $\kappa$ B RelA.

The NF $\kappa$ B family member RelA is a ubiquitously expressed potent transcriptional activator that is induced by exposure to pathogens and inflammatory cytokines to activate the

expression of a large number inflammatory and immune-response genes (Hayden and Ghosh, 2008; Hoffmann and Baltimore, 2006). The signaling mechanisms involved in regulating NF $\kappa$ B RelA activity have been elucidated in detail (Basak et al., 2012; Mitchell et al., 2016), but there is much more uncertainty about how it controls endogenous target genes. Indeed, while many genes have been identified to be potentially NF $\kappa$ B regulated (<http://www.bu.edu/nf-kb/gene-resources/target-genes/>), there is no database that lists the NF $\kappa$ B target genes in a particular physiological condition, defined cell type and stimulus.

RelA's domain organization is characterized by the Rel Homology Region (RHR), which mediates dimerization and DNA binding functions (Baeuerle and Baltimore, 1989) and was structurally characterized by X-ray crystallography (Chen et al., 1998; Chen et al., 2000). However, it is possible that for some endogenous target genes, promoter recruitment of RelA is mediated primarily by protein-protein interactions, for example via pre-bound CBP (Mukherjee et al., 2013).

RelA's C-terminus contains two transactivation domains, TA1 and TA2 (Moore et al., 1993; Schmitz and Baeuerle, 1991). TA1 consists of the last 30 amino acids in sequence in the very C-terminus, while TA2 is directly adjacent to TA1. The initial thought of TA1 being the principal transactivation domain for RelA transcriptional activity is due to the fact that structural features of TA1 domain are highly conserved across species and that it has been shown to be sufficient and potent in inducing transcriptional activity (Schmitz and Baeuerle, 1991); however, when deleting these residues, the authors showed that the unique C-terminal third of RelA contained at least another distinct transcriptional activation domain that is directly adjacent to TA1. TA1 consists of an amphipathic helix characteristic of an acidic activation domain. TA2

interacts with CBP/p300, and its structure with the CBP-derived TAZ1 peptide was characterized by nuclear magnetic resonance (Mukherjee et al., 2013; Nyqvist et al., 2019). However, CBP/p300 was also reported to interact with the RHR via phosphorylated S276 (Zhong et al., 2002), and knock-in mutations of the S276A or S276E mutation showed complex mouse phenotypes and transcriptional defects (Dong et al., 2008). To add to this complexity, it also remains possible that trans-activation of some target genes is mediated by other sequences within RelA, for example between RHR and TA2/TA1.

Interestingly, a key difference between TA1 and TA2 is the role of post-translational modification. Unlike TA2, TA1's conformation is thought to be regulated (Savaryn et al., 2016) by phosphorylation of any of 7 potential sites (S529, S535, S536, S543, S547, S550, and S551 in human RelA) altering cofactor interactions (Milanovic et al., 2014), and hence transcriptional activation potential (Hochrainer et al., 2013). In particular, S536 is a prominent phospho-acceptor site (Christian et al., 2016), that is a reliable biomarker for RelA activity. This suggests a model in which TA1's transactivation activity is dependent on a phosphorylation event that integrates the activity of other signaling pathways, such as CKII, CaMKIV, RSK1, TAK1/TAB1, PI3K/Akt, ATM, and IKK $\epsilon$  (Bae et al., 2003; Bao et al., 2010; Bird et al., 1997; Bohuslav et al., 2004; Buss et al., 2004; Haller et al., 2002; Moreno et al., 2010; Sabatel et al., 2012; Sakurai et al., 2003; Wang et al., 2000; Yoboua et al., 2010), whereas TA2's transactivation potential is intrinsic to its biochemical structure. Remarkably, however, it remains unknown whether NF $\kappa$ B response genes show differential regulation by TA1 vs. TA2; this is an important question as TA2-regulated genes would be expected to provide for a core NF $\kappa$ B-mediated inflammatory response, whereas TA1-regulated genes are dependent on other signaling pathways as well.

Here, we report the stringent identification of endogenous NF $\kappa$ B target genes induced by TNF in primary fibroblasts, and a genetic complementation system for RelA variants to probe their regulatory strategies. We found that all RelA target gene binding was dependent on base-specific contacts within the  $\kappa$ B sequence, and all transactivation was dependent on the two C-terminal activation domains; neither protein-protein interactions proved sufficient for target gene selection, nor was the RHR sufficient to drive transcriptional activation. However, we discovered remarkable gene-specific regulatory strategies involving TA1 and TA2. Though most genes were regulated by both TA1 and TA2, the two transactivation functioned either redundantly or synergistically, forming logical OR or AND gates in a gene-specific manner. While OR gate genes were robustly activated by the constitutive TA2 activity, on AND gate genes TA2's role is to boost the PTM-regulated TA1 activity. Thus, our study distinguishes NF $\kappa$ B RelA target genes as being largely signaling context independent vs. largely context-dependent.



## RESULTS

### Stringent identification of TNF-responsive NFκB RelA target genes

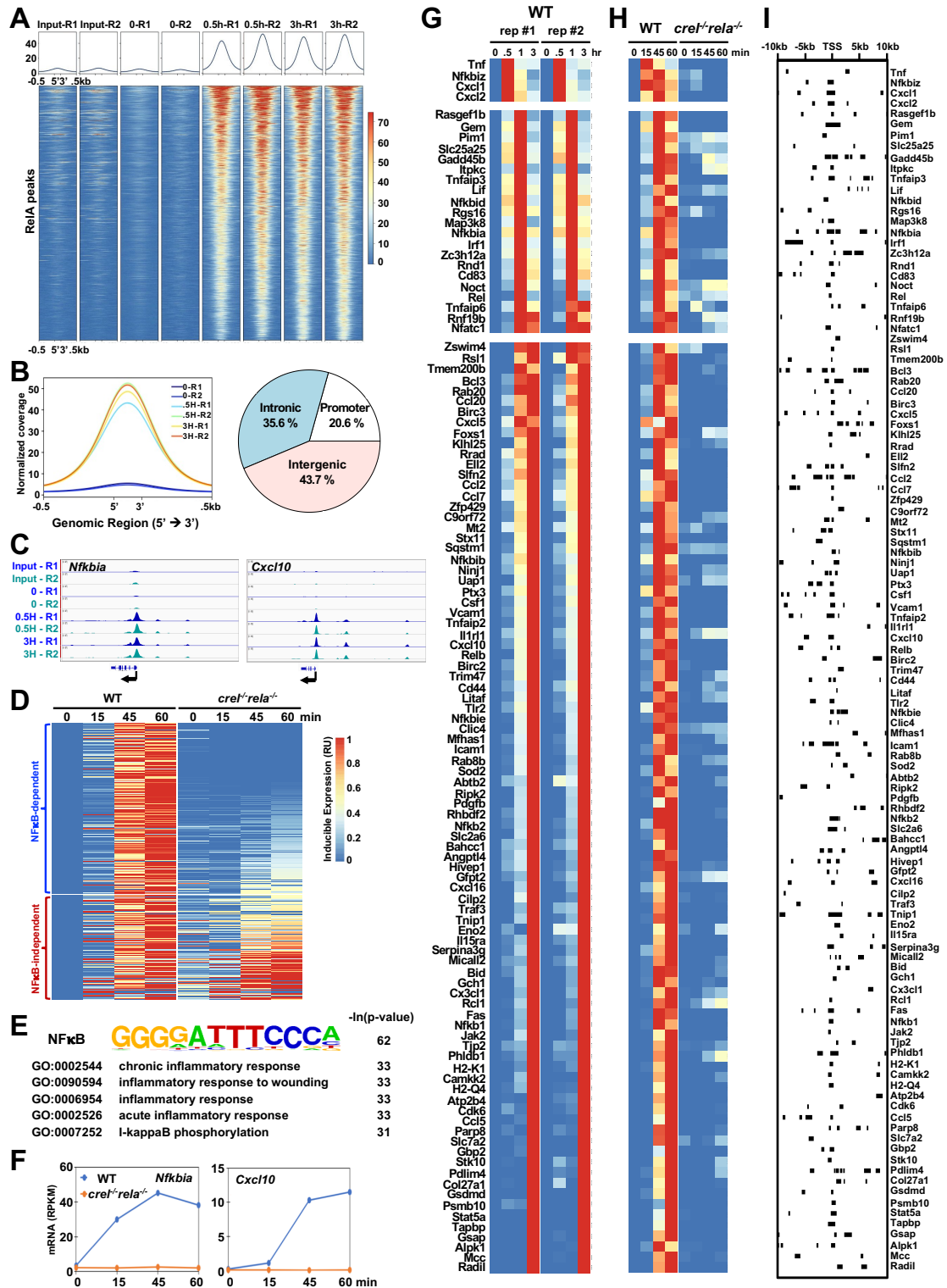
To identify high-confidence NFκB RelA target genes, we applied two rigorous criteria, namely: (i) TNF-induced NFκB/RelA binding to the target gene's regulatory regions, and (ii) TNF-induced transcriptional activation that is genetically NFκB-dependent. To examine the genome-wide binding pattern of NFκB, we performed chromatin immunoprecipitation followed by sequencing (ChIP-seq) with RelA-specific antibody during a short time-course of TNF stimulation of 0, 0.5hr and 3hr in wild-type (WT) primary murine embryonic fibroblasts (MEFs). Bioinformatic analysis of the replicate datasets (FDR<0.01) identified in 9,829 RelA peaks that were TNF-inducible at 0.5hr or 3hr (Figure 2.1A). Overall, these ChIP-enriched RelA binding events were notably enhanced at 0.5hr and largely remained at 3hr (Figure 2.1B, left panel). We identified the locations of these RelA peaks to be 44% intergenic, 21% within promoter regions, and 36% within intronic regions of genes (Figure 2.1B, right panel). Genome browser tracks of two known NFκB target genes, *Nfkb1a* and *Cxcl10* confirmed easily discernible peaks above a low background that are highly inducible in response to TNF and highly reproducible between the two datasets (Figure 2.1C).

To assess the NFκB-dependent transcriptional response to TNF, we performed gene expression analysis of nascent transcripts via chromatin-associated RNA-seq (caRNA-seq) in WT and *crel<sup>-/-</sup>rela<sup>-/-</sup>* MEF cells (Figure 2.1D). We chose caRNA-seq analysis rather than polyA+ RNA-seq to ensure that we identified transcriptional induction rather than changes in mRNA levels mediated by post-transcriptional mechanisms, for example, changes in mRNA half-life. Previous work had shown that the absence of RelA can be partially compensated by the NFκB

family member cRel (Hoffmann et al., 2003), necessitating the use of the combination knockout to assess RelA-dependent gene expression. Our 1-hour time-course analysis revealed 419 TNF-inducible genes in WT MEFs whose caRNA levels were more than two-fold induced in WT MEFs at any time point after TNF stimulation relative to the unstimulated (0hr) time point (Figure 2.1D). Setting the maximum RPKM for each gene to 1 and the basal RPKM in unstimulated WT cells to be 0, we plotted data from *crel<sup>-/-</sup>rela<sup>-/-</sup>* MEF cells next to WT data. We found that 259 genes had peak expression values that were less than half in the mutant relative to WT, and 160 genes showed expression that was more than half, leading us to label the former as largely “NFκB-dependent” and the latter largely “NFκB-independent”. Motif enrichment analysis of the regulatory DNA regions associated with transcription start sites using HOMER (Heinz et al., 2010) revealed a preponderance of κB sites in the NFκB-dependent genes but no highly significant motif for NFκB-independent genes (Figure 2.1E). Focusing on those that are protein-coding (229 and 120, respectively), we undertook gene ontology (GO) analysis with Enrichr Ontologies (Kuleshov et al., 2016) for over-represented functional pathways in each category. We found that the top five most highly enriched GO terms (by p-value) for the NFκB-dependent genes described the inflammatory response and NFκB activation (Figure 2.1E), whereas the NFκB-independent genes did not yield highly significant terms. Line graphs of two NFκB-dependent genes, *Nfkb1a* and *Cxcl10* (Figure 2.1F) exemplify the high degree of NFκB-dependence in their TNF-induced expression.

To develop the list of stringent NFκB RelA-regulated target genes, we intersected the above-described physical/binding data (within 10kb of each gene’s transcription start site) and the genetic/functional data and further ensured that the nascent transcripts are indeed processed

into mature mRNA by performing polyA+ RNA-seq from total RNA isolated from WT MEF cells in response to TNF, extending our time course analysis to 3 hours (0.5, 1, and 3 hr time points). Selecting for peak fold-change in response to TNF of  $\geq 2$ , an FDR of  $<0.01$ , and  $\geq 50\%$  NF $\kappa$ B dependence of the maximum value in the time course, we generated a list of 113 stringently selected NF $\kappa$ B/RelA-regulated target genes (Figure 2.1G). The replicate datasets showed a high level of concordance. The corresponding caRNA-seq data (Figure 2.1H) indicates that aside from the very early gene group, the timing of peak mRNA abundance may not be driven by transcriptional mechanisms, but rather post-transcriptional, such as mRNA processing (Pandya-Jones et al., 2013) or mRNA half-life (Hao and Baltimore, 2009). Mapping the RelA ChIP-seq data associated with each gene (Figure 2.1I) identified probable RelA binding events responsible for gene induction, but did not reveal a correlation between RelA binding location and transcriptional induction dynamics.

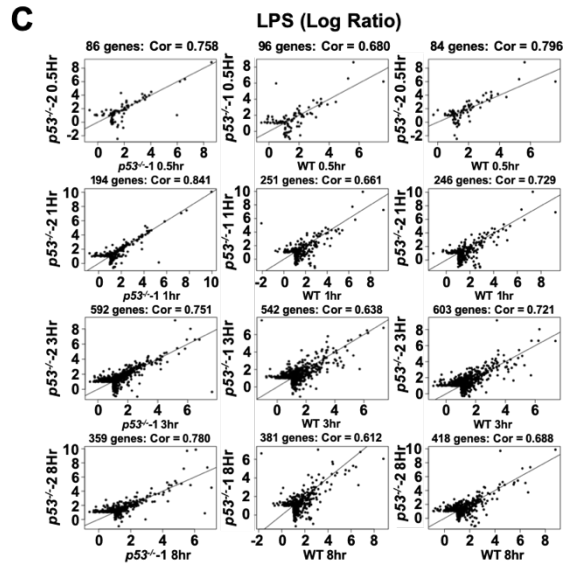
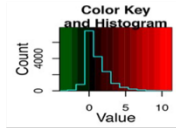
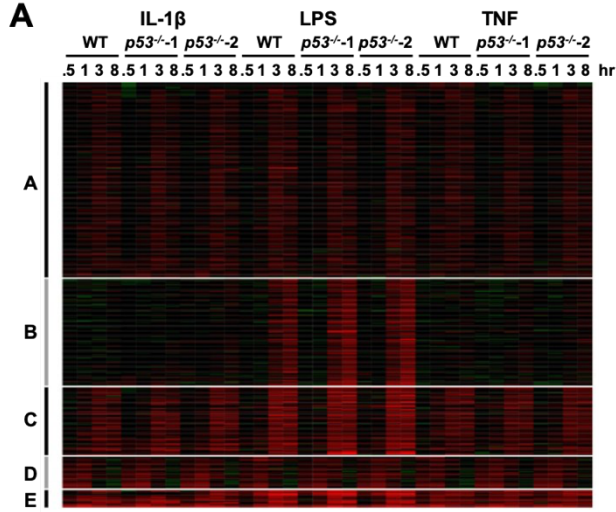


**Figure 2.1 Identifying NFκB RelA target genes in the TNF response of murine embryonic fibroblasts.** (A) Genome-wide binding of NFκB RelA in wild-type (WT) primary murine embryonic fibroblasts (MEF) stimulated with TNF (10ng/mL) at 0.5hr and 3hr by chromatin immunoprecipitation followed by sequencing (ChIP-seq) with RelA specific antibody. 9,829 RelA binding events were identified in two independent replicate experiments. Heatmap shows read density along  $\pm 0.5$ kb of DNA centered around the peak read density for each binding event and ordered by high to low read density. (B) (Left panel) The normalized RelA ChIP-seq density over identified peaks within the genome. (Right panel) Pie chart shows where RelA peaks are found to be located. (C) Genome browser tracks of two replicates (R1, R2) of RelA binding events in WT MEFs for two known NFκB target genes, *Nfkb1a* and *Cxcl10*. (D) Heatmap of the relative induced expression of 419 nascent transcripts measured by via chromatin-associated RNA sequencing (caRNA-seq), whose maximal induced expression was  $\geq 1$  RPKM and  $\geq 2$  fold over basal. Of these 419 genes, 229 genes were protein-coding and NFκB-dependent, as their maximal expression was less than 50% in *crel<sup>-/-</sup>rela<sup>-/-</sup>* compared to WT MEF. The heatmap of gene expression is ordered by high to low NFκB dependence. (E) *De novo* motif and gene ontology analyses for NFκB-dependent genes identified the most highly enriched motif (within -1.0 to 0.3kb of TSS) and GO terms (using Enrichr Ontologies tool (Kuleshov et al., 2016)). For NFκB-independent genes top motifs and GO terms showed substantially less significance. (F) Line plots of chromatin-associated RNA (caRNA) abundance (RPKM) for known NFκB target genes *Nfkb1a* and *Cxcl10* genes. (G) Heatmap of mature mRNA (polyA+RNA) relative induced expression (as in D) for 113 NFκB target genes, which were defined by the presence of RelA ChIP-seq peak and TNF-inducible NFκB-dependent caRNA expression. Two biological replicates of WT MEFs are shown, ordered by their peak time of expression. (H) Heatmap of relative induced expression of nascent transcripts determined by caRNA-seq for these 113 NFκB-dependent genes shown in the same order as in G. (I) A map of 297 RelA-binding peaks identified by ChIP-seq for each of the 113 NFκB target genes within  $\pm 10$ kb of TSS, shown in the same order as in G and H.

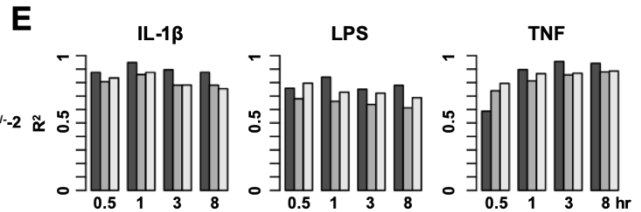
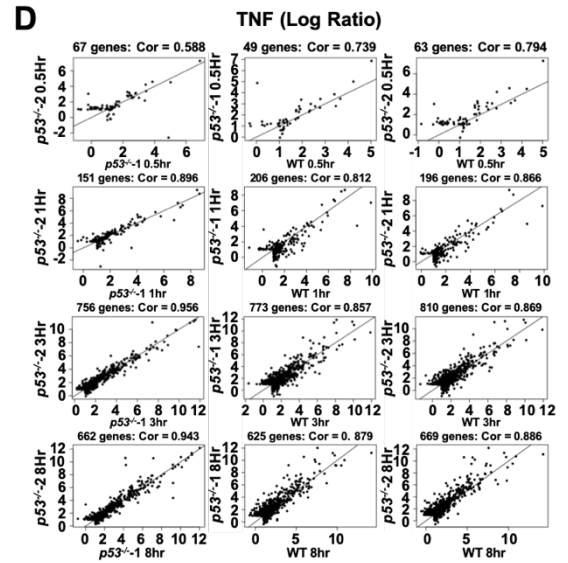
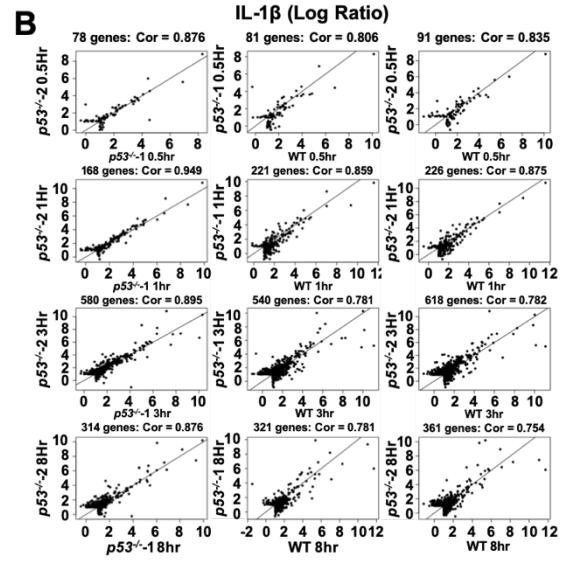
## **An experimental system to dissect regulatory strategies of NFκB RelA target genes**

To characterize the regulatory strategies of NFκB RelA target genes by probing them for their requirements of RelA functional domains, we developed an experimental workflow for retroviral complementation of RelA-deficient MEF cells with specifically engineered variants of RelA, and subsequent transcriptomic analysis in response to TNF. In order to prolong the lifespan of primary MEFs (Todaro and Green, 1963), which would otherwise not be amenable for such genetic manipulation, we investigated whether we could use MEFs deficient in p53. Transcripts induced by TNF, IL-1β, or LPS, revealed similar gene expression patterns between two biological replicates of p53-deficient MEFs and their littermate WT control (Figure 2.2A). Pairwise comparisons revealed high reproducibility in inducible gene expression between *p53<sup>-/-</sup>* and WT MEFs at each time point (Figure 2.2B-E), justifying the use of p53-deficient MEFs for studies of inflammatory response genes.

To develop the primary MEF RelA complementation system, we bred knockout mouse strains to produce a strain that is not only deficient in NFκB subunits but also p53, which allowed production of primary *p53<sup>-/-</sup>crel<sup>-/-</sup>rela<sup>-/-</sup>* MEF cells from E12.5 embryos (prior to embryonic lethality of this genotype at E13). Following expansion of these cells for about a week, we retrovirally transduced them with RelA-WT (Figure 2.3A), selected transduced cells with puromycin, and examined complementation by biochemical assays. Immunoblotting revealed RelA expression in reconstituted cells at about the same level as WT control MEFs (Figure 2.4A). Electrophoretic mobility shift assay (EMSA) with a κB site probe showed strong DNA binding activity following TNF stimulation (Figure 2.4B).



■ *p53*<sup>-/-</sup>-1 vs *p53*<sup>-/-</sup>-2  
 □ *p53*<sup>-/-</sup>-1 vs WT  
 □ *p53*<sup>-/-</sup>-2 vs WT

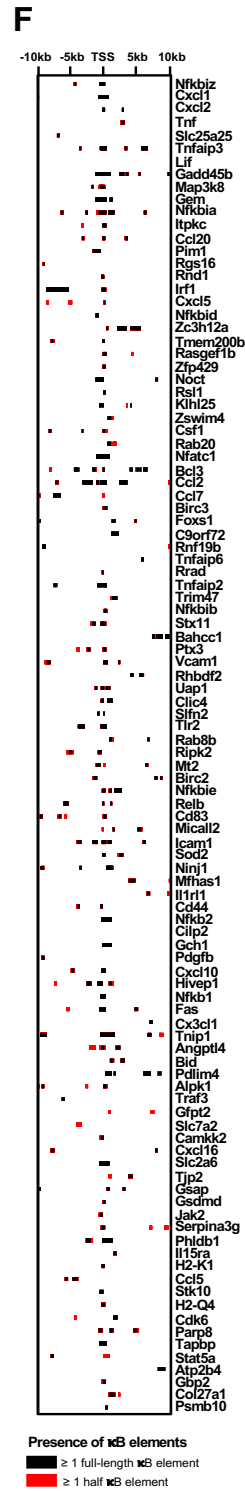
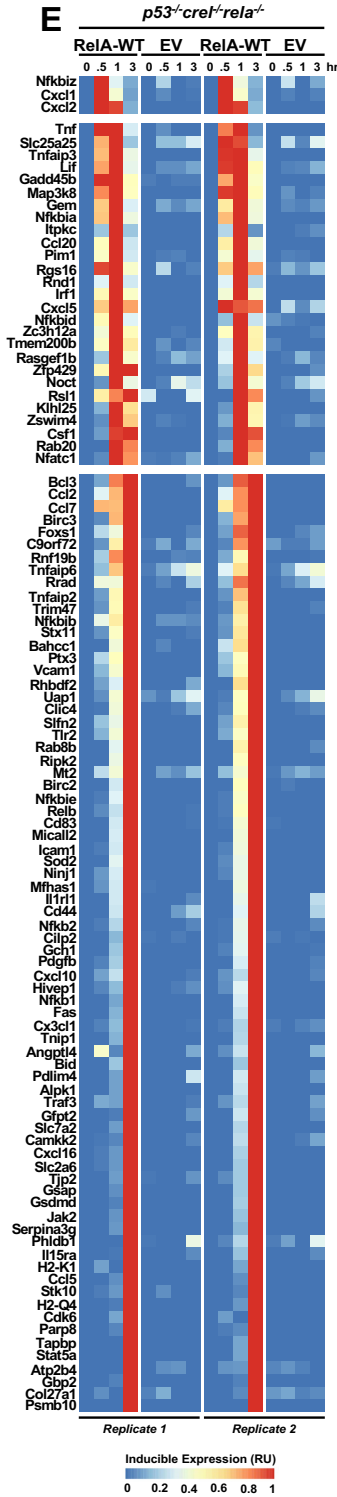
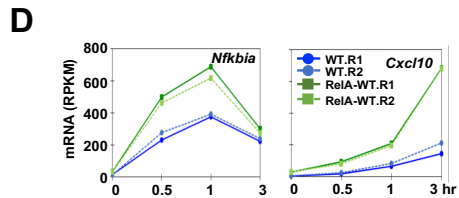
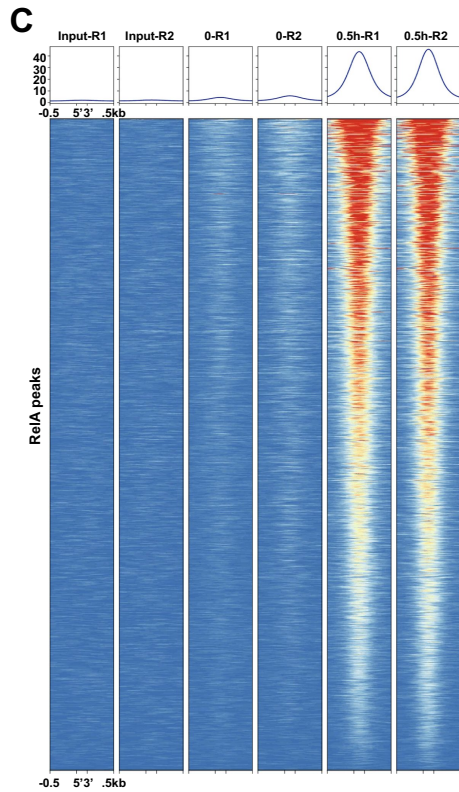
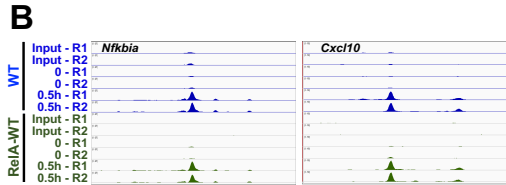
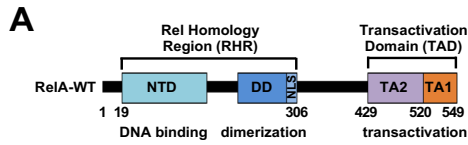


**Figure 2.2 p53 deficiency does not affect TNF-induced gene expression.** (A) Heatmap visualization of upregulated genes in response to IL-1 $\beta$  (10ng/mL), TNF (10ng/mL), or LPS (100ng/mL) stimulations at indicated times in WT or *p53*<sup>-/-</sup> MEFs. One biological replicate of WT and two biological replicates of *p53*<sup>-/-</sup> MEFs are shown. Genes with  $\geq 100$  normalized counts in at least one condition and an induction  $\geq 4$  were sorted into five groups via K-means clustering. (B) Scatterplots between significantly up-regulated genes in all genotypes at all time points of IL-1 $\beta$  stimulation are plotted, with number of genes and R<sup>2</sup> value indicated. Rows are 0.5, 1, 3 and 8hr respectively. Columns are *p53*<sup>-/-2</sup> vs. *p53*<sup>-/-1</sup>, *p53*<sup>-/-1</sup> vs. WT, and *p53*<sup>-/-2</sup> vs. WT, respectively. We restricted our analysis to genes that were up-regulated by at least 2-fold in one of the two conditions compared. (C) Scatterplots between significantly up-regulated genes in all genotypes at all time points of LPS stimulations are plotted, with number of genes and R<sup>2</sup> value indicated. (D) Scatterplots between significantly up-regulated genes in all genotypes at all time points of TNF stimulations are plotted, with number of genes and R<sup>2</sup> value indicated. (E) Summary of correlations between different stimuli conditions where bar plots of the R<sup>2</sup> values from panels B-D are shown.

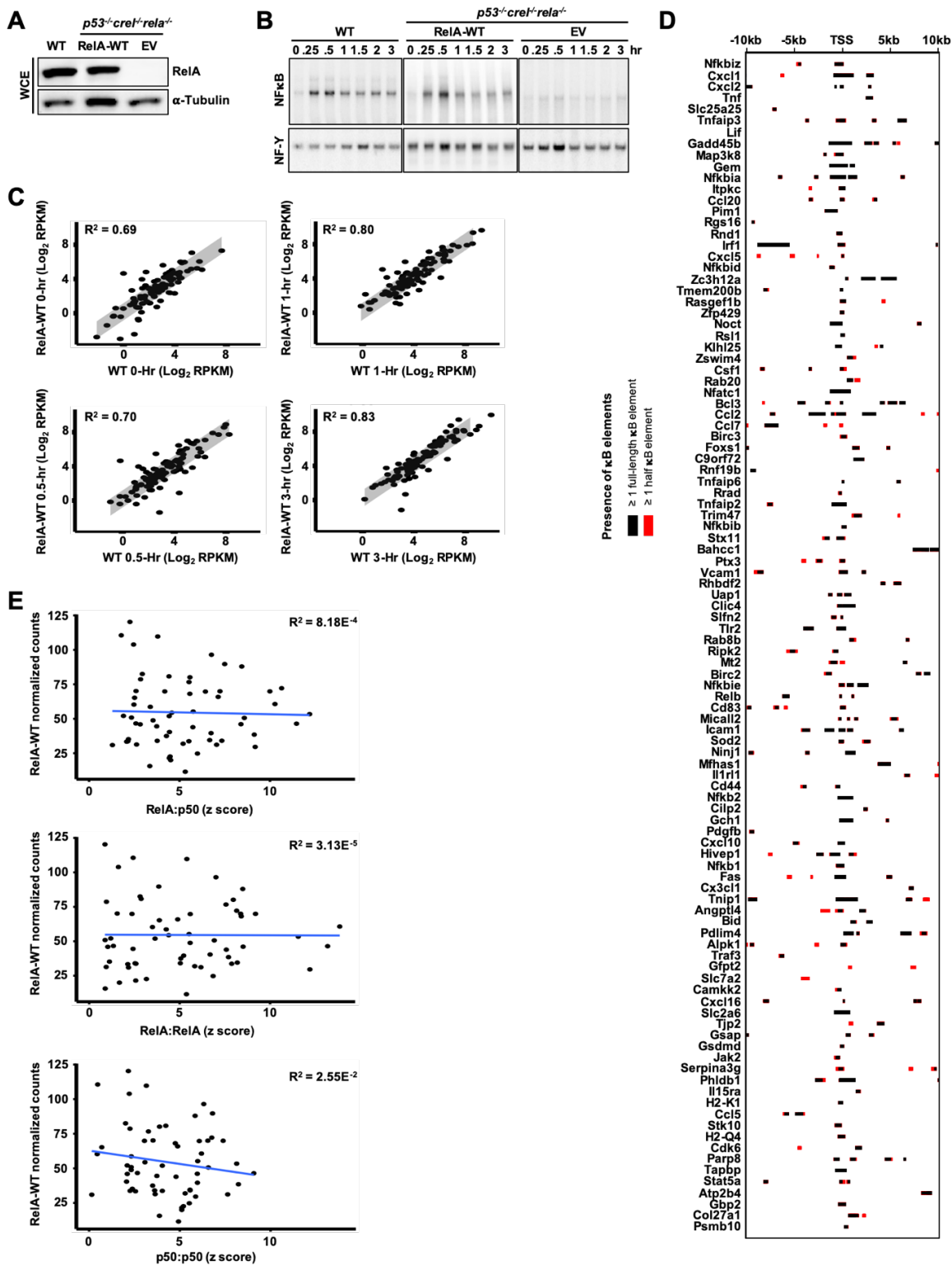


To further test the genetic complementation system, we examined NF $\kappa$ B RelA binding via RelA ChIP-seq using RelA-WT reconstituted MEFs with and without 0.5hr of TNF stimulation, on previously identified endogenous NF $\kappa$ B target genes (Figure 2.1G), such as *Nfkb1a* and *Cxcl10* (Figure 2.3B). Importantly, we found that RelA binding peaks identified in WT MEF control were indeed also present in the reconstituted RelA-WT cells (Figure 2.3C).

Next, we examined gene expression responses to TNF in reconstituted MEFs stimulated with TNF using polyA+ RNA-seq. We found high reproducibility in replicate reconstituted MEFs on *Nfkb1a* and *Cxcl10* (Figure 2.3D). Extending our analysis to the 113 NF $\kappa$ B target genes, a scatter plot analysis demonstrated good correlations in polyA+RNA expression patterns between WT MEF control and the reconstituted RelA-WT MEFs at each time point analysis (Figure 2.4C). Specifically, we found that 104 genes satisfied the same criteria applied to WT and *crel-rela* MEFs, namely TNF fold change over time of  $\geq 2$ , an FDR of  $< 0.01$  and  $\geq 50\%$  NF $\kappa$ B dependence of the maximum expression value in the time-course (Figure 2.3E), thereby validating the primary MEF complementation system. In sum, our analysis revealed 104 NF $\kappa$ B target genes (Supplementary Table 2.1) that showed robust RelA DNA binding and RelA-dependent TNF-inducible expression at both nascent and mature mRNA transcript level.



**Figure 2.3 A RelA genetic complementation system for studying the control of endogenous NFκB RelA target genes.** (A) Schematic of the domain structure of the mouse RelA protein (with relevant amino acid numbers) and the primary cells to be complemented, and the experimental assays to be performed. (B) Genome browser tracks of RelA binding events on the *Nfkb1a* and *Cxcl10* genes in WT MEFs and *p53<sup>-/-</sup>crel<sup>-/-</sup>rela<sup>-/-</sup>* MEFs reconstituted with RelA-WT, data from two independent experiments (R1, R2) are shown. (C) Heatmap of the read density along ±0.5kb of RelA ChIP-seq peaks following 0.5hr TNF treatment for 104 genes identified as NFκB-dependent genes in WT MEFs and *p53<sup>-/-</sup>crel<sup>-/-</sup>rela<sup>-/-</sup>* MEFs reconstituted with RelA-WT. (D) Line plots of polyA+RNA expression (RPKM) of *Nfkb1a* and *Cxcl10* genes. (E) Heatmap of relative induced expression in reconstituted RelA-WT and Empty Vector (EV) in *p53<sup>-/-</sup>crel<sup>-/-</sup>rela<sup>-/-</sup>* MEFs as determined by polyA+RNA. Two independent experiments are shown. (F) A map of the NFκB binding sites (κB DNA sequences) within each of the 223 RelA ChIP-seq peaks identified with an FDR <0.01 and associated with the 104 NFκB target genes. Full κB elements refer to 9, 10, and 11 bp sequences conforming to the consensus: 5'-GGR(N<sub>3,5</sub>)YCC-3', where R = A or G; Y = C or T; N = any nucleotide (A, C, G, or T). Half κB elements refer to 5'-GGR-3' and 5'-YCC-3'.



**Figure 2.4 Retroviral transduction of RelA in  $p53^{+}crel^{-}rela^{-}$  MEF provide a suitable complementation system for studying NF $\kappa$ B RelA target genes.** (A) Western blotting of RelA levels and  $\alpha$ -Tubulin as loading control in unstimulated WT MEFs and  $p53^{+}crel^{-}rela^{-}$  MEFs reconstituted RelA-WT and empty pBABE-puro (EV). (B) Analysis of nuclear NF $\kappa$ B DNA-binding activity by Electrophoretic Mobility Shift Assay (EMSA) for  $\kappa$ B DNA and NF-Y (loading control) probes of nuclear extracts prepared at indicated times after TNF stimulation from same cells as (B). (C) Scatter plots for all 113 identified genes with polyA<sup>+</sup> RNA-seq showing their RPKM in log<sub>2</sub> for each time point (0, 0.5hr, 1hr, and 3hr) in response to TNF between WT MEF cells and  $p53^{+}crel^{-}rela^{-}$  MEF reconstituted with RelA-WT. R<sup>2</sup> values of 0.69 to 0.83 are found across all time points and outliers were removed to produce the list of 104 target genes in subsequent analyses. (D) A map of the NF $\kappa$ B binding sites ( $\kappa$ B DNA sequences) within each of the 234 RelA ChIP-seq peaks identified with an FDR <0.05 and associated with the 104 NF $\kappa$ B target genes. Full  $\kappa$ B elements refer to 9, 10, and 11 bp sequences conforming to the consensus: 5'-GGR(N<sub>3,5</sub>)YCC-3', where R = A or G; Y = C or T; N = any nucleotide (A, C, G, or T). Half  $\kappa$ B elements refer to 5'-GGR-3' and 5'-YCC-3'. (E) Correlation between RelA peak size and relative affinity of  $\kappa$ B site sequence. Normalized counts of RelA ChIP-seq peaks retrieved from RelA ChIP-seq data with RelA-WT expressing MEFs are plotted against PBMA-determined z-scores of strongest  $\kappa$ B binding site sequences for RelA:RelA, RelA:p50, and p50:p50 dimer retrieved from (Siggers et al., 2012).

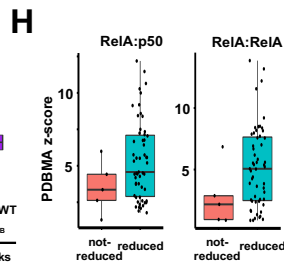
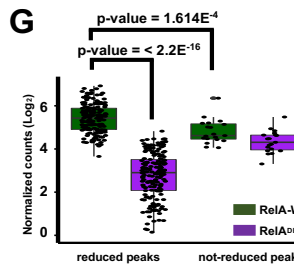
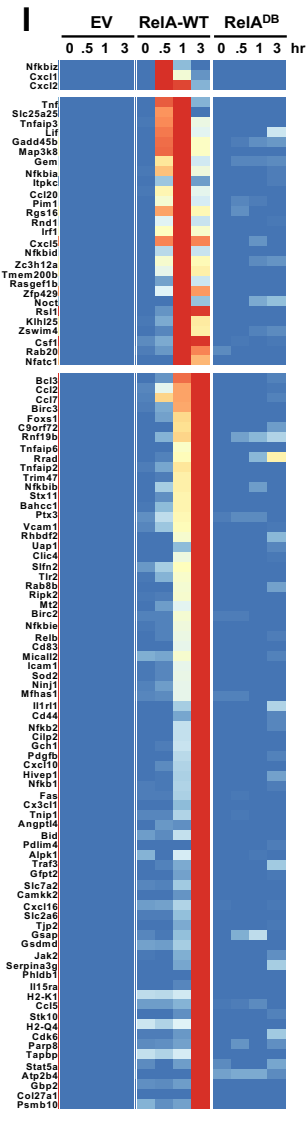
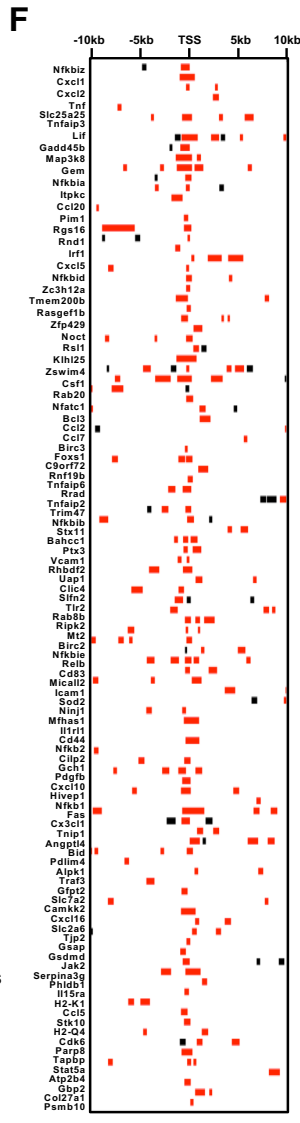
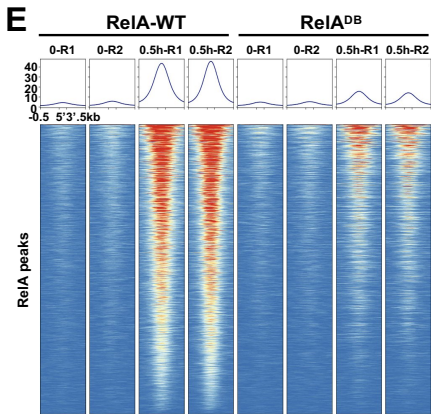
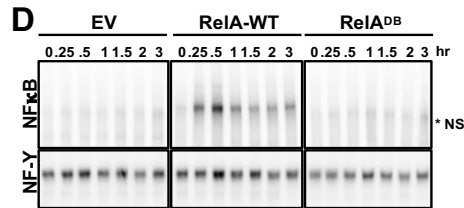
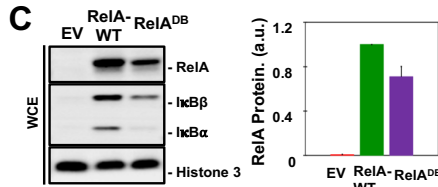
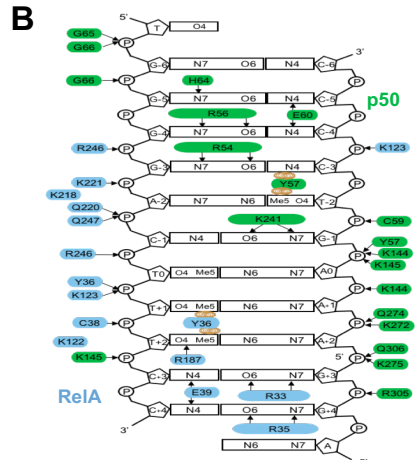
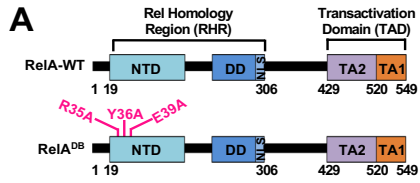
## **All TNF-induced NFκB target genes require that RelA makes base-specific contacts within the κB element**

Prior structural and functional studies of NFκB-DNA complexes demonstrated that NFκB binds to a variety of κB sites where NFκB recognizes 9 to 11 base pair palindromic κB DNA elements to the sequence: 5'-GGR(N<sub>35</sub>YCC)-3' (Hoffmann et al., 2006). Using this information, we identified all κB DNA elements that are associated with all identifiable RelA ChIP-seq peaks (Figure 2.1I) for each of the 104 genes (Supplementary Table 2.1). Mapping the RelA ChIP-seq data and κB DNA elements associated with each gene within 10kb of their TSS (Figure 2.3F), we found κB DNA elements for 223 RelA binding peaks on 104 genes. These 223 RelA binding events harbor 617 full κB and 12,768 half κB DNA elements with an FDR of <0.01. When the FDR is relaxed to <0.05, 234 RelA binding events are identified harboring 663 full κB and 14,072 half κB DNA elements, and the conclusions are confirmed (Figure 2.4D). Overall, we did not observe a correlation between the relative affinity of the κB site sequence determined by *in vitro* protein binding-DNA microarrays (Siggers et al., 2012) and the number of reads within a peak (Figure 2.4E).

To determine whether DNA-base-specific contacts of the RelA protein are in fact required for recruiting NFκB to target sites and for activating target genes upon inflammatory stimulation, we generated a triple amino acid mutation (R35A, Y36A, and E39A), depicted in Figure 2.5A, termed the RelA DNA-binding mutant (RelA<sup>DB</sup>). The mutations abrogate base-specific contacts within the κB sequence (Figure 2.5B) (Chen et al., 1998a). We retrovirally transduced this DNA-binding mutant into primary *p53<sup>-/-</sup>crel<sup>-/-</sup>rela<sup>-/-</sup>* MEFs and examined NFκB by

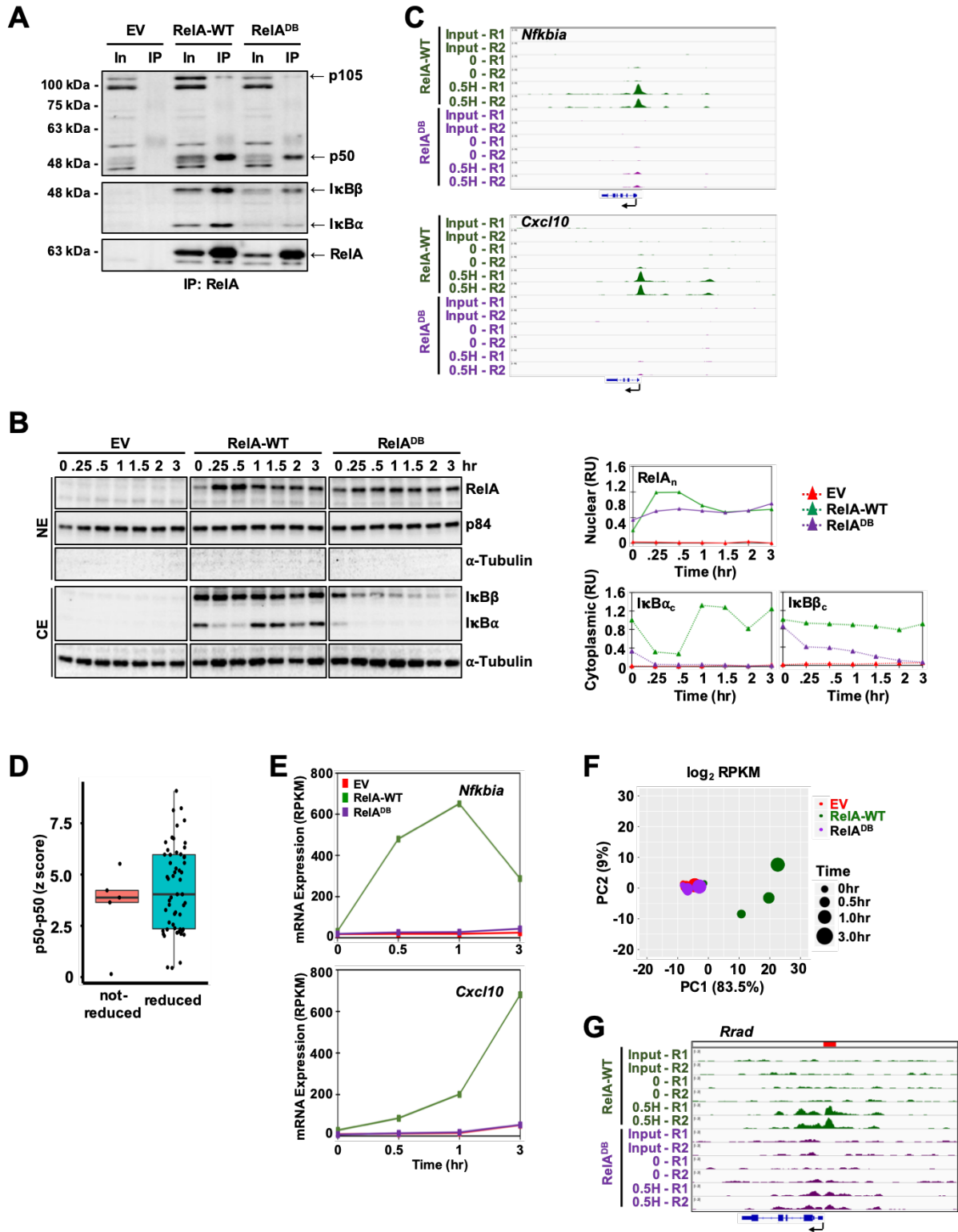
biochemical assays. Immunoblotting confirmed expression of reconstituted RelA<sup>DB</sup> protein, albeit at slightly lower levels (about 75%) than RelA-WT (Figure 2.5C). Co-immunoprecipitation confirmed that the RelA<sup>DB</sup> mutant is able to associate with p50 to form dimeric NFκB and to interact with p105, IκBα and IκBβ to form higher order IκB-NFκB complexes, characteristic of latent NFκB in unstimulated cells (Figure 2.6A). We next assessed the NFκB DNA-binding activity via EMSA and found that RelA<sup>DB</sup> showed no κB site-binding activity in response to TNF stimulation unlike the RelA-WT control (Figure 2.5D), though immunoblotting of nuclear extracts confirmed nuclear presence (Figure 2.6B). In sum, the RelA<sup>DB</sup> mutant does not support high affinity NFκB DNA-binding *in vitro*.

We next examined NFκB RelA binding *in vivo* by RelA ChIP-seq. On previously identified 9,829 endogenous chromatin sites (Figure 2.1A), RelA<sup>DB</sup> mutant showed dramatically diminished TNF-induced RelA binding (Figure 2.5E). For example, on *Nfkb1a* and *Cxcl10* genes, TNF-induced RelA binding was dramatically reduced (Figure 2.6C). Focusing on the 104 NFκB target genes (Figure 2.3E), we evaluated every previously identified RelA binding peak and found that the vast majority showed a substantial > 2-fold reduction in the RelA<sup>DB</sup> mutant (Figure 2.5F). Detailed differential RelA ChIP peak analysis (Supplementary Table 2.1) revealed that those few RelA peaks that were less affected by the RelA<sup>DB</sup> mutant were generally less prominent in wild-type cells (Figure 2.5G), which we interpreted to be indicative of the strong contribution of high affinity DNA binding ability. Furthermore, they generally showed poorer κB site motifs, as quantified by *in vitro* protein-DNA microarray studies (Figure 2.5H and Figure 2.6D). Overall, our analysis reveals that NFκB RelA selects the majority of inflammatory response target genes via direct RelA-DNA interactions via base-specific contacts.





**Figure 2.5 High affinity binding by RelA is required for the TNF-induced expression of all NFκB target genes.** (A) Schematic representation of the targeted mutations in the DNA binding mutant of murine RelA (R35A, Y36A, E39A). (B) Schematic of the κB DNA contacts made by RelA:p50 NFκB heterodimer, adapted from (Chen et al., 1998a). The heterodimer structure reveals base-specific contacts made by specific amino acids in the RelA protein, indicating the critical roles of R35, Y36 and E39. Arrows denote hydrogen bonds; brown ovals indicate van der Waals contacts. (C) Protein expression of RelA, IκBβ, IκBα, and Histone 3 as loading control, by immunoblotting in unstimulated cells genetically complemented with indicated EV, RelA-WT and RelA<sup>DB</sup>. Quantified protein expression is shown on right. (D) Analysis of nuclear NFκB activity by EMSA with κB and NF-Y (loading control) probes of nuclear extracts prepared at indicated times after TNF stimulation of genetically complemented cells shown in (C). \*NS is non-specific. The data is representative of two independent experiments. (E) Heatmap of RelA peaks at 9,829 locations defined in Figure 2.1A, in genetically complemented (RelA WT and RelA<sup>DB</sup>) *p53<sup>-/-</sup>crel<sup>-/-</sup>rela<sup>-/-</sup>* MEFs in response to 0.5hr of TNF stimulation. (F) A map of RelA binding events associated with 104 NFκB target genes indicating whether RelA-binding is reduced  $\geq 2$  fold in the RelA<sup>DB</sup> mutant (red bar). (G) Quantification and comparison of RelA peaks shown in (F). Averaged normalized counts from two replicates of RelA ChIP-seq experiments in RelA-WT or RelA<sup>DB</sup> expressing MEFs are plotted to compare RelA peaks that highly dependent on high affinity binding by RelA vs. those that are less dependent. For each category, Mann-Whitney U-test indicates that peaks less dependent on high affinity binding by RelA show a lower read count in RelA-WT control cells. (H) Correlation between RelA ChIP-seq peaks and PBMA-determined z-scores of strongest κB binding site sequences for RelA:p50 and RelA:RelA dimers retrieved from Siggers et al. Of the 7 10-bp κB site sequences within not-reduced RelA peaks, 5 with the strongest z-scores were plotted. (I) Heatmap for the transcriptional TNF response of the 104 target genes in genetically complemented RelA-WT and RelA<sup>DB</sup> cells, analyzed by polyA+RNA-seq.



**Figure 2.6 High affinity DNA binding by RelA is required for all TNF-induction of NFκB target genes.** (A) RelA DNA binding mutant shows normal interactions with p50, IκBα and IκBβ as detected by RelA immunoprecipitation using whole-cell extracts (WCE) from unstimulated cells followed by immunoblotting. (B) Nuclear extracts (NE) and cytoplasmic extracts (CE) from TNF-stimulated MEFs were analyzed by immunoblotting for antibodies against RelA, IκBβ, IκBα, p105/p50, p84 (nuclear loading control), and α-Tubulin (cytoplasmic loading control). (C) Genome browser tracks of RelA binding events in reconstituted RelA-WT and RelA<sup>DB</sup> cells for known NFκB target genes, *Nfkb1a* and *Cxcl10*, in response to 0.5 hr of TNF stimulation. Data is representative of two independent experiments. (D) Correlation between RelA peak dependence on RelA's high DNA affinity and PBMA-determined z-scores of strongest κB binding site sequences for p50:p50 dimer retrieved from Siggers et al. Of the seven 10-bp κB site sequences within not-reduced RelA peaks, the five with the strongest z-scores were plotted. (E) Line plots of polyA+RNA-seq data for *Nfkb1a* and *Cxcl10* genes shown in RPKM in response to TNF at indicated times in WT and RelA<sup>DB</sup>-reconstituted in *p53<sup>+</sup>crel<sup>+</sup>rela<sup>-</sup>* MEFs. (F) Principal Component Analysis (PCA) plot of the 104 NFκB-dependent genes in response to TNF at indicated times using log<sub>2</sub> of RPKM. (G) Genome browser tracks of RelA ChIP-seq for *Rrad* gene in reconstituted RelA-WT and RelA<sup>DB</sup> mutant cells.

Next, we investigated whether the reduced  $\kappa$ B recruitment of the DNA binding mutant results in a diminished transcriptional response of NF $\kappa$ B target genes. We performed polyA+ RNA-seq in reconstituted MEFs stimulated with TNF over a 3-hour time-course analysis (0.5, 1, and 3 hr). Examining the model target genes, *Nfkb1a* and *Cxcl10*, we found that RelA<sup>DB</sup> mutant did not support their gene expression (Figure 2.6E). Extending the analysis to the 104 NF $\kappa$ B target genes, we found that the TNF-induced gene expression response was almost entirely abolished in the RelA<sup>DB</sup> mutant cells (Figure 2.5I). This is also evident in a principal component analysis of the 104 genes (Figure 2.6F) which shows that the transcriptional response of the mutant largely overlaps with the empty vector control. Only one gene retained 50% transcriptional activation, *Rrad* (Ras related glycolysis inhibitor and calcium channel regulator). Close examination revealed some residual RelA binding within the promoter region (Figure 2.6G), including a  $\kappa$ B binding site at -123 bp (5'-GGGAATCCCC-3') whose 4G-stretch could provide sufficient affinity to heterodimeric NF $\kappa$ B via the p50 binding partner (Cheng et al., 2011).

In sum, our analysis showed that for the vast majority of genes the triple amino acid mutation abrogates TNF-induced *in vivo* DNA binding (RelA CHIP data) and target gene expression. Our results suggest that RelA target gene selection depends on base-specific interactions between RelA and the  $\kappa$ B site; our data do not rule out that protein-protein interactions with chromatin-bound factors contribute to binding site selectivity, but indicates that such interactions do not suffice for the activation of inflammatory response NF $\kappa$ B target genes.

## All TNF-induced NFκB target genes are regulated by two C-terminal TA domains

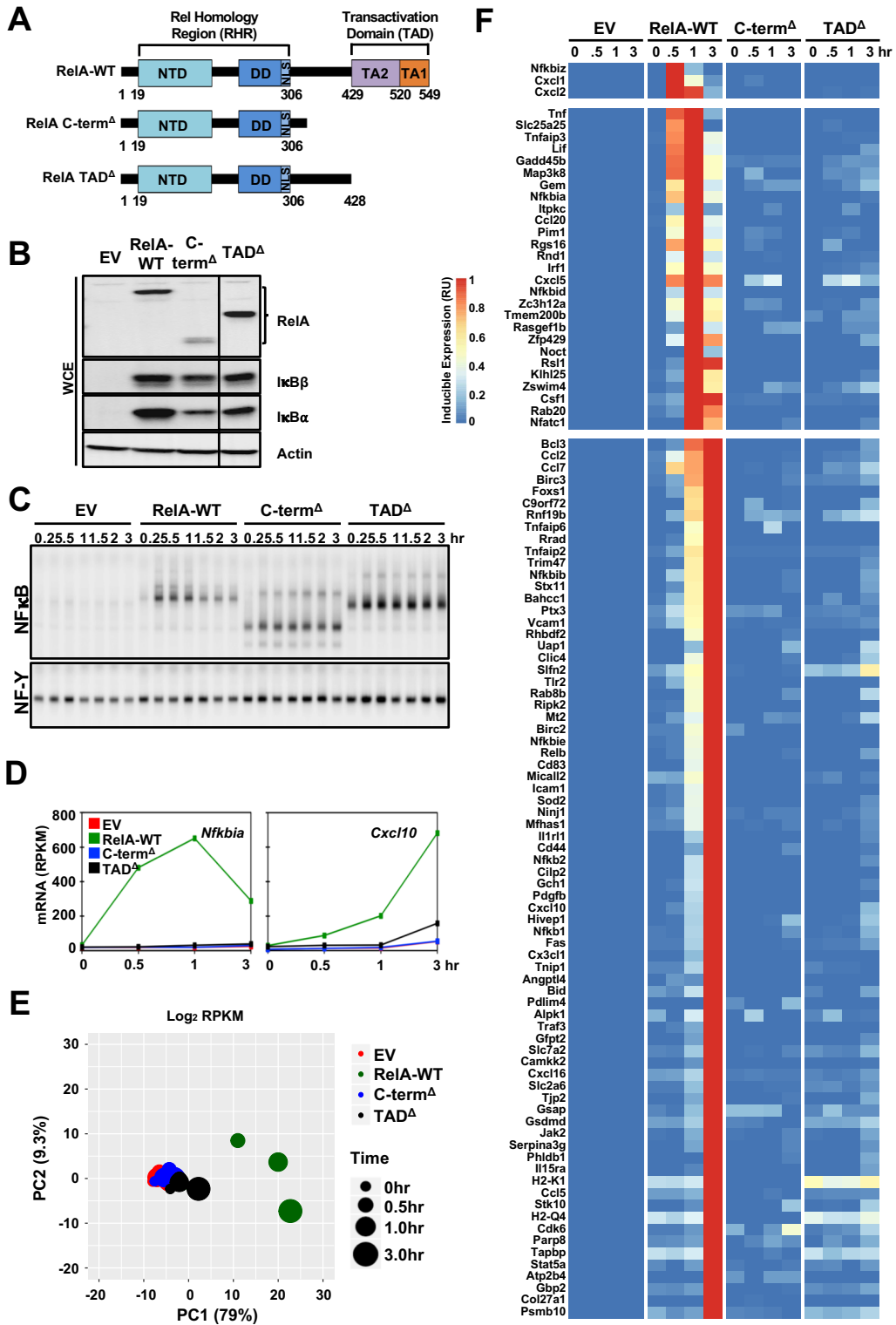
To investigate the role of RelA's C-terminal region in the transcriptional activation of endogenous NFκB target genes, we first generated two truncated variant forms of murine RelA; a full truncation of its C-terminal region (deleting amino acids 326-549; Δ326-549), referred to as C-term<sup>Δ</sup>, and a deletion specifically of its two TA domains (deleting residues 429-549; Δ429-549), referred to as TAD<sup>Δ</sup> (Figure 2.7A).

Immunoblotting of reconstituted MEFs showed close to WT expression of the TAD<sup>Δ</sup> mutant but slightly lower levels of RelA, IκBα and IκBβ in C-term<sup>Δ</sup> mutant (Figure 2.7B). Nevertheless NFκB DNA-binding activity was detected by EMSA at comparable levels to that of reconstituted RelA-WT controls (Figure 2.7C). Upon stimulation, both mutants showed a normal onset of TNF-inducible binding activity of NFκB; however, post-induction repression characteristic of TNF-induced NFκB activity was abrogated, indicative of defective negative feedback control. Indeed, no TNF-induced *Nfkb1a* mRNA expression was observed in either mutant (Figure 2.7D).

Extending the analysis to RNA-seq data of the 104 NFκB target genes, the PCA plot showed that both mutations result in severe deficiency in TNF-induced gene expression response (Figure 2.7E), largely equivalent to the EV control. Single gene analysis by heatmap visualization confirmed this global picture (Figure 2.7F): none of the 104 genes showed normal TNF induction, with only one gene, *Slfn2*, being induced to about 50% in the TAD<sup>Δ</sup> mutant. In sum, despite the elevated TNF-induced NFκB activity in these mutant cells (due to deficient

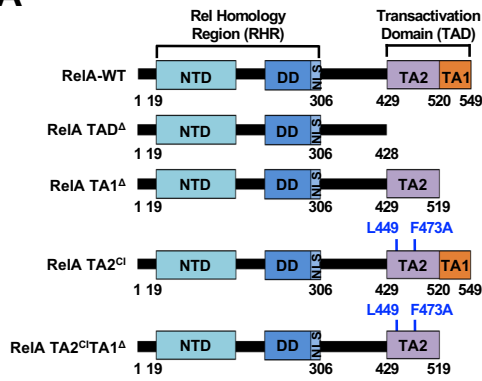
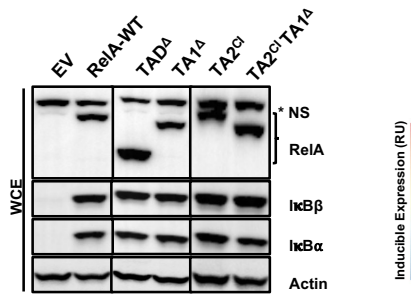
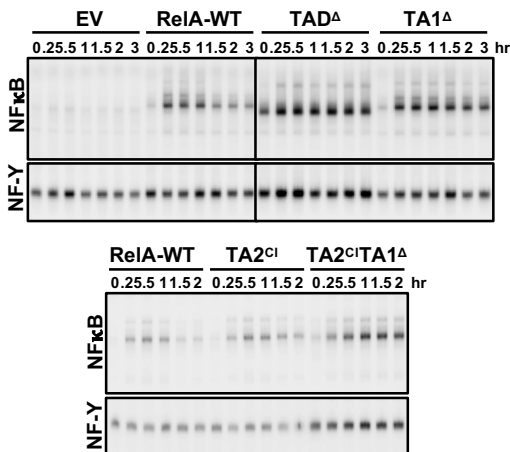
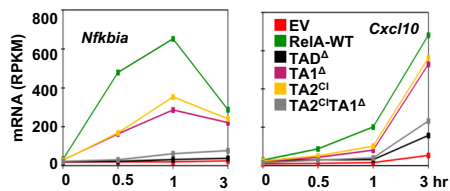
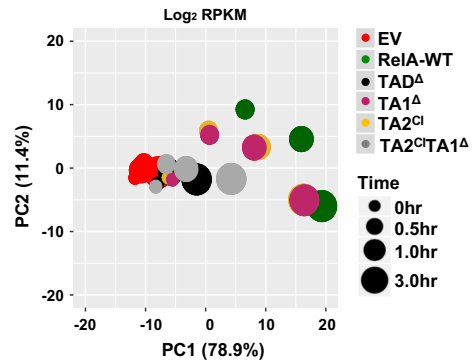
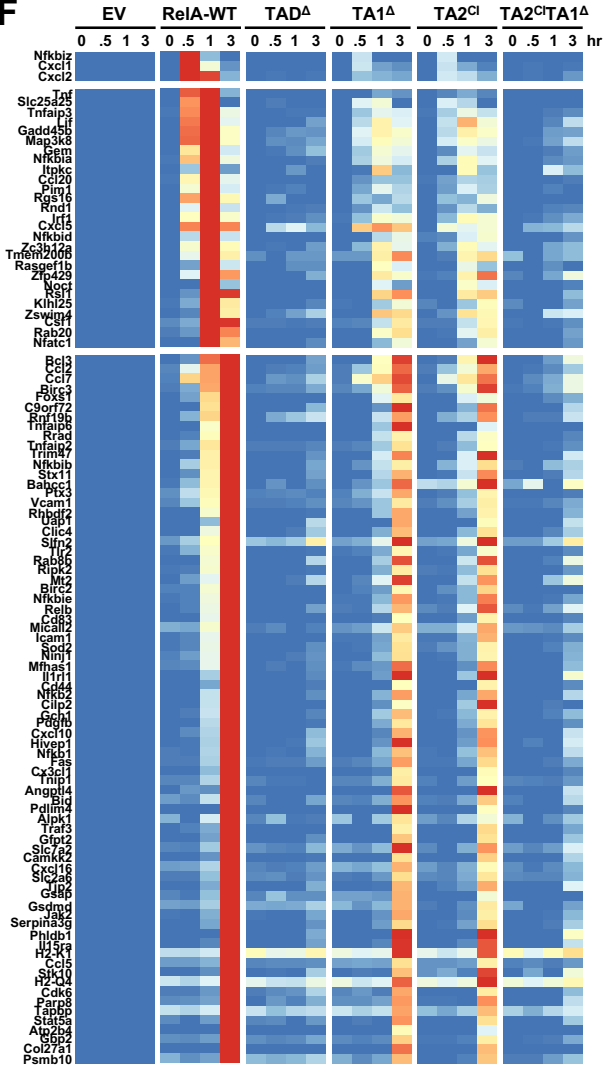
negative feedback control), the data indicates that all transcriptional activation functions of NFκB require the C-terminal activation domains TA1 and TA2.

To determine whether NFκB target genes have differential requirements for either TA1 or TA2, we constructed variants of RelA (Figure 2.8A), a deletion mutant lacking residues 520 to 549 that define the TA1 (hereafter is referred to as TA1<sup>Δ</sup>), a double amino acid mutant L449A and F473A, which abrogates the RelA TA2 function of interacting with the TAZ1 domain of transcriptional coactivator, CBP/p300 (Mukherjee et al., 2013), referred to as (TA2<sup>o</sup>), and a double mutant (TA2<sup>o</sup>TA1<sup>Δ</sup>). (Internal deletion of TA2 appeared to disrupt the function of TA1, which prompted us to design point mutations within the domain.) Following reconstitution of *p53<sup>-/-</sup>crel<sup>-/-</sup>rela<sup>-/-</sup>* MEFs, we confirmed that expression levels of RelA variants and the canonical IκBs were close to those in RelA-WT control (Figure 2.8B). Further, gel mobility shift analysis confirmed that these targeted mutations did not interfere with NFκB dimerization, activation, and DNA binding to κB sites upon TNF stimulation (Figure 2.8C). However, similar to C-term<sup>Δ</sup> and TAD<sup>Δ</sup> mutants examined previously we found that NFκB DNA-binding activity was persistent over the 3-hour time course indicative of a loss of proper negative feedback control. Indeed, TNF-induced *Nfkb1a* mRNA expression was substantially diminished in single mutants and abrogated in the double mutant (Figure 2.8D).



**Figure 2.7 The RelA C-terminal portion is required for TNF induction of all NFκB target genes.** (A) Schematic illustrates the RelA variants to be tested: RelA C-term<sup>Δ</sup> (aa 1-325) and RelA TAD<sup>Δ</sup> (aa 1-428). (B) Protein expression of RelA, IκBβ, IκBα, and Actin as loading control, in indicated unstimulated cells assayed by immunoblotting. (C) Analysis of nuclear NFκB activity by EMSA with κB and NF-Y (loading control) probes of nuclear extracts prepared at indicated times after TNF stimulation of genetically complemented cells shown in (B). (D) Line plots of mRNA expression for NFκB target genes *Nfkb1a* and *Cxcl10* genes in response to TNF in same cells. (E) PCA plot of all 104 NFκB target genes in response to TNF in same cells. (F) Heatmap of the transcriptional response to TNF of the 104 target genes in same cells. Relative induced expression is shown.



**A****B****C****D****E****F**

**Figure 2.8 RelA transactivation domains TA1 and TA2 both contribute to the TNF response of NF- $\kappa$ B target genes.** (A) The schematic illustrates the RelA variants to be tested: a deletion mutant of TA1, a CBP-interaction mutant of TA2 (TA2<sup>o</sup>) and a combination mutant. (B) Protein expression of RelA, I $\kappa$ B $\beta$ , I $\kappa$ B $\alpha$ , and Actin as loading control, in indicated unstimulated cells assayed by immunoblotting with antibodies specific to RelA, I $\kappa$ B $\beta$ , I $\kappa$ B $\alpha$ , and  $\beta$ -Actin. (C) Analysis of nuclear NF $\kappa$ B activity by EMSA with  $\kappa$ B and NF-Y (loading control) probes of nuclear extracts prepared at indicated times after TNF stimulation of genetically complemented cells shown in (B). (D) Line plots of mRNA expression for *Nfkbia* and *Cxcl10* genes in response to TNF stimulation in same cells. (E) PCA plot of all 104 NF $\kappa$ B target genes in response to TNF in same cells. (F) Heatmap of the transcriptional response of the 104 target genes in same cells. Relative induced expression is shown.

To extend the gene expression analysis to the 104 NFκB target genes, we analyzed RNA-seq data for all described mutants. PCA revealed that both single mutants showed global deficiencies in the TNF-induced gene expression response, while the double mutant appears almost entirely deficient in transcriptional activation, akin to the complete TAD<sup>A</sup> mutant (Figure 2.8E). Interestingly, visualizing the data at single gene resolution in the heatmap format (Figure 2.8F) revealed subtle differences in the functionality of the mutants that warranted a quantitative analysis.

### **A model-aided analysis reveals gene-specific logic gates formed by RelA TA1 and TA2**

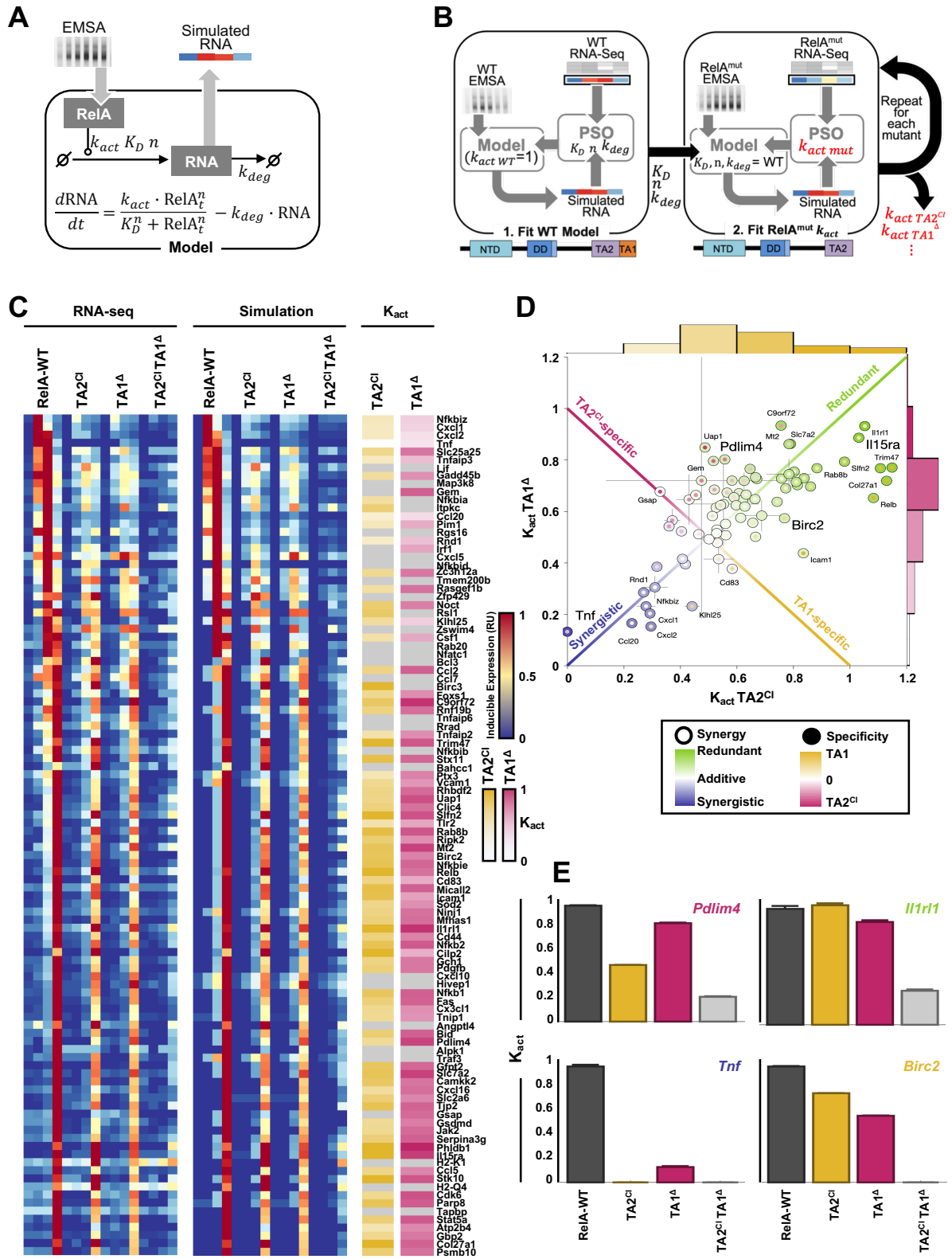
For each RelA target gene to assess the functional requirements of TA1 and TA2 quantitatively, we had to address the potentially confounding effect of alterations in the NFκB activation time course (Figure 2.8C). We developed a mathematical formalism that considers both the measured time courses of mRNA and NFκB DNA-binding activity that drives transcription; hence, an ordinary differential equation (ODE) model of RelA-dependent gene expression was constructed (Figure 2.9A). The model consists of a single ODE representing the rate of change of mRNA that results from NFκB-driven synthesis and mRNA decay (see Methods). NFκB-driven mRNA synthesis is a function of the amount of NFκB DNA binding activity and the specific activation activity ( $k_{act}$ ) of the particular RelA variant.

Given the DNA binding activity measured for each RelA TA mutant, we could identify the activation rate ( $k_{act}$ ) for each gene that optimally accounts for the measured mRNA profile (Figure 2.9B). Other parameters ( $K_D$ ,  $n_{hill}$ ,  $k_{deg}$ ) were also fit but assumed to be the same for all RelA variants, as they represent intrinsic properties of the gene promoter of mRNA. Particle

swarm optimization was used to minimize the distance between simulated RNA time courses and the measured RNA-seq data for each of the 104 genes and the model was able to recapitulate the experimental findings indicating that altered activation strengths associated with each TA mutant could explain the altered RNA-seq results (Figure 2.9C). A stringent criterion ( $\ln(\text{dist}) < -2.5$ , see Methods) was applied to exclude 28 genes with unsatisfactory fits. For the remaining genes a wide range of activation strengths ( $k_{act}$ ) values were identified for the TA1<sup>Δ</sup> and TA2<sup>Δ</sup> mutants, from ~1 (where TA mutation did not affect gene induction strength relative to RelA-WT) to 0 (where TA mutation of a single TA domain entirely abrogated gene expression) (Figure 2.9C).

Our hope for this analysis was to identify differences in relative dependence on TA1 vs. TA2 among the 104 RelA target genes, and we found modest specificity: for example inflammatory genes Cxcl2, Cd83 and ICAM1 were more TA1-dependent, whereas Pdlim4 (Src inhibitor), Gsap (protease) showed a higher degree of TA2-dependence. However, for many genes the optimally parameterized  $k_{act}$  values for TA1<sup>Δ</sup> and TA2<sup>Δ</sup> mutants were correlated (Figure 2.9C) with marked differences in the degree of the decrease associated with both mutants (Figure 2.9D). For example, Cxcl1, Cxcl2, and Tnf, showed a substantial decrease in transcriptional activity with mutating either TA domain (Figure 2.9D and E bottom left), whereas Il15ra and Il1rl1 when either TA domain was removed (Figure 2.9D and E top right). On the former class of genes, the inability of either TA domain to function effectively on its own suggests that TA1 and TA2 function synergistically, whereas on the latter class of genes, they seem to function redundantly or independently. Thus, the unexpected conclusion from this analysis is that RelA target genes differ whether they impose an AND gate or OR gate logic on the two TA domains within RelA. Given that the activity of TA1 is dependent on the

phosphorylation status of serines in its amphipathic helix, an AND vs OR gate logic determines distinct regulatory role of TA2: in the latter case, TA2 may be primary driver of transcriptional activation, but in the former case, TA2 merely assists or boosts TA1-driven gene activation.



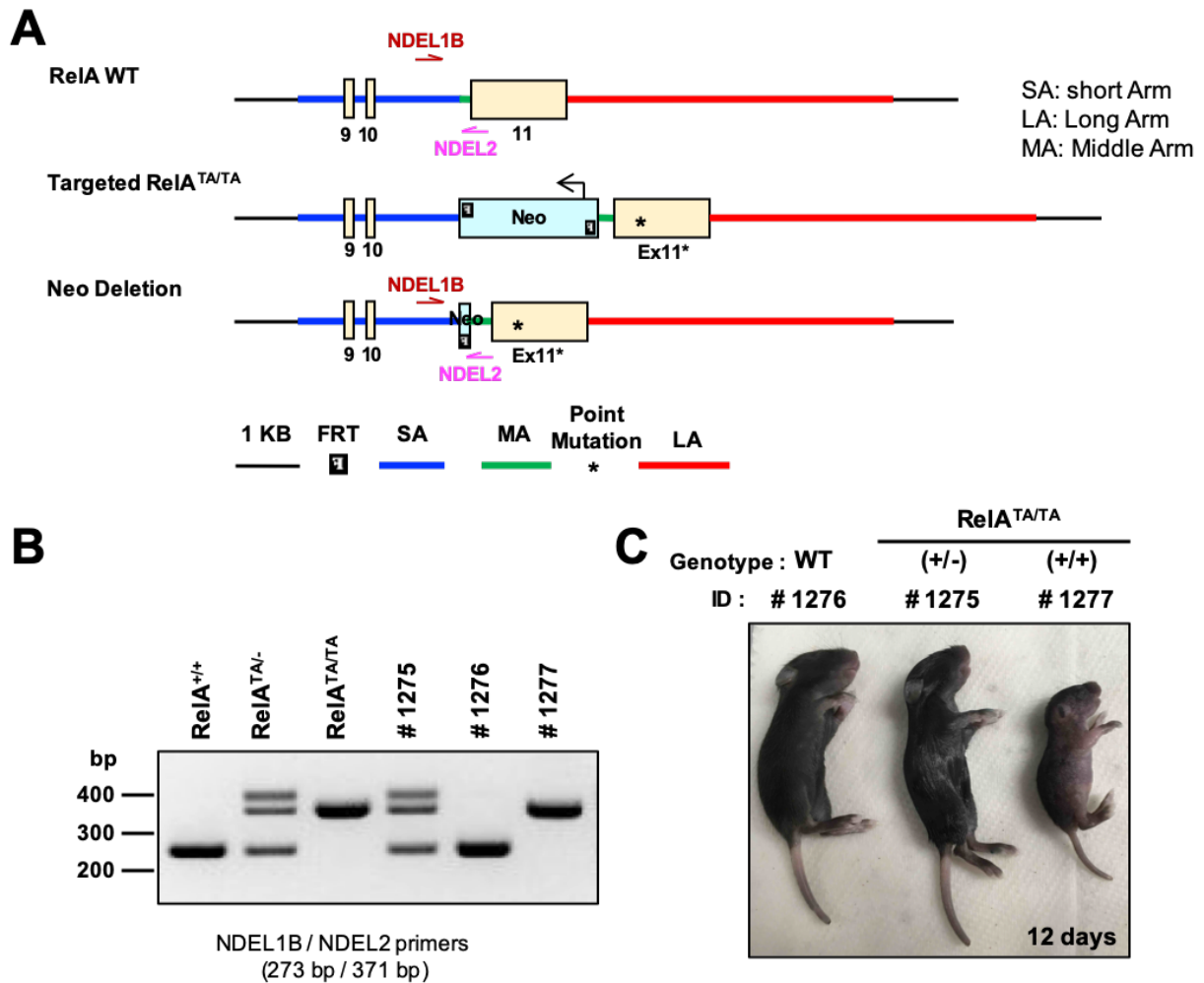
**Figure 2.9 A math model-aided analysis reveals gene-specific requirements for TA1 and TA2.** (A) Schematic of the ordinary differential equation (ODE) used to obtain simulated mRNA dynamics from quantified NFκB activity timecourses. (B) Schematic of the Particle Swarm Optimization (PSO) pipeline used to quantify activation strengths ( $k_{act}$ ) for TAD mutants. First  $K_D, n_{hill}, k_{deg}$  are fit to RelA-WT data with  $k_{act} = 1$ . The identified parameters are then maintained with new  $k_{act}$  fit for each TAD mutant to obtain remaining activation strength (see Methods). (C) experimental (left, RNA-seq) and simulated best-fit mRNA time-course (middle) heatmaps, along with identified  $k_{act}$  for TA2<sup>cl</sup> (yellow) and TA1<sup>Δ</sup> (pink).  $k_{act}$  is shown relative to RelA-WT with brighter colors indicating closer activity to RelA-WT (no effect of mutation) and white indicating complete loss of activity in the mutant ( $k_{act} = 0$ ). Gray indicated a fit with  $\ln(\text{dist}) < -2.5$  (see methods) was not found. (D) Scatter plot of  $k_{act}$  for TA2<sup>cl</sup> and TA1<sup>Δ</sup> for 76 genes with good fit in panel C. Center color represents effect of either single mutation (from green  $k_{act} = 1$  with no change from RelA-WT and redundancy with respect to a single mutation, to blue  $k_{act} = 0$  where either mutation abrogates gene induction and both domains work synergistically to achieve full gene activation). Border color represents off-diagonal effect where a gene shows specific loss of induction in TA2<sup>cl</sup> (pink) or TA1<sup>Δ</sup> (yellow). Gray lines indicate standard deviation of  $k_{act}$  from 3 repeated runs of optimization pipeline. (E) Bar graphs of  $k_{act}$  (relative to mean RelA-WT  $k_{act}$ ) for RelA-WT, TA2<sup>cl</sup>, TA1<sup>Δ</sup> and TA2<sup>cl</sup>TA1<sup>Δ</sup> mutants, shown for 4 example genes arranged to indicate their relative positions in panel D. Error bars indicate standard deviation of  $k_{act}$  from 3 repeated runs of optimization pipeline.

## **A knock-in mouse reveals that regulatory strategies of RelA target genes are generally conserved in different cell types but are often stimulus-specific**

The complementation of RelA-deficient primary MEF cells with mutated variants of RelA allowed us to study the effects of numerous specific mutations on the TNF-response. To dissect regulatory strategies of endogenous target genes in other cell types and in response to other stimuli, we engineered a mouse strain that harbors the previously described RelA TA2<sup>off</sup>TA1<sup>A</sup> variant as a knock-in mutation, termed *RelA<sup>TA</sup>* (Figure 2.10A). Homozygous *RelA<sup>TA/TA</sup>* mice are not embryonic lethal, unlike *RelA<sup>-/-</sup>* mice, but are sickly and smaller than their heterozygous littermates (Figure 2.10B), whose genotype was verified by PCR (Figure 2.10C). To examine whether RelA target genes showed similar or differential regulatory strategies in other cell types and other inflammatory stimuli, we produced an extensive RNA-seq data by stimulating wild-type and *RelA<sup>TA/TA</sup>* primary MEFs and BMDMs with TNF or Toll-Like 4 Receptor ligand lipopolysaccharide (LPS).

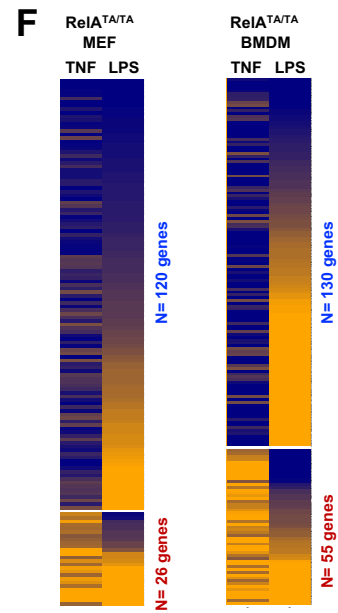
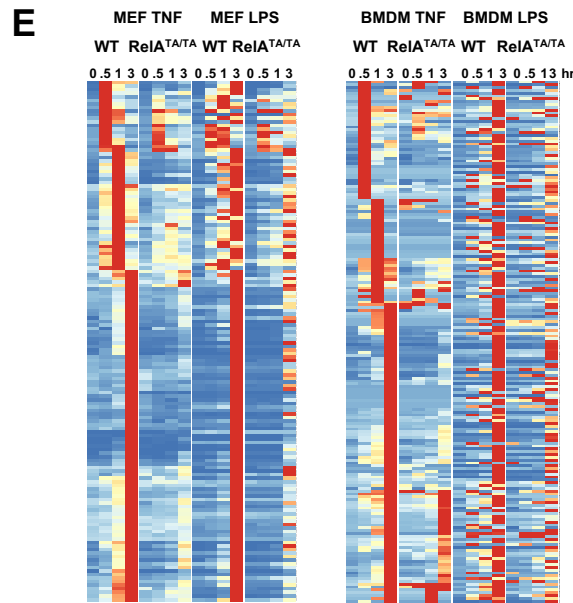
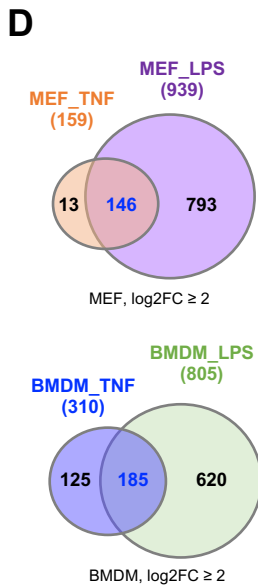
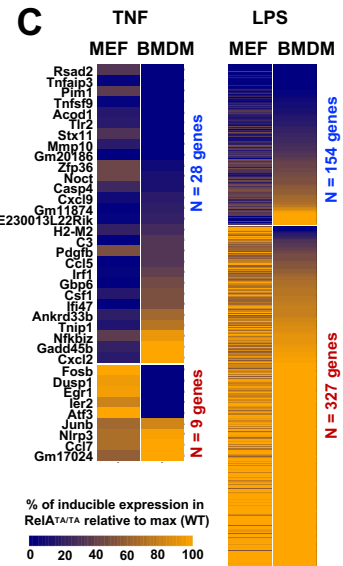
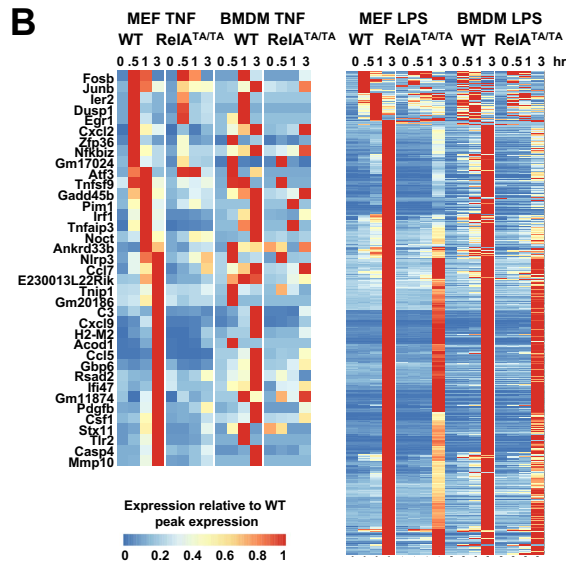
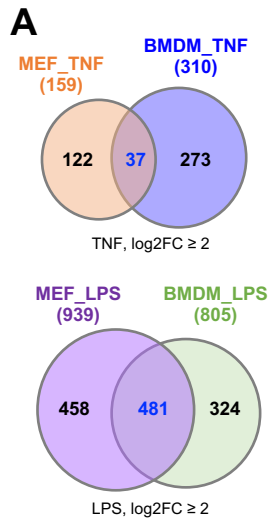
We first identified genes that were activated in both MEFs and BMDMs by a stringent log<sub>2</sub> fold change >2 threshold (Figure 2.11A). We found 37 such genes in response to TNF stimulation and 481 in response to LPS (Figure 2.11A). After peak-normalizing the data for each gene, we plotted the relative expression data from WT and *RelA<sup>TA/TA</sup>* MEFs and BMDMs in order of induction peak time in WT MEFs and subsequent hierarchical clustering (Figure 2.11B). We found that the majority of gene activation events were diminished in both mutant MEFs and BMDMs. We evaluated the phenotype by plotting the percentage of expression in *RelA<sup>TA/TA</sup>* cells relative to the WT peak expression at the same time point for each gene (Figure 2.11C). In MEFs





**Figure 2.10 Generation of a RelA Transactivation Domain mutant knock-in mouse strain.**

(A) Schematic of the knock-in strategy, first targeting the RelA gene with a mutant allele containing the CI mutation in TA2 and deletion of TA1, as well as a Neo gene that is flanked by FRT sites, then deleting Neo with FRT. (B) Confirmation of genotype. PCR product using primer set NDEL1B and NDEL2 with genomic DNA from tail DNA isolated from indicated pups was used to screen mice. PCR product for wild-type band showed at 273 bp, mutant band at 371 bp, visualized by 2% agarose gel. Genotyping results for Mouse IDs corresponds to the mice in (C). (C) Photo of 12 day-old littermate mice of indicated genotypes (WT, RelA<sup>TA/-</sup>, and RelA<sup>TA/TA</sup>) prior to isolation of bone-marrow.



**Figure 2.11 A knock-in mouse reveals that the dual TAD-requirement pertains to other cell-types and stimuli.** (A) Venn diagrams indicating of overlap in induced transcriptional response in MEFs and BMDMs. Induced genes satisfy two criteria:  $\log_2$  fold-change  $\geq 2$  and max RPKM  $> 1$ , by polyA+RNA-seq over a 3 hr timecourse analysis. (*Left panel*) In response to TNF (10ng/mL) 159 genes are induced in WT MEFs and 310 are induced in WT BMDMs. (*Right panel*) In response to LPS (100ng/mL), 939 genes are induced in WT MEFs and 805 induced genes in WT BMDMs. (B) Heatmaps of relative expression of induced genes in WT and RelA<sup>TATA</sup> mutant MEFs or BMDMs in response to (*Left panel*) TNF or (*Right panel*) LPS. Gene names and data plotted in heatmaps are listed in Supplementary Table 2.2 and Table 2.3 for TNF and LPS, respectively. (C) NF $\kappa$ B dependence of induced genes: percentage of peak expression in RelA<sup>TATA</sup> mutant vs. WT. (*Left panel*) Genes induced by TNF in MEFs and BMDMs. Gene names and data plotted in heatmap are listed in Supplementary Table 2.4. (*Right panel*) Genes induced by LPS in MEFs and BMDMs. Gene names and data plotted in heatmap are listed in Supplementary Table 2.5. (D) Venn diagrams indicating of overlap in induced transcriptional response to TNF and LPS (*Left panel*) In WT MEFs, 159 genes were induced by TNF and 939 by LPS. (*Right panel*) In WT BMDMs, 310 genes were induced by TNF and 805 were induced by LPS. (E) Heatmaps of relative expression of TNF- vs. LPS-induced genes in WT and RelA<sup>TATA</sup> mutant (*Left panel*) MEFs or (*Right panel*) BMDMs. Gene names and data plotted in heatmap are listed in Supplementary Table 2.6 and Table 2.7 for MEFs and BMDMs, respectively. (F) NF $\kappa$ B dependence of induced genes: percentage of peak expression in RelA<sup>TATA</sup> mutant vs. WT. (*Left panel*) Genes induced by MEFs by TNF and LPS. Gene names and data plotted in heatmap are listed in Supplementary Table 2.8. (*Right panel*) Genes induced by BMDMs by TNF and LPS. Gene names and data plotted in heatmap are listed in Supplementary Table 2.9.

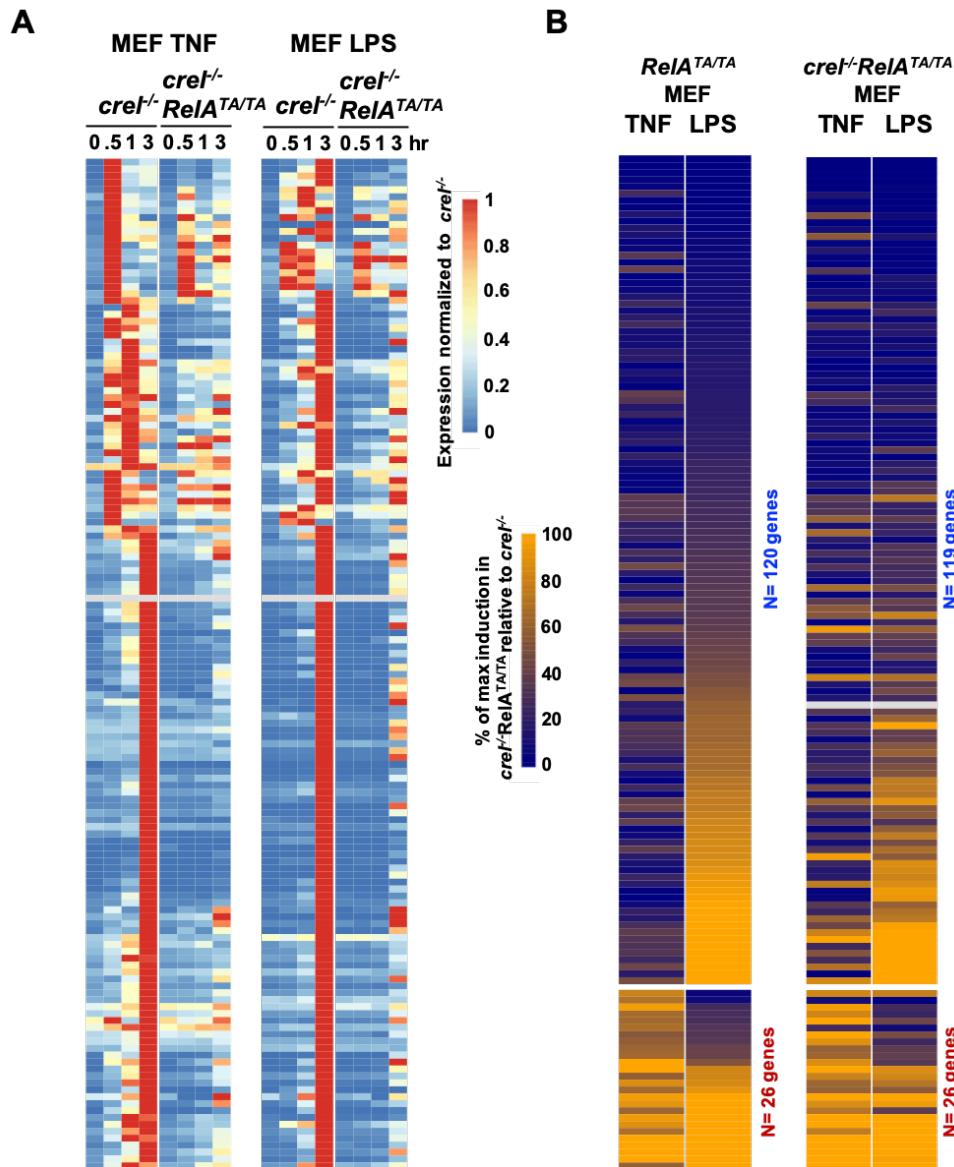
the majority of genes were TA-dependent (28/37), and most of these (25/28) were also TA-dependent in BMDMs. In response to LPS, the majority of genes were TA-independent in both MEFs and BMDMs, given the strong activation of NF $\kappa$ B-independent signaling pathways of IRF3/ISGF3 and MAPK p38. However, of the 154 genes that were identified as TA-dependent in MEFs, about 90% showed an equivalent degree of TA-dependence in BMDMs. These data suggest that regulatory strategies of RelA target genes are generally conserved in different cell types when induced by the same stimulus.

We then asked whether regulatory strategies of NF $\kappa$ B target genes may be stimulus-specific. To this end we identified 146 genes that were induced by both TNF and LPS in MEFs and 185 that were induced by both stimuli in BMDMs (Figure 2.11D). Heatmap visualization of the gene expression timecourses revealed that most genes induced rapidly by TNF peaked later in response to LPS (Figure 2.11E left and right panels). Examining their RelA TA-dependence by collapsing the data to the peak timepoint, we found that of the 120 MEF genes that were TA-dependent in response to TNF, only 60% showed an equivalent degree of TA-dependence in response to LPS, and 15% were entirely TA-independent (Figure 2.11F left and right panels). Similarly, of the 26 genes whose TNF induction was TA-independent half showed TA-dependence in response to LPS. In BMDMs the lack of equivalence was even more pronounced: only 25% showed an equivalent degree of TA-dependence (or independence) in response to TNF and LPS, and more than 40% showed entirely opposite regulatory requirements for RelA's TA domains.

We wondered whether compensation by cRel, which was documented in *RelA*<sup>-/-</sup> MEFs (Hoffmann et al., 2003), was affecting our results. We thus bred the RelA<sup>TA</sup> knock-in strain to a

*crel*<sup>-/-</sup> background and produced RNA-seq data from *crel*<sup>-/-</sup>*RelA*<sup>TATA</sup> and *crel*<sup>-/-</sup> MEFs in response to TNF and LPS stimulations. Focusing on the previously mentioned list of 146 genes that were found induced by both TNF and LPS in WT MEFs, we found 145 also induced in *crel*<sup>-/-</sup> MEF controls (Figure 2.12A, only *Mmp10* gene did not satisfy the stringent criteria of log<sub>2</sub>FC >2 and max RPKM >1; thus, it was grayed out). Our results with *crel*<sup>-/-</sup>*RelA*<sup>TATA</sup> and *RelA*<sup>TATA</sup> MEFs demonstrate that the lack of RelA TA-dependence is generally not due to cRel compensation (Figure 2.12B).

In sum, our transcriptomic analysis using newly developed *RelA*<sup>TATA</sup> mice revealed that regulatory strategies of RelA target genes were generally conserved between MEFs and BMDMs when the same stimulus was used, but that in either cell type, RelA TA dependence observed in response to TNF was not well correlated with dependence in response to LPS. These data indicate that many NFκB target genes engage differential regulatory strategies to different stimuli, consistent with the notion that RelA transactivation activity may integrate signaling pathways that are triggered by some stimuli but not others.



**Figure 2.12 Lack of RelA-TAD-dependence in the transcriptional response of MEFs to TNF or LPS is not due to cRel compensation.** (A) Heatmaps of the transcriptional response 146 genes that are induced in *cRel*<sup>-/-</sup> MEFs in response to TNF and LPS. Shown is the relative expression in *cRel*<sup>-/-</sup> and *cRel*<sup>-/-</sup>*RelA*<sup>TAD/TAD</sup> mutant MEFs in response to (*Left panel*) TNF or (*Right panel*) LPS. Gene names and data plotted in heatmap are listed in Supplementary Table 2.10. (B) NFκB dependence of TNF- and LPS-induced genes in MEFs: percentage of peak expression in (*Left panel*) *RelA*<sup>TAD/TAD</sup> mutant vs. WT, and (*Right panel*) *cRel*<sup>-/-</sup>*RelA*<sup>TAD/TAD</sup> mutant vs. WT. Gene names and data plotted in heatmap are listed in Supplementary Table 2.8.

## SUPPLEMENTARY TABLES

### Supplementary Table 2.1 List of RelA binding locations and TNF-induced gene expression

**for 104 NFκB target genes.** The table shows all identifiable RelA-binding peaks and their associated κB DNA elements for each of the 104 NFκB target genes, from -10kb to gene TSS and to +10kb downstream of gene TSS.

Column A: Genomic location of each RelA ChIP-seq peak.

Column B: Distance from gene TSS for start of RelA peak.

Column C: Distance from gene TSS for end of RelA peak.

Column D: Gene coding strand direction (-1 refers to antisense or negative strand, 1 refers to sense or positive strand).

Column E: each κB sequence respective to its RelA ChIP-seq peak.

Column F: Genomic location of each κB sequence relative to gene TSS

Column G: ChIP-seq score for RelA peak in reconstituted RelA-WT (Figure 2.3 and Figure 2.5).

Column H: ChIP-seq score for RelA peak in reconstituted RelA<sup>DB</sup> mutant (Figure 2.5).

Column I: Ratio of RelA ChIP-seq score (RelA<sup>DB</sup> mutant over RelA-WT).

Column J: RelA ChIP-seq peak classification based on results in Column I (not\_reduced is defined by ratio of RelA<sup>DB</sup> mutant over RelA-WT  $\geq 0.5$  and reduced is if ratio of RelA<sup>DB</sup> mutant over RelA-WT  $< 0.5$ ).

Column K: Percentage of dependence on NFκB based on nascent transcript expression, analyzed by caRNA-seq in WT vs *crel<sup>-/-</sup>rela<sup>-/-</sup>* MEFs stimulated with TNF.

Column L: Fold-induction ( $\log_2$ ) of nascent transcript expression (caRNA-seq) in response to TNF in WT MEFs. Peak expression in WT divide by its unstimulated condition.

Column M: Mean of fold-induction ( $\log_2$ ) of mRNA, analyzed by polyA+RNA-seq in WT MEFs stimulated with TNF.

Column N: Ensemble Gene ID for each gene annotated with biomaRt (R).

Column O: Gene symbol.

Column P: Description of Gene.

### Supplementary Table 2.2

The table contains the relative expression data plotted in heatmap visualized in Figure 2.11B. 37 genes were found upregulated in both WT MEFs and BMDMs in response to TNF stimulation by a stringent  $\log_2$  fold change  $> 2$  threshold. For each gene, relative expression data in WT or

*RelA<sup>TATA</sup>* MEFs and BMDMs were plotted by peak-normalizing the data in order of the time point of peak induction in their respective WT control (see Materials and Methods) and subsequent hierarchical clustering was performed within each peak timing of induction. Of note, averaged RPKMs from WT and *RelA<sup>TATA</sup>* MEFs data (from two replicate) were used to calculate relative expression for each gene. Same ordering of genes were plotted in WT and *RelA<sup>TATA</sup>* BMDMs data. Scale of 0 to 1; 0 corresponds to no inducible expression and 1 corresponds to similar expression in WT control, respectively.

### **Supplementary Table 2.3:**

The table contains the relative expression data plotted in heatmap visualized in Figure 2.11B. 481 genes were found upregulated in both WT MEFs and BMDMs in response to LPS stimulation by a stringent Log<sub>2</sub> fold change >2 threshold. For each gene, relative expression data in WT or *RelA<sup>TATA</sup>* MEFs and BMDMs were plotted by peak-normalizing the data in order of the time point of peak induction in their respective WT control and subsequent hierarchical clustering was performed within each peak timing of induction. Same ordering of genes were plotted in WT and *RelA<sup>TATA</sup>* BMDMs data. Scale of 0 to 1; 0 corresponds to no inducible expression and 1 corresponds to similar expression in WT control, respectively.

### **Supplementary Table 2.4:**

The table contains the percentage of expression data for the 37 TNF-responsive genes in *RelA<sup>TATA</sup>* MEFs and BMDMs that were plotted in Figure 2.11C heatmap. For each gene in response to TNF stimulation, averaged percentage of expression data (from two replicate) in *RelA<sup>TATA</sup>* MEFs and BMDMs (1 replicate) relative to their respective WT peak expression at the same time point were



plotted. Same ordering of genes were plotted for percentage of expression data in WT and *RelA*<sup>TATA</sup> BMDMs. For heatmap visualization, these genes were first identified by their TA-dependence relative to WT MEFs (<50% referred to as TA-dependent and ≥50% referred to as TA-independent). Within each category, genes were furthered ordered by their TA-dependence found in BMDM data. Scale of 0 to 100 corresponds to no expression and 100 is similar expression to WT control, respectively.

**Supplementary Table 2.5:**

This table contains the percentage of expression data for the 481 LPS-responsive genes in *RelA*<sup>TATA</sup> MEFs and BMDMs that were plotted in Figure 2.11C heatmap. For each gene, percentage of expression in *RelA*<sup>TATA</sup> MEFs and BMDMs relative to their respective WT peak expression at the same time point were calculated. For heatmap visualization, these genes were first identified by their TA-dependence relative to WT MEFs (<50% referred to as TA-dependent and ≥50% referred to as TA-independent). Within each category, genes were furthered ordered by their TA-dependence found in BMDM data. Scale of 0 to 100 corresponds to no expression and 100 is similar expression to WT control, respectively.

**Supplementary Table 2.6:**

The table contains the relative expression data for 146 genes induced in WT and *RelA*<sup>TATA</sup> MEFs by TNF and LPS stimulation found by a stringent log<sub>2</sub> fold change >2 threshold that were plotted in Figure 2.11E (left panel) heatmap. For each gene, relative expression data in WT and *RelA*<sup>TATA</sup> MEFs in response to either TNF or LPS stimulation were calculated. Of note, averaged RPKMs from WT and *RelA*<sup>TATA</sup> MEFs data (from two replicate) in response to TNF were used to calculate relative

expression for each gene. Ordering of gene list is based on TNF-stimulated data in WT and same ordering of genes (from top to bottom of heatmap and table) were shown for LPS-stimulated data. Scale of 0 to 1; 0 corresponds to no inducible expression and 1 corresponds to similar expression in WT control, respectively.

#### **Supplementary Table 2.7:**

The table shows the relative expression data for 185 genes induced in BMDMs by TNF and LPS stimulation identified in WT BMDMs data. Heatmap visualization of this data in WT and *RelA<sup>TATA</sup>* BMDMs is shown in Figure 2.11E (right panel) heatmap. For each gene, relative expression data in WT and *RelA<sup>TATA</sup>* BMDMs in response to either TNF or LPS stimulation were calculated. Ordering of gene list is based on TNF-stimulated data in WT and same ordering of genes (from top to bottom of heatmap) were shown for LPS-stimulated data. Scale of 0 to 1; 0 corresponds to no inducible expression and 1 corresponds to similar expression in WT control, respectively.

#### **Supplementary Table 2.8:**

The table shows the percentage of expression data for the 146 upregulated genes in *RelA<sup>TATA</sup>* and 146 genes in *crel<sup>-/-</sup>RelA<sup>TATA</sup>* MEFs in response to TNF and LPS stimulation, visualized in Figure 2.11F and Figure 2.12B, respectively. These heatmaps represent the degree of RelA TAD dependence by evaluating the phenotype of *RelA<sup>TATA</sup>* and *crel<sup>-/-</sup>RelA<sup>TATA</sup>* mice. For each gene, percentage of expression data in *RelA<sup>TATA</sup>* or *crel<sup>-/-</sup>RelA<sup>TATA</sup>* relative to their respective WT or *crel<sup>-/-</sup>* peak expression at the same time point. Scale of 0 to 100 corresponds to no expression and 100 is similar expression to WT or *crel<sup>-/-</sup>* control, respectively.

**Supplementary Table 2.9:**

The table shows the percentage of expression data for the 185 upregulated genes in *RelA<sup>TATA</sup>* BMDMs in response to TNF and LPS stimulation, visualized in Figure 2.11F (right panel). These heatmaps represent the degree of RelA TAD dependence by evaluating the phenotype of *RelA<sup>TATA</sup>* mice. For each gene, percentage of expression data in *RelA<sup>TATA</sup>* BMDMs relative to their respective WT peak expression at the same time point. Scale of 0 to 100 corresponds to no expression and 100 is similar expression to WT control, respectively.

**Supplementary Table 2.10:**

The table shows the relative expression data for 146 genes induced in *crel<sup>-/-</sup>* and *crel<sup>-/-</sup>RelA<sup>TATA</sup>* MEFs by TNF and LPS stimulation. Heatmap visualization of these genes in *crel<sup>-/-</sup>* and *crel<sup>-/-</sup>RelA<sup>TATA</sup>* MEFs are visualized in Figure 2.12A. Of note, *Mmp10* gene is included in this gene list to preserve the ordering of genes as in WT MEFs control; however, the gene did not satisfy the stringent criteria of  $\log_2FC > 2$  and  $\max RPKM > 1$  in *crel<sup>-/-</sup>* and *crel<sup>-/-</sup>RelA<sup>TATA</sup>* MEFs and thus, “NA” was filled in for the data. Only 145 genes were also induced in *crel<sup>-/-</sup>* MEF controls and was plotted in Figure 2.12A (left panels).

## MATERIALS AND METHODS

### Reagents

For cell stimulations we used 10ng/mL mouse TNF (R&D Systems # 410-MT), 100ng/mL LPS (Sigma, B5:055), and 10ng/mL mouse IL-1 $\beta$  (R&D Systems, catalog #401-ML-CF) to stimulate cells. pBABE-puro plasmid vector is commercially available through Addgene cat #1764. Antibodies used for western blotting were specific for RelA (Santa Cruz Biotechnology, sc-372, sc-109), I $\kappa$ B $\alpha$  (Santa Cruz Biotechnology, sc-371), I $\kappa$ B $\beta$  (Santa Cruz Biotechnology, sc-945), p50 (BioBharati LifeScience #BB-AB0080),  $\alpha$ -Tubulin (Santa Cruz Biotechnology, sc-5286),  $\beta$ -actin (Santa Cruz Biotechnology, sc-1615), Histone 3 (Abcam, #ab1791), and p84 (Abcam, #ab131268).

### Construction of Mutant RelA Plasmids

The pBABE-puro plasmid vector containing RelA was constructed by ligating the polymerase chain reaction (PCR) amplified coding region of murine RelA (amino acids 1 to 549) restricted with *EcoRI* and *Sall*. Agilent QuikChange II Site-Directed Mutagenesis Kit (Agilent Technologies) was used for all RelA point mutation and deletion variants. DNA binding mutant (RelA<sup>DB</sup>) within amino-terminal were mutated by a triple substitution at residues Arg35, Tyr36, and Glu39 to Ala (R35A, Y36A, R39A). Mutagenesis of the carboxyl-terminal region for C-term <sup>$\Delta$</sup> , TAD <sup>$\Delta$</sup> , and TA1 <sup>$\Delta$</sup>  were performed by displacing residues Pro326, Ala429, and Ser520, respectively, with a STOP codon sequence. All site-specific mutations were verified by Sanger

sequencing analysis and sequencing analyses of the resulting RelA mutants showed that the targeted sites were the only changes in the DNA sequence.

## **Cell Culture**

Wild-type or mutant primary MEFs were generated from E11.5-13.5 embryos and cultured in Dulbecco's Modified Eagle's Medium (DMEM) supplemented with 10% bovine calf serum (BCS), 1% penicillin-streptomycin and 1% L-Glutamine. BMDMs were made through the isolation of  $5 \times 10^6$  bone marrow cells from mouse femurs of WT or *RelA<sup>TATA</sup>*C57BL/6 mice following red blood cell lysis and seven-day culture with 30% L929-conditioned medium.

## **Genetic Complementation of MEFs**

For transfection, Platinum-E (Plat-E) retroviral packaging cell line (Morita et al., 2000), a modified cell line derived from HEK-293T, were plated on 10-cm plates 16-hr the day before transfection at 50% confluent in DMEM supplemented with 10% fetal calf serum, 1% penicillin-streptomycin and 1% L-Glutamine. Cells were transfected using 300 $\mu$ L of Opti-MEM medium (ThermoFisher Scientific) and polyethylenimine (PEI; 1 $\mu$ g/ $\mu$ L in 1xPBS pH4.5, Polysciences #23966-2) with 7 $\mu$ g of retroviral construct DNA, pBABE-puro EV control or RelA expressing constructs (4:1 ratio of PEI ( $\mu$ L):plasmid DNA ( $\mu$ g)). Transfection complex (Opti-MEM medium, PEI reagent, plasmid DNA) were incubated for 20-min at room temperature then added drop-wise to Plat-E cells for 6 hours. Transfected media was replaced with fresh DMEM media containing 10% fetal calf serum, 1% penicillin-streptomycin and 1% L-Glutamine. Cells were further incubated for a total of 48-hr post-transfection and prior to collecting viruses. Viruses-

containing supernatant were filtered through a 0.45  $\mu\text{m}$  filter and used to infect *p53<sup>-/-</sup>crel<sup>-/-</sup>rela<sup>-/-</sup>* MEFs with the addition of 4 $\mu\text{g}/\text{mL}$  Polybrene. 48-hr post-infection of cells with viruses the stably transduced cells were selected with 2 $\mu\text{g}/\text{mL}$  puromycin for a total of 72 hours. Post selection with puromycin, puromycin-containing medium is removed and cells are passaged twice for recovery prior to being expanded in culture for experiments. pBABE-puro empty vector without the *RelA* gene fragment is used as a negative control, to maintain a stable retrovirally transduced RelA knockout cell line, meanwhile pBABE-puro containing full-length RelA (RelA-WT) is used as a positive RelA cell line control.

### **Western Blotting**

For whole cell extracts,  $3 \times 10^6$  cells were lysed with RIPA buffer containing 1mM PMSF and 1mM DTT followed by lysing with 1x SDS-PAGE sample buffer containing 5%  $\beta$ -mercaptoethanol. Cell lysates were separated by SDS-PAGE and subjected to western blotting. Nuclear and cytoplasmic extracts were performed with standard methods as described previously (Hoffmann *et al*, 2002; Werner *et al*, 2005). Western blots were probed with antibodies against RelA (Santa Cruz Biotechnology, sc-372), RelA (Santa Cruz Biotechnology, sc-109), I $\kappa$ B $\alpha$  (Santa Cruz Biotechnology, sc-371), I $\kappa$ B $\beta$  (Santa Cruz Biotechnology, sc-945), p50 (BioBharati LifeScience #BB-AB0080),  $\alpha$ -Tubulin (Santa Cruz Biotechnology, sc-5286),  $\beta$ -actin (Santa Cruz Biotechnology, sc-1615), Histone 3 (Abcam, #ab1791), p84 (Abcam, #ab131268).

## **Electrophoretic Mobility Shift Assay (EMSA)**

EMSA was carried out with standard methods as described previously (Hoffmann *et al*, 2002; Werner *et al*, 2005). In brief, 2.5 $\mu$ L total normalized nuclear extracts were incubated for 15-min with 0.01pmol of P<sup>32</sup>-labeled 38bp double-stranded oligonucleotide containing two consensus  $\kappa$ B sites (5'-GCTACAAGGGACTTTCCGCTGGGGACTTTCCAGGGAGG-3'; or with NF-Y loading control (5'-GATTTTTTTCCTGATTGGTTAAA-3' ; 5'-ACTTTTAACCAATCAGGAAAAA-3') in binding buffer [10mM Tris-Cl (pH 7.5), 50mM NaCl, 10% glycerol, 1% NP-40, 1mM EDTA, 0.1mg/mL Poly(deoxyinosinic-deoxycytidylic)], in a final reaction of 6 $\mu$ L. The reaction mixtures were run on a non-denaturing 5% acrylamide (30:0.8) gel containing 5% glycerol and 1X TGE buffer [24.8mM Tris, 190 mM glycine, 1mM EDTA] at 200 volts for 2 hours. The gel was visualized by Typhoon Scanner (GE Healthcare Life Sciences), in which the NF-Y loading control gel was used to normalize for loading variability.

## **Immunoprecipitation**

Whole cell extracts (WCE) were lysed with RIPA buffer containing 1mM PMSF and 1mM DTT. Anti-RelA antibody (Santa Cruz Biotechnology, sc-372G) was conjugated to prewashed magnetic protein-G beads (Life Technologies Dynabeads) for 30-min at room temperature followed by addition unstimulated WCE in RIPA buffer containing 1mM PMSF and 1mM DTT and incubation overnight (~ 16-hr). The beads were then washed thoroughly with 1X TBS-T buffer and IP samples were eluted with 1X SDS-sample buffer containing 5%  $\beta$ -

mercaptoethanol. Samples were resolved on SDS-PAGE and western blotting with antibodies specific for anti-RelA, anti-I $\kappa$ B $\alpha$ , anti-I $\kappa$ B $\beta$ , and anti-p50.

### **RNA Isolation and Sequencing (RNA-seq)**

MEF cells at ~80% confluence were serum-starved by overnight incubation in Dulbecco's Modified Eagle's Medium supplemented with 0.5% bovine calf serum (BCS), 1% penicillin-streptomycin and 1% L-Glutamine prior to stimulation. For chromatin-associated RNA-seq (caRNA-seq), nascent RNA transcripts were prepared from the chromatin fraction (Tong et al., 2016) using TRIzol according to the manufacturer's instruction (Life Technologies) and purified using Direct-zol RNA Microprep Kit (Zymo Research cat#R2060). RNA libraries were prepared from ribo-depleted using KAPA Stranded RNA-Seq Kit with RiboErase (KAPA Biosystems, cat#KK8483) with 400ng of starting total RNA material. For polyA+RNA-seq analysis, total RNA was isolated with the Qiagen RNeasy Mini Kit according to the manufacturer's instructions, quantified using Epoch Spectrophotometer System (Biotek), and purified from 1 $\mu$ g of starting total RNA material using oligo (dT) magnetic beads before fragmenting at high temperature with divalent cations. Complementary DNA libraries were generated using KAPA Stranded mRNA-Seq Kit (KAPA Biosystems, cat#KK8421), and quantitation was performed using Qubit 2.0 fluorometer using dsDNA BR assay kit #Q32853. Sequencing was performed on Illumina HiSeq 2000 and HiSeq 4000 with single-end 50-bp sequencing, according to manufacturer's recommendations and prepared by Broad Stem Cell Research Center core facility at the University of California, Los Angeles.



## **RNA-seq Data Analysis**

Reads were aligned with STAR to Gencode mouse mm10 genome and RefSeq genes and featureCounts were used to obtain aligned raw counts. Only uniquely mapped reads with a mapping quality score of  $\geq 20$  were kept for further analysis, using samtools. Read counts were normalized for library size and transcript length by conversion to RPKM and gene below the maximum RPKM  $< 1$  were excluded from downstream analysis. DESeq2 was used identify induced genes for subsequent analysis using the following criteria:  $\geq 2$ -fold increase in expression at any one time point over basal with FDR threshold of 0.01. Principal components were calculated with prcomp package and plotted with ggplot. caRNA-seq and polyA+RNA-seq heatmaps were plotted using pheatmap package. HOMER (Heinz et al., 2010) was used to assess for enrichment of *de novo* and known transcription factor binding motifs for NF $\kappa$ B dependent genes with promoter sequences 1 kb upstream and 0.3 kb downstream of the transcription start site. An in-depth description of this software can be found at [homer.ucsd.edu/homer](http://homer.ucsd.edu/homer). Gene ontology analysis in biological processes for NF $\kappa$ B target genes were performed using Enrichr (Chen et al., 2013; Kuleshov et al., 2016). The 5 most enriched GO terms were selected for NF $\kappa$ B-dependent genes.

## **Chromatin Immunoprecipitation and Sequencing (ChIP-seq)**

MEF cells ( $8 \times 10^6$  cells per plate) were serum-starved overnight with 0.5% BCS medium, then stimulated with 10ng/mL TNF at indicated time points. For ChIP, cells were double cross-linked with 100mM disuccinimidyl glutarate/PBS solution (DSG, ThermoFisher Scientific #20593) for 30-min followed by 1% methanol-free Formaldehyde/PBS solution (ThermoFisher

Scientific #28908) for 15-min. Cross-linked cells were quenched with 125mM Glycine for 5 min and washed twice with cold PBS followed by snap freezing with dry ice. The cell pellets were thawed and lysed in Lysis Buffer 1, on ice. Cells were briefly sonicated with Diagenode Bioruptor 300 sonication system (medium power, 15 sec ON/15 sec OFF, 2 cycles) in Diagenode 1.5mL TPX microtubes (100µl-max 300 µl/tube). After centrifugation, cell pellets were lysed in Lysis Buffer 2 and incubated for 10 min at room temperature. Following centrifugation, cell nuclear pellets were lysed in Lysis Buffer 3. Nuclear lysates were sonicated with Diagenode Bioruptor 300 sonication system (low power, 30 sec ON/30 sec OFF, 12 cycles) in Diagenode 1.5mL TPX microtubes. Sonication was stopped every 4 cycles for incubation on ice for 1 min, gentle inversion and pulse-spin. Sonicated nuclear supernatant containing DNA fragments were consolidated with the same sample into a single 1.5 mL polypropylene tube. The lysates were centrifuged at max speed for 10 min at 4°C. The supernatants were transferred to 2 mL no-stick microtubes (Phenix Research cat# MH-820S) with 3 volumes of Dilution buffer and 5µg anti-RelA antibody (Santa Cruz Biotechnology, sc-372), incubated overnight at 4°C. Next day, antibody-chromatin complexes were incubated with 30µL magnetic protein G beads (Life Technologies Dynabeads protein G #1004D) for 5 hours at 4°C. Chromatin-immunoprecipitates were washed 3 times (4 min wash at 4°C) with each of the following buffer in this order: low-salt wash buffer, high-salt wash buffer, LiCl buffer, and TE buffer. ChIP DNA was eluted in elution buffer overnight at 65°C. 1% inputs and ChIP DNA fragments were subjected to reverse cross-linking, RNase A digestion (50µg), Proteinase K digestion (50µg), and purification with AMPure XP beads (Beckman Coulter). Input DNA samples were quantified with dsDNA BR assay kit #Q32853, and ChIP DNA samples were quantified with dsDNA HS assay kit

(Q32854). Quantitation was performed using Qubit 2.0 fluorometer. ChIP-Seq DNA libraries were prepared from 5ng of Inputs or ChIP DNA using NEBNext Ultra DNA Library Prep Kit for Illumina (New England BioLabs, # E7370L).

***ChIP Buffer composition***

Lysis Buffer 1: 50mM HEPES-KOH (pH 7.6), 140mM NaCl, 1mM EDTA, 10% Glycerol, 0.5% NP-40, 0.25% Triton X-100 [with freshly added 1X EDTA-free protease inhibitors].

Lysis Buffer 2: 10mM Tris-Cl (pH 8.0), 200mM NaCl, 1mM EDTA, 0.5mM EGTA [with freshly added 1X EDTA-free protease inhibitors].

Lysis Buffer 3: 10mM Tris-Hcl (pH 8.0), 100mM NaCl, 1mM EDTA, 0.5mM EGTA, 0.1% Na Deoxycholate, 0.5% N-lauroylsarcosine sodium salt, 0.2% SDS [with freshly added 1X EDTA-free protease inhibitors].

Dilution Buffer: 10mM Tris-Cl (pH 8.0), 160mM NaCl, 1mM EDTA, 0.01% SDS, 1.2% Triton X-100 [with freshly added 1X EDTA-free protease inhibitors].

Low Salt Wash Buffer: 50mM HEPES-KOH (pH 7.6), 140mM NaCl, 1mM EDTA, 1% Triton X-100, 0.1% Na Deoxycholate, 0.1% SDS [with freshly added 0.5X EDTA-free protease inhibitors].

High Salt Wash Buffer: 50mM HEPES-KOH (pH 7.6), 500mM NaCl, 1mM EDTA, 1% Triton X-100, 0.1% Na Deoxycholate, 0.1% SDS [with freshly added 0.5X EDTA-free protease inhibitors].

LiCl Buffer: 20mM Tris-HCl (pH 8.0), 250mM LiCl, 1mM EDTA, 0.5% Na Deoxycholate, 0.5% NP-40

TE Buffer: 10mM Tris-HCl (pH 8.0), 1mM EDTA

Elution Buffer: 10mM Tris-HCl (pH 8.0), 1mM EDTA, 1% SDS

### **ChIP-seq Data Analysis**

Sequencing reads were aligned to the mouse mm10 genome and RefSeq genes using Bowtie 2 (Langmead and Salzberg, 2012) and filtered using Samtools. Uniquely mapped reads were used to identify peaks for each sample individually with MACS2 version 2.1.0 using default settings except for FDR of 0.01. Differential RelA binding events were plotted as heatmap using plotHeatmap from deepTools (Ramírez et al., 2016). ChIP-seq peak annotation for genomic locations were plotted as pie chart using ChIPseeker (Yu et al., 2015). For mapping of  $\kappa$ B elements to NF $\kappa$ B target genes, any TNF-inducible RelA ChIP-seq peaks within  $\pm 10$ kb from gene TSS were annotated to  $\kappa$ B elements (unique half and full  $\kappa$ B DNA sequences were annotated within the mm10 genome) and were mapped to each RelA ChIP-seq peak centered at 500bp window ( $\pm 250$ bp from each peak of  $\kappa$ B sequence) on every gene using Bedtools intersect. Full-length  $\kappa$ B elements were defined by the consensus sequence 5'GGRNNNNNYCC-3' for unique 9, 10, or 11bp DNA sequence; where R is a A or G, Y is a T or C, and N is any nucleotide.  $\kappa$ B half sites were defined by the consensus sequence 5'GGR or YCC-3' DNA sequence.  $\kappa$ B motifs were extracted from UCSC mm10 genome using Biostrings and BSgenome packages. Mapping of  $\kappa$ B motifs and RelA ChIP-seq peaks were visualized by ggplot2 geom\_segment. Scatter plots and box plots of RelA ChIP-seq data were visualized by ggplot. Wilcox.test function in R was used to find the statistical significance of reduced vs non-reduced RelA peaks (Mann-Whitney U-test). Integrative Genomics Viewer (IGV) was used to acquire RelA ChIP-seq tracks for example genes (Robinson et al., 2011).

## Computational Modeling

An ODE model was constructed representing the rate of change of mRNA for each gene.

$$\frac{d\text{RNA}}{dt} = \frac{k_{act} \cdot \text{RelA}_t^n}{K_D^n + \text{RelA}_t^n} - k_{deg} \cdot \text{RelA}$$

RelA is a time-dependent variable obtained by quantifying RelA DNA-binding activity from EMSA and linearly interpolating between discrete timepoints. Basal mRNA for a given parameter set was obtained by analytically solving the ODE with RelA fixed at the basal value:

$$\text{RNA}_0 = \frac{k_{act} \cdot \text{RelA}_0^n}{k_{deg} \cdot (K_D^n + \text{RelA}_0^n)}$$

Induced time-course response was obtained using ode23s in MATLAB (The MathWorks, Inc.).

The distance between experimental and modeled mRNA time courses was quantified using a combination of Pearson correlation and MSE to take into account both dynamics and absolute values ( $\text{dist} = (1 - \text{Pearson}) + \text{MSE}$ ). As  $K_D, n_{hill}, k_{deg}$  are assumed to be gene-specific properties, unaffected by TAD mutations these were first fit to WT data using particle swarm optimization (PSO) to minimize the distance between modelled mRNA time-course and measured RNA-seq (50 particles, terminating at either 100 epochs or distance below 0.001). As the RNA-seq time-course did not capture a decrease in mRNA levels for late-induced genes,  $k_{deg}$  could not be fit but was assumed to be equivalent to an 8 hour half-life. Following the fit to the WT data  $K_D, n_{hill}, k_{deg}$  were fixed for data from mutant cells and a new  $k_{act}$  was obtained for each TAD mutation using the same optimization approach.

## **Animal Use**

Wild-type and gene-deficient C57BL/6 mice were maintained in specific pathogen-free condition at the University of California, Los Angeles. The animal protocol for this study were approved by the Institutional Animal Care and Use Committee and by the University of California, Los Angeles Division of Laboratory Animal Medicine. Targeted Neo deleted RelA transactivation domain heterozygous knock-in mutant mice were generated by ingenious Technology Lab (iTTL, [www.genetargeting.com](http://www.genetargeting.com)).

## **Data Availability**

All sequencing data presented in this publication have been deposited to the NCBI Gene Expression Omnibus (GEO) and accessible under SuperSeries accession number GSE132540, <https://www.ncbi.nlm.nih.gov/geo/query/acc.cgi?acc=GSE132540>.

## **ACKNOWLEDGEMENTS**

The work presented in this chapter was a collaborative effort and is currently unpublished. The CBP-interacting mutant plasmid, pBABE-puro RelA-TA2<sup>α</sup>, and the anti-p50 antibody were generous gifts from Dr. Gourisankar Ghosh (UCSD). Roberto Spreafico and Zhang Cheng helped process ChIP-seq and RNA-seq data. Jeremy Davis-Turak helped with analysis in the control gene expression (Figure 2.2). Kensei Kishimoto and Aditya Pimplaskar helped analyze ChIP-seq and RNA-seq data. Emily Yu Hsin Chen helped with the chromatin-associated RNA-seq experiment. Mathematical modeling was performed by Simon Mitchell with

assistance from Amy Tam. Ning Wang helped with HOMER motif enrichment analysis. Yi Liu helped with BMDM isolation. Eason Lin helped with documenting knock-in mutant mice phenotype. Diane Lefaudeux provided technical advice in R programming. The dissertation author is the primary researcher and author of this study. Kensei Kishimoto, Jeremy Davis-Turak, Aditya Pimplaskar, Zhang Cheng, Roberto Spreafico, Emily Yu Hsin Chen, Amy Tam, and Simon Mitchell are co-authors. Alexander Hoffmann is the corresponding author.

## REFERENCES

- Bae, J.S., Jang, M.K., Hong, S., An, W.G., Choi, Y.H., Kim, H.D., and Cheong, J. (2003). Phosphorylation of NF-kappa B by calmodulin-dependent kinase IV activates anti-apoptotic gene expression. *Biochem. Biophys. Res. Commun.* *305*, 1094–1098.
- Baeuerle, P.A., and Baltimore, D. (1989). A 65-kappaD subunit of active NF-kappaB is required for inhibition of NF-kappaB by I kappaB. *Genes Dev.* *3*, 1689–1698.
- Bao, X., Indukuri, H., Liu, T., Liao, S.-L., Tian, B., Brasier, A.R., Garofalo, R.P., and Casola, A. (2010). IKKε modulates RSV-induced NF-κB-dependent gene transcription. *Virology* *408*, 224–231.
- Basak, S., Behar, M., and Hoffmann, A. (2012). Lessons from mathematically modeling the NF-κB pathway: Mathematical modeling the NF-κB pathway. *Immunological Reviews* *246*, 221–238.
- Bird, T.A., Schooley, K., Dower, S.K., Hagen, H., and Virca, G.D. (1997). Activation of nuclear transcription factor NF-kappaB by interleukin-1 is accompanied by casein kinase II-mediated phosphorylation of the p65 subunit. *J. Biol. Chem.* *272*, 32606–32612.
- Bohuslav, J., Chen, L.-F., Kwon, H., Mu, Y., and Greene, W.C. (2004). p53 induces NF-kappaB activation by an IkappaB kinase-independent mechanism involving phosphorylation of p65 by ribosomal S6 kinase 1. *J. Biol. Chem.* *279*, 26115–26125.
- Buss, H., Dörrie, A., Schmitz, M.L., Hoffmann, E., Resch, K., and Kracht, M. (2004). Constitutive and interleukin-1-inducible phosphorylation of p65 NF-κB at serine 536 is mediated by multiple protein kinases including IκB kinase (IKK)-α, IKKβ, IKKε, TRAF family member-associated (TANK)-binding kinase 1 (TBK1), and an unknown kinase and couples p65 to TATA-binding protein-associated factor II31-mediated interleukin-8 transcription. *J. Biol. Chem.* *279*, 55633–55643.
- Chen, E.Y., Tan, C.M., Kou, Y., Duan, Q., Wang, Z., Meirelles, G.V., Clark, N.R., and Ma'ayan, A. (2013). Enrichr: interactive and collaborative HTML5 gene list enrichment analysis tool. *BMC Bioinformatics* *14*, 128.
- Chen, F.E., Huang, D.-B., Chen, Y.-Q., and Ghosh, G. (1998a). Crystal structure of p50/p65 heterodimer of transcription factor NF-κB bound to DNA. *Nature* *391*, 410–413.
- Chen, Y.-Q., Ghosh, S., and Ghosh, G. (1998b). A novel DNA recognition mode by the NF-κB p65 homodimer. *Nature Structural & Molecular Biology* *5*, 67–73.
- Chen, Y.-Q., Sengchanthalangsy, L.L., Hackett, A., and Ghosh, G. (2000). NF-κB p65 (RelA) homodimer uses distinct mechanisms to recognize DNA targets. *Structure* *8*, 419–428.



- Cheng, C.S., Feldman, K.E., Lee, J., Verma, S., Huang, D.-B., Huynh, K., Chang, M., Ponomarenko, J.V., Sun, S.-C., Benedict, C.A., et al. (2011). The Specificity of Innate Immune Responses Is Enforced by Repression of Interferon Response Elements by NF- $\kappa$ B p50. *Sci. Signal.* 4, ra11–ra11.
- Christian, F., Smith, E.L., and Carmody, R.J. (2016). The Regulation of NF- $\kappa$ B Subunits by Phosphorylation. *Cells* 5.
- Corton, J., Moreno, E., and Johnston, S. (1998). Alterations in the GAL4 DNA-binding Domain Can Affect Transcriptional Activation Independent of DNA Binding. *JBC* 273, 13776–13780.
- Dong, J., Jimi, E., Zhong, H., Hayden, M.S., and Ghosh, S. (2008). Repression of gene expression by unphosphorylated NF- $\kappa$ B p65 through epigenetic mechanisms. *Genes Dev.* 22, 1159–1173.
- Haller, D., Russo, M.P., Sartor, R.B., and Jobin, C. (2002). IKK beta and phosphatidylinositol 3-kinase/Akt participate in non-pathogenic Gram-negative enteric bacteria-induced RelA phosphorylation and NF-kappa B activation in both primary and intestinal epithelial cell lines. *J. Biol. Chem.* 277, 38168–38178.
- Hao, S., and Baltimore, D. (2009). The stability of mRNA influences the temporal order of the induction of genes encoding inflammatory molecules. *Nat. Immunol.* 10, 281–288.
- Hayden, M.S., and Ghosh, S. (2008). Shared Principles in NF- $\kappa$ B Signaling. *Cell* 132, 344–362.
- Heinz, S., Benner, C., Spann, N., Bertolino, E., Lin, Y.C., Laslo, P., Cheng, J.X., Murre, C., Singh, H., and Glass, C.K. (2010). Simple combinations of lineage-determining transcription factors prime cis-regulatory elements required for macrophage and B cell identities. *Mol. Cell* 38, 576–589.
- Hochrainer, K., Racchumi, G., and Anrather, J. (2013). Site-specific Phosphorylation of the p65 Protein Subunit Mediates Selective Gene Expression by Differential NF- $\kappa$ B and RNA Polymerase II Promoter Recruitment. *J Biol Chem* 288, 285–293.
- Hoffmann, A., and Baltimore, D. (2006). Circuitry of nuclear factor  $\kappa$ B signaling. *Immunological Reviews* 210, 171–186.
- Hoffmann, A., Levchenko, A., Scott, M.L., and Baltimore, D. (2002). The I $\kappa$ B-NF- $\kappa$ B Signaling Module: Temporal Control and Selective Gene Activation. *Science* 298, 1241.
- Hoffmann, A., Leung, T.H., and Baltimore, D. (2003). Genetic analysis of NF-kappaB/Rel transcription factors defines functional specificities. *EMBO J.* 22, 5530–5539.
- Hoffmann, A., Natoli, G., and Ghosh, G. (2006). Transcriptional regulation via the NF-kappaB signaling module. *Oncogene* 25, 6706–6716.

- Keegan, L., Gill, G., and Ptashne, M. (1986). Separation of DNA binding from the transcription-activating function of a eukaryotic regulatory protein. *Science* *231*, 699–704.
- Kovesdi, I., Reichel, R., and Nevins, J.R. (1986). Identification of a cellular transcription factor involved in E1A trans-activation. *Cell* *45*, 219–228.
- Kuleshov, M.V., Jones, M.R., Rouillard, A.D., Fernandez, N.F., Duan, Q., Wang, Z., Koplev, S., Jenkins, S.L., Jagodnik, K.M., Lachmann, A., et al. (2016). Enrichr: a comprehensive gene set enrichment analysis web server 2016 update. *Nucleic Acids Res.* *44*, W90-97.
- Langmead, B., and Salzberg, S.L. (2012). Fast gapped-read alignment with Bowtie 2. *Nature Methods* *9*, 357–359.
- Milanovic, M., Kracht, M., and Schmitz, M.L. (2014). The cytokine-induced conformational switch of nuclear factor  $\kappa$ B p65 is mediated by p65 phosphorylation. *Biochem J* *457*, 401–413.
- Mitchell, S., Vargas, J., and Hoffmann, A. (2016). Signaling via the NF $\kappa$ B system. *Wiley Interdisciplinary Reviews: Systems Biology and Medicine* *8*, 227–241.
- Moore, P.A., Ruben, S.M., and Rosen, C.A. (1993). Conservation of transcriptional activation functions of the NF-kappa B p50 and p65 subunits in mammalian cells and *Saccharomyces cerevisiae*. *Mol. Cell. Biol.* *13*, 1666–1674.
- Moreno, R., Sobotzik, J.-M., Schultz, C., and Schmitz, M.L. (2010). Specification of the NF-kappaB transcriptional response by p65 phosphorylation and TNF-induced nuclear translocation of IKK epsilon. *Nucleic Acids Res.* *38*, 6029–6044.
- Morita, S., Kojima, T., and Kitamura, T. (2000). Plat-E: an efficient and stable system for transient packaging of retroviruses. *Gene Therapy* *7*, 1063.
- Mukherjee, S.P., Behar, M., Birnbaum, H.A., Hoffmann, A., Wright, P.E., and Ghosh, G. (2013). Analysis of the RelA:CBP/p300 Interaction Reveals Its Involvement in NF- $\kappa$ B-Driven Transcription. *PLOS Biology* *11*, e1001647.
- Nyqvist, I., Andersson, E., and Dogan, J. (2019). Role of Conformational Entropy in Molecular Recognition by TAZ1 of CBP. *J. Phys. Chem. B* *123*, 2882–2888.
- Pandya-Jones, A., Bhatt, D.M., Lin, C.-H., Tong, A.-J., Smale, S.T., and Black, D.L. (2013). Splicing kinetics and transcript release from the chromatin compartment limit the rate of Lipid A-induced gene expression. *RNA* *19*, 811–827.
- Ramírez, F., Ryan, D.P., Grüning, B., Bhardwaj, V., Kilpert, F., Richter, A.S., Heyne, S., Dündar, F., and Manke, T. (2016). deepTools2: a next generation web server for deep-sequencing data analysis. *Nucleic Acids Res* *44*, W160–W165.

- Robinson, J.T., Thorvaldsdóttir, H., Winckler, W., Guttman, M., Lander, E.S., Getz, G., and Mesirov, J.P. (2011). Integrative Genomics Viewer. *Nat Biotechnol* 29, 24–26.
- Sabatel, H., Di Valentin, E., Gloire, G., Dequiedt, F., Piette, J., and Habraken, Y. (2012). Phosphorylation of p65(RelA) on Ser(547) by ATM represses NF- $\kappa$ B-dependent transcription of specific genes after genotoxic stress. *PLoS ONE* 7, e38246.
- Sakurai, H., Suzuki, S., Kawasaki, N., Nakano, H., Okazaki, T., Chino, A., Doi, T., and Saiki, I. (2003). Tumor necrosis factor- $\alpha$ -induced IKK phosphorylation of NF- $\kappa$ B p65 on serine 536 is mediated through the TRAF2, TRAF5, and TAK1 signaling pathway. *J. Biol. Chem.* 278, 36916–36923.
- Savaryn, J.P., Skinner, O.S., Fornelli, L., Fellers, R.T., Compton, P.D., Terhune, S.S., Abecassis, M.M., and Kelleher, N.L. (2016). Targeted analysis of recombinant NF kappa B (RelA/p65) by denaturing and native top down mass spectrometry. *Journal of Proteomics* 134, 76–84.
- Schmitz, M.L., and Baeuerle, P.A. (1991). The p65 subunit is responsible for the strong transcription activating potential of NF- $\kappa$ B. *EMBO J.* 10, 3805–3817.
- Schmitz, M.L., Silva, M.A. dos S., Altmann, H., Czisch, M., Holak, T.A., and Baeuerle, P.A. (1994). Structural and functional analysis of the NF- $\kappa$ B p65 C terminus. An acidic and modular transactivation domain with the potential to adopt an alpha-helical conformation. *J. Biol. Chem.* 269, 25613–25620.
- Siggers, T., Chang, A.B., Teixeira, A., Wong, D., Williams, K.J., Ahmed, B., Ragoussis, J., Udalova, I.A., Smale, S.T., and Bulyk, M.L. (2011). Principles of dimer-specific gene regulation revealed by a comprehensive characterization of NF- $\kappa$ B family DNA binding. *Nature Immunology* 13, 95.
- Siggers, T., Chang, A.B., Teixeira, A., Wong, D., Williams, K.J., Ahmed, B., Ragoussis, J., Udalova, I.A., Smale, S.T., and Bulyk, M.L. (2012). Principles of dimer-specific gene regulation revealed by a comprehensive characterization of NF- $\kappa$ B family DNA binding. *Nature Immunology* 13, 95–102.
- Todaro, G., and Green, H. (1963). Quantitative studies of the growth of mouse embryo cells in culture and their development into established lines. *J Cell Bio* 17, 299–313.
- Tong, A., Liu, X., Thomas, B., Lissner, M., Baker, M., Senagolage, M., Allred, A., Barish, G., and Smale, S. (2016). A Stringent Systems Approach Uncovers Gene-Specific Mechanisms Regulating Inflammation. *Cell* 165, 165–179.
- Wang, D., Westerheide, S.D., Hanson, J.L., and Baldwin, A.S. (2000). Tumor Necrosis Factor  $\alpha$ -induced Phosphorylation of RelA/p65 on Ser529 Is Controlled by Casein Kinase II. *J. Biol. Chem.* 275, 32592–32597.

Werner, S.L., Barken, D., and Hoffmann, A. (2005). Stimulus Specificity of Gene Expression Programs Determined by Temporal Control of IKK Activity. *Science* 309, 1857.

Yoboua, F., Martel, A., Duval, A., Mukawera, E., and Grandvaux, N. (2010). Respiratory syncytial virus-mediated NF-kappa B p65 phosphorylation at serine 536 is dependent on RIG-I, TRAF6, and IKK beta. *J. Virol.* 84, 7267–7277.

Yu, G., Wang, L.-G., and He, Q.-Y. (2015). ChIPseeker: an R/Bioconductor package for ChIP peak annotation, comparison and visualization. *Bioinformatics* 31, 2382–2383.

Zhong, H., May, M.J., Jimi, E., and Ghosh, S. (2002). The Phosphorylation Status of Nuclear NF-KB Determines Its Association with CBP/p300 or HDAC-1. *Molecular Cell* 9, 625–636.

# **CHAPTER 3:**

## **Conclusions and Future Directions**

In Chapter 2 of this dissertation, we focused on the RelA subunit of the transcription factor NF $\kappa$ B. We revealed gene-specific regulatory strategies of endogenous RelA target genes in primary cells by probing their stimulus-induced expression with engineered RelA variants. We stringently identified target genes by both functional and physical binding criteria. We developed an experimental system to test mutational variants in primary cells, and systematically analyzed both chromatin DNA recruitment and transcriptional trans-activation at single gene resolution. A key transcriptional activation domain mutation was introduced by a knock-in mouse line to examine other cell types and stimuli and a mathematical modeling approach enabled a quantitative analysis to reveal gene-specific logic gates formed by the two TA domains. Although we focused only on inducible genes that are expressed when NF $\kappa$ B is functionally active, the genes that NF $\kappa$ B can down-regulate via gene repression are also worth exploring in future work. Identifying endogenous genes that are expressed or repressed by NF $\kappa$ B activity can explain the differential outcomes of NF $\kappa$ B activation in healthy versus unhealthy cells that may be important for developing novel therapeutic interventions designed to target NF $\kappa$ B responses.

In this study, we first showed that in primary fibroblasts, RelA recruitment and transcriptional activation of all endogenous NF $\kappa$ B target genes induced by TNF are dependent on direct high-affinity DNA binding of RelA. A previously report had shown in X-ray structures of NF $\kappa$ B dimer-DNA complex that binding to only one half-site of  $\kappa$ B DNA targets is sufficient for DNA recognition (Chen et al., 2000). Here in our study, we observed that the DNA base-specific contacts made by both NF $\kappa$ B subunits to  $\kappa$ B DNA targets are indispensable for the downstream gene activation of target genes. In our RelA<sup>DB</sup> mutant analysis, the dimerization partner p50 may still contribute to DNA binding, but it appears insufficient to mediate

downstream gene expression. Hence, the transcriptional activation potential of NF $\kappa$ B was inhibited as loss of NF $\kappa$ B transcriptional activity was observed (Figure 2.5H). Nevertheless, to confirm our findings in Chapter 2 and our observations that p50 binding in our RelA<sup>DB</sup> mutant analysis is insufficient for TNF-induced activation of NF $\kappa$ B target genes, ChIP -seq experiments with a p50-specific antibody could confirm whether the genomic locations where RelA binding was inhibited in the RelA<sup>DB</sup> mutant cell line show unaltered p50 binding. Alternatively, for a deeper understanding of the mechanisms of DNA binding, we could use biophysical approaches to assess DNA binding in the RelA<sup>DB</sup> mutant. In this regard, performing structural characterization of the RelA<sup>DB</sup> mutant in complex with DNA through X-ray crystallography or nuclear magnetic resonance (NMR) may address whether base-specific contacts with  $\kappa$ B DNA are fully prevented in RelA<sup>DB</sup>. Solving the structures of RelA<sup>DB</sup> mutant as a RelA homodimer or as a heterodimer with p50 could allow a more accurate assessment of the physical properties of RelA-containing dimers binding to DNA and possibly confirm that p50 is required for DNA binding, but insufficient for NF $\kappa$ B-mediated transcription of genes in a RelA<sup>DB</sup> mutant context.

While the gene expression response to TNF is rapid, future studies may address whether the dependence on DNA base-specific contacts also pertains to long-term expression dynamics mediated by NF $\kappa$ B. An example of inducers that mediate longer NF $\kappa$ B activity and long-term expression dynamics is bacterial lipopolysaccharide (LPS) that activates toll-like receptor 4 (TLR4) signaling. NF $\kappa$ B activation in response to LPS stimulation has been shown to result in more delayed and persistent NF $\kappa$ B activity (Werner et al., 2005). Additionally, LPS-induced activation of the TLR4 signaling pathways is more complex as it results in the activation of other transcription factor activity in addition to NF $\kappa$ B, such as interferon regulatory factors (IRFs).

Although IRFs are known to co-regulate TLR4-induced genes with NF $\kappa$ B (Lu et al., 2008), e.g. the expression of Ccl5/RANTES gene (Tong et al., 2016), we predict that the dependence on DNA base-specific contacts in NF $\kappa$ B RelA may also pertain to TLR4-response genes.

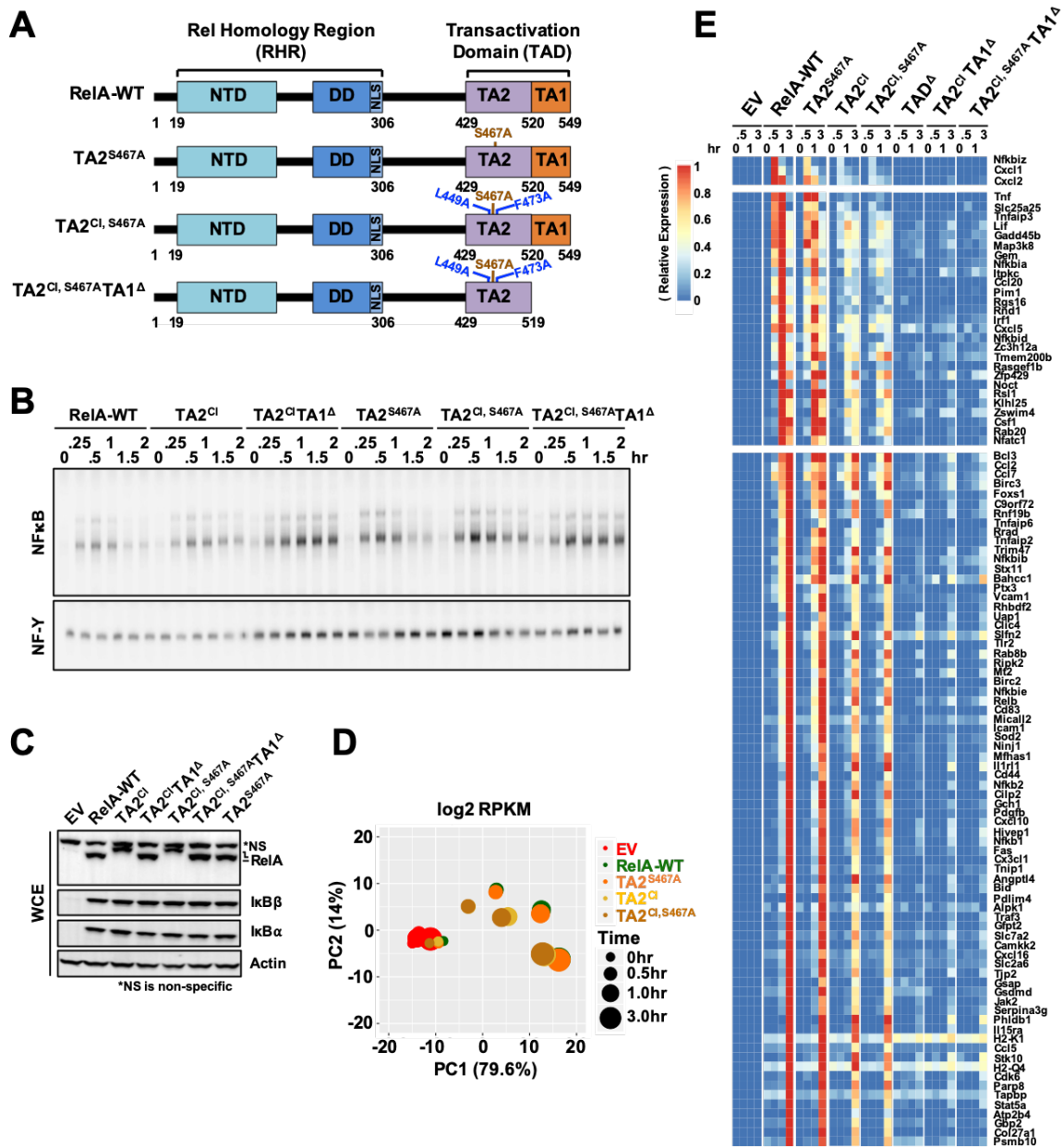
Our studies further indicate that all endogenous target genes induced by TNF require the C-terminal region of RelA that harbors two transactivation domains, TA1 and TA2. That is remarkable given that phosphorylation of RelA at S276 was reported to play critical roles in recruiting CBP/p300 (Zhong et al., 1998), and knock-in mutant mice harboring the S276A mutation showed striking animal phenotypes and alterations in the expression of many genes, including some known NF $\kappa$ B target genes (Dong et al., 2008). Our analysis suggests that the intact N-terminal RHR containing phosphorylated S276 is insufficient for TNF-induced NF $\kappa$ B target gene activation and may support the notion that the phenotype of S276 mutation may be due to alterations at larger time and epigenetic scales (Cheng et al., 2008).

In this dissertation, mathematical modeling was also used to assess the functional requirements of each RelA transactivation domain quantitatively, which may be confounded in the experimental system (i.e. alterations in the NF $\kappa$ B activation time course, Figure 2.8C). Hence, by probing target genes for the roles of the two C-terminal activation domains, TA1 and TA2, we found remarkable gene-specificity in our mathematical model-aided analysis. Target genes did not differ very much in whether they were more highly regulated by TA1 vs. TA2, but they differed in whether they required only either TA or required both TAs for gene activation. In other words, some NF $\kappa$ B target genes allow TA1 and TA2 to function independently, forming a logical OR gate while other NF $\kappa$ B target genes require the synergistic function of TA1 and TA2, with the TAs forming a logical AND gate. These distinct regulatory strategies may be



mediated by distinct mechanistic requirements for the recruitment of molecular co-activators. For example, genes that exhibit an OR gate logic, might be activated sufficiently by recruiting CBP/p300 via TA2, but genes exhibiting an AND gate logic might need to recruit not only CBP/p300 but also additional co-activators via TA1.

The functionality of TA1 was characterized as being regulated by PTMs, particularly phosphorylation, while TA2 has intrinsic transactivation activity via its interaction with CBP/p300. Yet S467 within TA2 was reported as a potential phosphorylation site that may dampen its activity (Buss et al., 2004a; Geng et al., 2009; Mao et al., 2009; Schwabe and Sakurai, 2005). To investigate whether S467 plays a role in the TNF-induced expression of NF $\kappa$ B target genes in fibroblasts, we constructed the S467A variant within full length RelA, TA1 deleted RelA, or the CBP-interaction mutant TA2<sup>ci</sup> (Figure 3.1A). Gel mobility shift analysis showed TA2<sup>S467A</sup> did not alter the DNA-binding activity of NF $\kappa$ B compared to each respective parent construct (Figure 3.1B, cf. Figure 2.8C), and protein expression levels of these RelA variants and the canonical I $\kappa$ B $\alpha$  and I $\kappa$ B $\beta$  were normal (Figure 3.1C). We then undertook polyA+ RNA-seq analysis and PCA revealed only minimal alteration in the TNF-induced gene expression response with S467A in the WT or TA2<sup>ci</sup> context (Figure 3.1D). Furthermore, in a heatmap with single-gene resolution (Figure 3.1E), we observed very little effect by the S467A mutation. Only chemokines Cxcl1, Cxcl2 and Ccl20, which are rapidly and highly induced, showed a slight reduction but no enhancement. Our data thus confirms that an intrinsic CBP/p300 interaction affinity (probed with the TA2<sup>ci</sup> mutation) is the primary mode of function of the TA2 domain. This contrasts with how TA1's functionality is enhanced by phosphorylation events mediated by coordinated kinases such as CKII and IKK $\epsilon$  (O'shea and Perkins, 2008; Buss et al., 2004b; Wang et al., 2000).



**Figure 3.1 The RelA TA2 domain functions primarily via intrinsic affinity for CBP/p300.**

(A) Schematic of the RelA variants involving mutation of the phosphorylation site S467. (B) Analysis of nuclear NFκB activity by EMSA of nuclear extracts prepared at indicated times after TNF stimulation of genetically complemented fibroblasts of indicated genotype. (C) Protein expression of RelA, IκBβ, IκBα, and Actin in unstimulated cells as assayed by immunoblotting. (D) PCA plot of the transcriptional TNF response of all 104 NFκB target genes at indicated times and cell variants. (E) Heatmap of relative induced expression in response to TNF stimulation of the 104 target genes in same cell variants, as analyzed by polyA+RNA-seq.

What are the implications of this regulatory distinction of TA1 vs. TA2 for the transcriptional control of NFκB target genes, which differ in how they employ TA1 and TA2? Considering NFκB target genes that are regulated redundantly by TA1 OR TA2, we would expect these genes to respond to all inflammatory stimuli that activate the IKK-NFκB axis as TA2 is effective for their induction, and regulated TA1 activity may merely provide some modulation. On the other hand, NFκB target genes that are regulated synergistically by TA1 AND TA2 will be strongly activated only by those inflammatory stimuli that also induce the phosphorylation of TA1 serines that potentiate its acidic activation function. Alternatively, TA1 phosphorylation may be a function of the micro-environmental context, thus rendering the activation of these genes tissue context-dependent. We note, for such genes, controlled by an AND gate of TA1 and TA2, the role of TA2 is to amplify the effect of phosphorylation-mediated regulation of TA1 in activity, rendering them more responsive to these PTMs than if they were regulated only by TA1.

Examining the types of genes that are regulated redundantly vs. synergistically by TA1 and TA2, we noted that many genes that provide for negative regulation of inflammation, such as *Il15ra*, *IL1rl1*, *Trim47*, *Slfn2* or *RelB* fall into the former category. For these genes, TA redundancy means that they constitute an inflammatory core response that includes provisions for inflammatory resolution. In contrast, the latter category includes genes that are key initiators of an inflammatory response such as *TNF*, *Ccl20*, *Ccl2*, *Cxcl1*. For these genes, TA synergy means that their expression is activated only in response to a subset of inflammatory stimuli, or when tissue-environmental context provides for the co-stimulatory signal that TA1 requires.

The here-described paradigm of NFκB RelA-responsive gene expression being either redundantly or synergistically mediated by TA1 and TA2 should prompt a range of further studies

that extend past work on the signals and pathways that control TA1 phosphorylation and the molecular mechanisms that determine whether a target gene requires the dual TA1/TA2 functionality. We may imagine that the involvement of differential co-activators, mediator complexes, the nucleosome movements or other complex chromatin interactions, or recruitment or release of RNA polymerase may play a role in determining diverse regulatory logics.

More broadly, the study in this dissertation suggests that the structure-function relationship of key transcription factors provides an informative probe to dissect the diverse gene regulatory strategies that govern their many target genes. Dissecting the regulatory mechanisms of how endogenous gene expression is regulated is important to understand the TFs' physiological function and can therefore help in the development of therapeutic interventions. Quantitative datasets produced by Next Generation Sequencing approaches allow a focus on endogenous genes that may be effectively quantitatively evaluated with gene-specific resolution using mathematical models of the gene expression process to reveal regulatory diversity instead of the more traditional bioinformatics methods focusing on average behavior, assuming certain commonalities. Thus, we hope that our study provides an analysis blueprint for future studies; indeed, advances of CRISPR/Cas9 technology that enable the engineering of variants into the endogenous gene locus is powering studies of endogenous gene regulatory circuits at single gene resolution.

## REFERENCES

- Buss, H., Dörrie, A., Schmitz, M.L., Frank, R., Livingstone, M., Resch, K., and Kracht, M. (2004a). Phosphorylation of Serine 468 by GSK-3 $\beta$  Negatively Regulates Basal p65 NF- $\kappa$ B Activity. *J. Biol. Chem.* 279, 49571–49574.
- Buss, H., Dörrie, A., Schmitz, M.L., Hoffmann, E., Resch, K., and Kracht, M. (2004b). Constitutive and interleukin-1-inducible phosphorylation of p65 NF- $\kappa$ B at serine 536 is mediated by multiple protein kinases including I $\kappa$ B kinase (IKK)- $\alpha$ , IKK $\beta$ , IKK $\epsilon$ , TRAF family member-associated (TANK)-binding kinase 1 (TBK1), and an unknown kinase and couples p65 to TATA-binding protein-associated factor II31-mediated interleukin-8 transcription. *J. Biol. Chem.* 279, 55633–55643.
- Chen, F.E., and Ghosh, G. (1999). Regulation of DNA binding by Rel/NF-kappaB transcription factors: structural views. *Oncogene* 18, 6845–6852.
- Chen, Y.-Q., Sengchanthalangsy, L.L., Hackett, A., and Ghosh, G. (2000). NF- $\kappa$ B p65 (RelA) homodimer uses distinct mechanisms to recognize DNA targets. *Structure* 8, 419–428.
- Cheng, C.S., Johnson, T.L., and Hoffmann, A. (2008). Epigenetic control: slow and global, nimble and local. *Genes Dev.* 22, 1110–1114.
- Dong, J., Jimi, E., Zhong, H., Hayden, M.S., and Ghosh, S. (2008). Repression of gene expression by unphosphorylated NF- $\kappa$ B p65 through epigenetic mechanisms. *Genes Dev.* 22, 1159–1173.
- Geng, H., Wittwer, T., Dittrich-Breiholz, O., Kracht, M., and Schmitz, M.L. (2009). Phosphorylation of NF- $\kappa$ B p65 at Ser468 controls its COMMD1-dependent ubiquitination and target gene-specific proteasomal elimination. *EMBO Rep.* 10, 381–386.
- Hoffmann, A., Leung, T.H., and Baltimore, D. (2003). Genetic analysis of NF-kappaB/Rel transcription factors defines functional specificities. *EMBO J.* 22, 5530–5539.
- Hoffmann, A., Natoli, G., and Ghosh, G. (2006). Transcriptional regulation via the NF-kappaB signaling module. *Oncogene* 25, 6706–6716.
- Lu, Y.-C., Yeh, W.-C., and Ohashi, P.S. (2008). LPS/TLR4 signal transduction pathway. *Cytokine* 42, 145–151.
- Mao, X., Gluck, N., Li, D., Maine, G.N., Li, H., Zaidi, I.W., Repaka, A., Mayo, M.W., and Burstein, E. (2009). GCN5 is a required cofactor for a ubiquitin ligase that targets NF- $\kappa$ B/RelA. *Genes Dev.* 23, 849–861.
- O’shea, J.M., and Perkins, N.D. (2008). Regulation of the RelA (p65) transactivation domain. *Biochem. Soc. Trans.* 36, 603–608.

Schwabe, R.F., and Sakurai, H. (2005). IKK $\beta$  phosphorylates p65 at S468 in transactivator domain 2. *FASEB J.* *19*, 1758–1760.

Tong, A.-J., Liu, X., Thomas, B.J., Lissner, M.M., Baker, M.R., Senagolage, M.D., Allred, A.L., Barish, G.D., and Smale, S.T. (2016). A Stringent Systems Approach Uncover Gene-Specific Mechanisms Regulating Inflammation. *Cell* *165*, 165–179.

Wang, D., Westerheide, S.D., Hanson, J.L., and Baldwin, A.S. (2000). Tumor Necrosis Factor  $\alpha$ -induced Phosphorylation of RelA/p65 on Ser529 Is Controlled by Casein Kinase II. *J. Biol. Chem.* *275*, 32592–32597.

Werner, S.L., Barken, D., and Hoffmann, A. (2005). Stimulus Specificity of Gene Expression Programs Determined by Temporal Control of IKK Activity. *Science* *309*, 1857.

Zhong, H., Voll, R.E., and Ghosh, S. (1998). Phosphorylation of NF- $\kappa$ B p65 by PKA Stimulates Transcriptional Activity by Promoting a Novel Bivalent Interaction with the Coactivator CBP/p300. *Mol. Cell* *1*, 661–671.